USAELRDL Technical Report 2261

HIGHER ORDER TEMPERATURE COEFFICIENTS OF THE ELASTIC STIFFNESSES AND COMPLIANCES OF ALPHA-QUARTZ

R. Bechmann
A. D. Ballato
T. J. Lukaszek

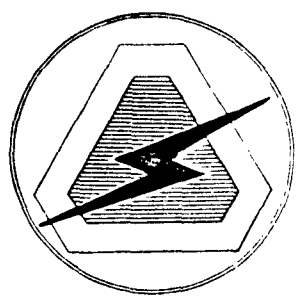

September 1963

UNITED STATES ARMY
ELECTRONICS RESEARCH AND DEVELOPMENT LABORATORY
FORT MONMOUTH, N.J.

U. S. ARMY ELECTRONICS RESEARCH AND DEVELOPMENT LABORATORY

FORT MONMOUTH, NEW JERSEY

September 1963

USAELRDL Technical Report Nr. 2261 has been prepared under the supervision of the Director, Electronic Components Department, and is published for the information and guidance of all concerned. Suggestions or criticisms relative to the form, content, purpose, or use of this publication should be referred to the Commanding Officer, U. S. Army Electronics Research and Development Laboratory, Attn: Chief, Piezoelectric Crystal and Circuitry Branch, Solid State and Frequency Control Division, Fort Monmouth, New Jersey.

J. M. KIMBROUGH, JR.
Colonel, Signal Corps
Commanding

OFFICIAL:
B. B. PALMER
Major, WAC
Adjutant

DISTRIBUTION:
Special

HIGHER ORDER TEMPERATURE COEFFICIENTS OF THE ELASTIC STIFFNESSES AND COMPLIANCES OF ALPHA-QUARTZ

R. Bechmann
A. D. Ballato
T. J. Lukaszek

DA Task No. 3A99-15-001-02

Abstract

The first-, second-, and third-order temperature coefficients of the elastic stiffnesses and compliances of alpha-quartz have been determined using thickness modes of double-rotated quartz plates based on the Christoffel theory of thickness vibrations. The temperature dependence of all possible thickness modes can be calculated from the values of the elastic stiffnesses and their temperature coefficients as derived during this investigation. A curve showing the locus of the first-order zero temperature coefficient of frequency of thickness-shear modes has been calculated and compared with experiments. The second- and third-order temperature coefficients of frequency of the first-order zero quartz cuts are given. Applications to AT, BT, CT, and DT cuts are made by comparing the calculated with the experimental values which characterize the frequency temperature behavior of crystals.

U. S. ARMY ELECTRONICS RESEARCH AND DEVELOPMENT LABORATORY

FORT MONMOUTH, NEW JERSEY

CONTENTS

HIGHER ORDER TEMPERATURE COEFFICIENTS OF THE ELASTIC STIFFNESSES AND COMPLIANCES OF ALPHA-QUARTZ

INTRODUCTION

The general theory of the propagation of plane waves in anisotropic media, as derived by Green [1] in 1839, results in three possible types of plane waves for any direction of propagation, each wave having a different velocity and the three directions of vibration being mutually perpendicular.

In 1877 Christoffel [2] wrote the differential equations of motion governing plane waves in terms of strain instead of stress. The six so-called Christoffel moduli Γ_{ik} which are combinations of the 21 stiffnesses $c_{\lambda\mu}$ ($\lambda,\mu = 1,2...,6$) and the direction cosines of the wave propagation were thereby introduced. In order to describe plane waves in a general triclinic material, only the six so-called Christoffel moduli are required as the strain components perpendicular to the direction of propagation are prohibited by lateral inertia.

The solution of the three second-order differential equations derived by Christoffel leads to three resulting stiffnesses c_m ($m = 1, 2, 3$) which are related to the velocities of wave propagation and the directions of the displacements which are generally neither parallel nor perpendicular to the direction of the wave propagation.

The resonance frequencies of thickness modes of an infinite crystal plate, based on Christoffel's equations, were derived in 1932 by Koga [3] in closed form, but correspondingly simple solutions for the thickness modes cannot be obtained for a bounded plate. The equations for thickness-shear and flexural vibrations of crystal plates have been solved in a series of papers by Mindlin [4]. Koga's solution, however, can be considered a zero-order approximation, and the resulting stiffness c_m, leading to values of the wave velocity for each of the three thickness modes of motion, approximates frequency expressions close to the values obtained by a higher approximation. The approximate equations can be used to determine the higher order temperature coefficients of the elastic stiffnesses.

The first-order temperature coefficients of the stiffnesses and compliances of alpha-quartz were originally derived by Bechmann [5] in 1934, based on Christoffel's theory, using measured values for the temperature coefficients of frequency of thickness modes of plates and extensional modes of bars in the 20° to 60°C temperature range. These temperature coefficients of the stiffnesses are of interest for practical application. The first-order zero temperature coefficients of frequency of AT- or BT-type quartz plates, for example, can be calculated using these values. The temperature coefficients of the elastic stiffnesses are not linear with temperature in a wider temperature range, and temperature coefficients of higher order have to be taken into consideration by use of a power series. It is sufficient to determine the first three orders of temperature coefficients of frequencies and stiffnesses to obtain satisfactory agreement between measurements and calculations. Difficulties would be encountered, however, if the temperature dependence were described using temperature coefficients of orders higher than three.

A modified theory of elasticity was considered by Laval [6] in 1951, and later by others, proposing that the asymmetrical part of the stress tensor enters into the constitutive relations, thereby increasing the number of elastic constants compared with the classical theory.

Laval's theory of elasticity demands, e.g., for the crystal class D_{2d}, two different stiffnesses c_{44} and c_{77} instead of the elastic-shear stiffness c_{44}. Jaffe and Smith [7] have carried out new measurements on ammonium dihydrogen phosphate by two methods: (1) measurements of the piezoelectric resonances, and (2) measurements using the pulse echo method, both giving the shear elastic stiffnesses directly. Measurements of shear wave velocities by the two simple methods show the velocities of the two waves involving shear between the Y- and Z-axes to be equal well within the experimental error limits.

According to Laval's theory of elasticity the number of elastic constants for the crystal class D_3 is increased by $c_{55} \neq c_{44}$ and c_{17}. Zubov and Firsova [8] carried out a new determination of the elastic stiffnesses of quartz using the increased number of elastic stiffnesses. Their values fall within the limits of accuracy of measurements. The experimental values for the frequency constants of various quartz plates vibrating in thickness modes, and previously used for determination of the elastic stiffnesses given by Bechmann [9], have been recalculated with respect to the new theory. He found that the values for c_{44} and c_{55}, c_{14} and c_{17} are so close and so critical that from an experimental point of view, no conclusions can be drawn nor decisions made as to whether the classical theory or the Laval theory is valid. Recent studies by Mindlin [10] show that the principles of conservation of momentum and energy are not fulfilled by Laval's theory. In the following, determination of the temperature coefficients of the stiffnesses is based on the classical theory of elasticity. Figure 1 shows the measured frequency-temperature behavior of the AT, BT, CT, DT, and RT cuts and, in addition, the so-called optimum angle of an AT cut, so defined that its frequency temperature dependence, in the temperature range $-40°$ to $90°C$, for example, is reduced to a minimum. Table 1 lists the angles of orientation θ for these cuts and the values for their second- and third-order temperature coefficients of frequency b and c respectively.

CHRISTOFFEL'S THEORY OF PLANE ELASTIC WAVES IN CRYSTALS

Christoffel's theory of the propagation of plane elastic waves in crystals is well known and treated in many papers and text books [11]. It is therefore unnecessary to repeat this theory.

The differential equation for plane waves in anisotropic media is written considering one dimension, that of the propagation s with the direction cosines α_1, α_2, α_3 in the form

$$\rho \frac{\partial^2 \xi}{\partial t^2} - c \frac{\partial^2 \xi}{\partial s^2} = 0 \ , \tag{1}$$

where c is

$$c = \Gamma_{11}p^2 + \Gamma_{22}q^2 + \Gamma_{33}r^2 + \Gamma_{23}qr + \Gamma_{31}rp + \Gamma_{12}pq \tag{2}$$

and

$$\Gamma_{ik} = \sum_{jl}^{3} c_{ij,kl} \ \alpha_j \alpha_l \ , \tag{3}$$

the Christoffel stiffnesses, a combination of the stiffnesses c_{ik} and the direction cosines. The constants p, q, r, when normalized by $p^2 + q^2 + r^2 = 1$, are the direction cosines for the displacement ξ_i. To solve Eq. (1) for an infinitely extended plate, the boundary conditions for the free plate

$$\frac{\partial \xi}{\partial s} = 0 \text{ for } s = 0 \text{ and } s = t \text{ (t is the thickness of the plate)}$$

have to be introduced.

When considering the propagation of elastic waves in a piezoelectric material, an additional piezoelectric stress due to the electric field E must be introduced. The elastic properties of an ionic lattice, which cannot be discussed separately, must be considered in conjunction with the theory of piezoelectric and dielectric effects. Because of the coupling of the strain and stress tensors with the vectors of electric field and electric displacement, a slight modification of the elastic stiffnesses $c_{\lambda\mu} = c_{\lambda\mu}^{E}$ occurs, becoming $c_{\lambda\mu}^{D_s}$, where D_s refers to constant normal displacement. For infinite plates, on the basis of Maxwell's equation, D_{normal} ($= D_s$) and $E_{tangent}$ must be continuous and therefore the related coefficients $c_{\lambda\mu}$ and Γ_{ik} are mixed with $D = 0$ normal to, $E = 0$ parallel to, the wavefront. Consequently, Γ_{ik}^{E} becomes Γ_{ik}^{D}, the direction cosines of the displacement change, and the resulting stiffnesses c_m^{E} become c_m^{D}. Between the displacement $\xi(p, q, r)$ and the resulting elastic stiffness c, the system of linear equations exists:

$$\begin{aligned} p\Gamma_{11} + q\Gamma_{12} + r\Gamma_{13} &= pc \\ p\Gamma_{12} + q\Gamma_{22} + r\Gamma_{23} &= qc \\ p\Gamma_{13} + q\Gamma_{23} + r\Gamma_{33} &= rc\ . \end{aligned} \tag{3a}$$

The secular equation defining the three resulting stiffnesses c_m of a piezoelectric material as a consequence of Eq. (3a) is given by

$$\begin{vmatrix} \Gamma_{11}^{D_s} - c^{D_s} & \Gamma_{12}^{D_s} & \Gamma_{13}^{D_s} \\ \Gamma_{12}^{D_s} & \Gamma_{22}^{D_s} - c^{D_s} & \Gamma_{23}^{D_s} \\ \Gamma_{13}^{D_s} & \Gamma_{23}^{D_s} & \Gamma_{33}^{D_s} - c^{D_s} \end{vmatrix}$$

$$\equiv \begin{vmatrix} \Gamma_{11}^{E} - c^{D_s} & \Gamma_{12}^{E} & \Gamma_{13}^{E} & \Xi_1 \\ \Gamma_{12}^{E} & \Gamma_{22}^{E} - c^{D_s} & \Gamma_{23}^{E} & \Xi_2 \\ \Gamma_{13}^{E} & \Gamma_{23}^{E} & \Gamma_{33}^{E} - c^{D_s} & \Xi_3 \\ \Xi_1 & \Xi_2 & \Xi_3 & -\epsilon_s \end{vmatrix} = 0. \tag{4}$$

The expressions for Γ_{ik}^{E} and $\Gamma_{ik}^{D_s}$ at constant electric field and constant normal displacement, respectively, in these equations are related by

$$\Gamma_{ik}^{D_s} = \Gamma_{ik}^{E} + \frac{1}{\epsilon_s} \Xi_i \Xi_k\ . \tag{5}$$

The direction cosines p_τ, q_τ, r_τ ($\tau = 1,2,3$) can be calculated from any two of the three equations (3a), for example, from the second and the third equations of (3a), one obtains

$$p_\tau = \frac{1}{W_\tau} \left[(\Gamma_{22} - c_\tau)(\Gamma_{33} - c_\tau) - \Gamma_{23}^{2} \right],$$

$$q_\tau = \frac{1}{W_\tau} \left[\Gamma_{13}\Gamma_{23} - \Gamma_{12}(\Gamma_{33} - c_\tau) \right],$$

$$r_\tau = \frac{1}{W_\tau} \left[\Gamma_{12}\Gamma_{23} - \Gamma_{13}(\Gamma_{22} - c_\tau) \right];$$

$$W_\tau = \{[(\Gamma_{22} - c_\tau)(\Gamma_{33} - c_\tau) - \Gamma_{23}^2]^2 + [\Gamma_{13}\Gamma_{23} - \Gamma_{12}(\Gamma_{33} - c_\tau)]^2 + [\Gamma_{12}\Gamma_{23} - \Gamma_{13}(\Gamma_{22} - c_\tau)]^2\}^{1/2}.$$

The effective piezoelectric constant, corresponding to the eigenvalue c_m, is

$$e_m = \sum_i^3 \beta_{im} \cdot \Xi_i ,$$

where the direction cosines β for the displacements follow from Eq. (4). When the components of the third-order piezoelectric tensor are written with three indices, the following conditions hold:

$$e_{n,kl} = e_{n,lk} ,$$

reducing the possible 27 combinations of coefficients to 18. Similarly, when the components of the fourth-order stiffness tensor are written with four indices, the following conditions hold:

$$c_{ij,kl} = c_{ij,lk} = c_{ji,kl} = c_{ji,lk} = c_{kl,ij} = c_{kl,ji} = c_{lk,ij} = c_{lk,ji} ,$$

reducing the 81 possible combinations of the indices to 21. The following table shows the scheme used for converting the double indices i,j (i,j = 1,2,3) to a single index μ (μ = 1, 2 . . . , 6).

ij		μ
11	→	1
22	→	2
33	→	3
23	→	4
31	→	5
12	→	6

The expressions for Christoffel's stiffnesses $\Gamma_{ik} = \Gamma_{ki}$, (i,k = 1,2,3), the piezoelectric stress constants Ξ_l (l = 1,2,3), and the permittivity ϵ_s of a general triclinic crystal as given in Eq. (4) follow from Table 2, e.g.,

$$\Gamma_{11} = c_{11}a_1^2 + c_{66}a_2^2 + c_{55}a_3^2 + 2c_{56}a_2a_3 + 2c_{51}a_3a_1 + c_{16}a_1a_2 . \qquad (6)$$

This scheme reduces considerably for quartz which belongs to the trigonal crystal class D_3. The stiffnesses c_{11}, c_{33}, c_{12}, c_{13}, c_{44}, c_{14} are finite. The following relationships hold: $c_{22} = c_{11}$, $c_{55} = c_{44}$, $c_{66} = \frac{1}{2}(c_{11} - c_{12})$, $c_{13} = c_{23}$ and $-c_{24} = c_{56} = c_{14}$. Further, $c_{15} = c_{16} = c_{25} = c_{26} = c_{35} = c_{36} = 0$. The piezoelectric constants are zero except $e_{11} = -e_{12} = -e_{26}$ and $e_{14} = -e_{25}$. For the dielectric constants $\epsilon_{22} = \epsilon_{11}$ and $\epsilon_{12} = \epsilon_{13} = \epsilon_{21} = \epsilon_{23} = \epsilon_{31} = \epsilon_{32} = 0$ hold. The scheme of the Christoffel stiffnesses Γ_{ik}, the piezoelectric stress constants Ξ_l, and the permittivity ϵ_s reduces for the trigonal crystal class D_3, which includes alpha-quartz, to the scheme shown in Table 3.

Considering the eigenfrequencies $\omega = 2\pi f$ of an infinitely extended plate vibrating in thickness modes, introducing $c = \frac{\rho\omega^2}{k^2}$, and taking into account the boundary conditions $\cos\frac{kt}{2} = 0$

having the solution $\frac{kt}{2} = \frac{n\pi}{2}$, the frequency in first approximation is

$$f_m^{(n)} = \frac{n}{2t}\sqrt{\frac{c_m{}^{D_s}}{\rho}}, \quad (m = 1, 2, 3) \tag{7}$$

where n is an odd integer. Correction terms, due to the piezoelectric effect and coupling with flexural modes, are omitted. The frequency $f_m^{(n)}$ for the nth overtone for mode m is determined by the eigenvalue $c_m{}^{D_s}$, the thickness of the plate t, and the density ρ. For practical purposes it is more convenient to consider the frequency constant $N = f \cdot t$, rather than the frequency, as the frequency f and the thickness t are the measured quantities. Generally, three solutions for the frequency f_m (m = 1, 2, 3) of the thickness vibrations and their overtones exist for each individual plate and in the following are designated as modes A, B, and C. Mode A is essentially the thickness-extensional mode while B and C are essentially thickness-shear modes. The frequencies for each plate always follow in the sequence $f_A > f_B > f_C$.

The equation for the temperature behavior of the frequency can be developed in the following power series

$$\frac{f - f_o}{f_o} = \frac{\Delta f}{f_o} = \sum_{n=1}^{3} Tf^{(n)} (T - T_o)^n , \tag{8}$$

where

$$Tf^{(n)} = \frac{1}{n!\, f_o}\left(\frac{\partial^n f}{\partial T^n}\right)_{T = T_o}, \tag{8a}$$

$Tf^{(n)}$ (n = 1, 2, 3) being designated a, b, and c respectively. T is the variable temperature and T_o the reference temperature.

The relationships between the first-order temperature coefficients of frequency $Tf^{(1)}$ and the first-order temperature coefficients of the stiffnesses $Tc_{\lambda\mu}{}^{(1)}$ are given by

$$2Tf^{(1)} = Tc^{(1)} - T\rho^{(1)} - 2Tt^{(1)} ; \tag{9}$$

the relations for the second-order temperature coefficients of frequency and stiffnesses are

$$\begin{aligned} 2\left[Tf^{(2)} - \tfrac{1}{2}(Tf^{(1)})^2\right] &= Tc^{(2)} - T\rho^{(2)} - 2Tt^{(2)} \\ &\quad -\tfrac{1}{2}\left[(Tc^{(1)})^2 - (T\rho^{(1)})^2 - 2(Tt^{(1)})^2\right] ; \end{aligned} \tag{10}$$

and for the third-order

$$\begin{aligned} 2\left[Tf^{(3)} - Tf^{(2)}Tf^{(1)} + 1/3(Tf^{(1)})^3\right] &= Tc^{(3)} - T\rho^{(3)} - 2Tt^{(3)} \\ &\quad - \left[Tc^{(2)}Tc^{(1)} - T\rho^{(2)}T\rho^{(1)} - 2Tt^{(2)}Tt^{(1)}\right] \\ &\quad + 1/3\left[(Tc^{(1)})^3 - (T\rho^{(1)})^3 - 2(Tt^{(1)})^3\right] , \end{aligned} \tag{11}$$

where $T\rho = -(2\alpha_x + \alpha_z)$ and α_x and α_z are the expansion coefficients. Tt is the temperature coefficient of the thickness of the plate. The essential term in these equations is the

temperature coefficient of the eigenvalue Tc determined by Eqs. (9) to (11); however, the terms resulting from the dimensions of the plate may be considered as corrections.

The elastic stiffnesses, the resulting elastic stress constants, and the first-order temperature coefficient of frequency have been calculated using a Burroughs 220 computer as a function of the orientation angles ϕ and θ for quartz in the interval

$$-90° \leq \theta \leq +90°, \qquad 0° \leq \phi \leq +30° .$$

The intervals of calculation were $\Delta\theta = 1°$ and $\Delta\phi = 1°$. The orientation of a plate is shown in Fig. 2. The direction cosines α_i (i = 1, 2, 3) defining the normal of the plate are given by

$$\alpha_1 = \sin \phi \cos \theta$$
$$\alpha_2 = \cos \phi \cos \theta$$
$$\alpha_3 = \sin \theta$$

when the Z-axis is chosen as the axis of the polar coordinate system and the angle ϕ is taken from the X-axis. Figure 3 shows the frequency constants N_m in kc·mm, the first-order temperature coefficient of frequency $Tf_m^{(1)}$ in $10^{-6}/°C$ and the piezoelectric stress constant e_m in 10^4 esu cm^{-2}, as plotted for modes A, B, and C corresponding to m = 1, 2, 3. The IRE notation [13] was used in these curves and throughout this report in describing a generally rotated plate as shown in Fig. 2 for the RT cut. By use of this notation, the Y cut is defined as $\phi = 0°$, $\theta = 0°$; an AT cut by $\phi = 0°$, $\theta = 35°$; the BT cut as $\phi = 0°$, $\theta = -49°$. The curves in Fig. 3 are plotted for the azimuth $\phi = 0°$, 6°, 12°, 18°, 24°, and 30°. From these curves three dimensional models have been made which are shown in Figs. 4-12.

METHODS AND EQUIPMENT FOR MEASUREMENTS

The measurements carried out included: 1) frequency measurements of the three modes of vibration at room temperature, and 2) frequency-temperature dependence of these three modes in an extended temperature range.

The frequency range for these three modes of vibration were approximately 4 to 8 Mc with $f_A > f_B > f_C$. Most of the crystals were excited in a CI Meter Type TS 330/TSM. A Heegner oscillator [12] was used sometimes to excite modes whose activity was too low for excitation in the CI Meter. The frequencies were determined with a Hewlett-Packard Counter, Model 524B.

The apparatus used for measuring the dependence of crystal frequency on temperature included: 1) a small aluminum cylinder having two cavities, with a canned crystal unit inserted in one of the cavities and a thermocouple in the other; 2) a calibrated precision bridge to determine the temperature; 3) a wire heating element which was wound around the aluminum cylinder; and 4) a well-insulated Dewar flask containing liquid nitrogen.

Measurements of the frequency-temperature behavior were conducted as follows: in order to obtain a very low initial temperature, the cylinder containing the crystal and a thermocouple were lowered into the flask containing liquid nitrogen. After the temperature within the two cavities approximated the temperature of liquid nitrogen, the liquid nitrogen was removed and the flask containing the cylinder was sealed to stabilize the temperature within the flask at the desired temperature. By means of the heating element described above and controlled by a variac, the temperature was gradually increased and frequency readings were taken at 5°C intervals over the temperature range of approximately −196° to +170°C.

DETERMINATION OF TEMPERATURE COEFFICIENTS OF STIFFNESSES AND COMPLIANCES OF ALPHA-QUARTZ

A large number of crystals vibrating in fundamental thickness modes and oriented at

different angles have been investigated with respect to their frequencies and temperature behavior at USAELRDL. In this report the IRE rotational symbol (yxwl)$\phi\theta$ is used to describe a generally rotated plate* [13]. Figure 2 shows schematically the orientation angles ϕ and θ for double-rotated quartz plates and, particularly, for the so-called RT cut having an orientation of $\phi = 15°$ and $\theta = -34°30'$. Most of the crystals were oriented at negative θ angles and various ϕ angles. The plates were square and had a length and width of approximately 0.5 inches, their edges were bevelled, and the blanks mounted in HC-6 holders. The plate thicknesses were adjusted so that in all cases, mode B was calibrated at the 5-mc frequency.** Some crystals oriented at positive angles of θ and at about $\phi = 20°$ were also investigated. The orientation $\phi = 20°$, $\theta = 34°20'$ is known as the IT cut† [14] when vibrating in the C mode. Several crystal plates with the orientation (xy)θ ($\theta = 0°$ to 60° at 10° intervals), (rotated X cuts) have been made at USAELRDL.

The values for the frequency constant N of the three fundamental modes A, B, and C were calculated using Eq. (4) and the recently published values for $c_{\lambda\mu}$ of quartz [9]. The elastic stiffnesses are given in Table 4 (mks units are used throughout this report), together with a new determination of the stiffnesses by Mindlin and Gazis [15]. Although the formulae on which the determination by Mindlin and Gazis is based do not include the piezoelectric and thermoelectric terms, they do account for mechanical coupling. The values derived by Mindlin and Gazis coincide most closely with the stiffnesses given by Bechmann [9] for both constant electric field and entropy and constant electric displacement and entropy.

The measured crystals had large electrode separations in order to obtain closer agreement between the measured and observed values.

The values for the temperature coefficients of the elastic stiffnesses $Tc_{\lambda\mu}$ are dependent on the accuracy of the measurements of the temperature coefficients of frequency Tf. It is well known that the temperature coefficients of frequency depend slightly on: state of the plate measured, e.g., the form of the plate (circular or square); the electrode size (ratio $\frac{\phi_e}{t}$ where ϕ_e is the diameter of the electrode and t is the thickness of the plate); the electrode separation (whether an air gap or plated blank is used); the order of overtone which changes the zero angles for the first-order zero temperature coefficients $Tf^{(1)}$; the bevelling of the plate which is necessary to avoid coupling with other modes which gives rise to errors; and the drive level of the resonator. Further, there are slight differences between the temperature coefficients of natural and synthetic quartz. Finally, the temperature coefficients of the stiffnesses are dependent on the approximation of the solution of the equations on which the determination is based.

Some previous investigations of the frequency-temperature behavior of double-rotated quartz crystals were conducted by Saunders and Hammond [16] based on the earlier calculation by Bechmann [5].

The frequency-temperature dependence of the quartz blanks mentioned was measured in the temperature range −196° to +170°C. All blanks used for frequency-temperature measurements were plated. The resulting frequency curve was developed in a power series with respect to the reference temperature $T_o = 25°C$ up to the third order. The first-, second-, and third-order temperature coefficients of frequency a, b, and c of a number of these crystals, which were used for the determination of the temperature coefficients of the stiffnesses, are also listed in Table 5.

*From this rotational symbol, the appropriate coordinate transformation can be easily derived [29].

**Most of these crystals were fabricated by McCoy Electronics Company, Mount Holly Springs, Pa.* The accuracy of the orientation angle was better than 10′ for the ϕ angle and better than 5′ for the θ angle, according to the manufacturer.

†These IT-cut crystals were furnished through the courtesy of Scientific Radio Products, Inc., Loveland, Colorado.

This table gives some of the measured and calculated values for the first-, second-, and third-order temperature coefficients a, b, and c, respectively, for modes A, B, and C. Crystals marked * indicate that the temperature coefficients of frequency of all three modes A, B, C have been measured. The calculation of the values for $Tc_{\lambda\mu}^{(n)}$ (n = 1, 2, 3) following from Eq. (4) by differentiation with respect to the temperature was made using a Burroughs Datatron 220 Computer.

The newly determined first-order temperature coefficients of the stiffnesses $Tc_{44}^{(1)}$, $Tc_{66}^{(1)}$, and $Tc_{14}^{(1)}$ are considered very accurate, as the values follow from rotated plates (yx1)θ. The behavior of the AT and BT cuts, their orientation angles for the zero temperature coefficient of frequency and the change of their temperature coefficients with respect to the angle θ are very well known [17] (see Table 6). In addition, the Y cut (yx) which has a first-order temperature coefficient of frequency of $92.5 \cdot 10^{-6}/°C$ has also been used.

When the angles for the first-order zero temperature coefficient of frequency are used, $\theta_o = 35°15'$ for the AT cut, and $-49°13'$ for the BT cut, and for the slope of the AT cut $\frac{\partial a}{\partial \theta} = -5.15 \cdot 10^{-6}/°C/°\theta$, the values in the first column of Table 6 are obtained. By exciting a high overtone [18] or using a large electrode gap, the zero angle θ_o for the AT cut is shifted to 35°22' and for the BT cut to $-49°40'$ and, assuming the same slope of $\frac{\partial a}{\partial \theta} = -5.15 \cdot 10^{-6}/°C/°\theta$ for the AT cut, values for $Tc_{44}^{(1)}$, $Tc_{66}^{(1)}$, and $Tc_{14}^{(1)}$ are obtained as shown on the right-hand side of Table 6. The difference between the two groups of values is also listed in Table 6 and this may be considered as the accuracy for determination of the temperature coefficients of the elastic stiffnesses $Tc_{44}^{(1)}$ $Tc_{66}^{(1)}$, and $Tc_{14}^{(1)}$.

$Tc_{11}^{(1)}$ follows from the X cut (xy) which has a value for the temperature coefficient of frequency of $Tf^{(1)} = -20.10^{-6}/°C$. $Tc_{33}^{(1)}$ was determined using the zero angles for the double-rotated plates (yxwl)$\pm\theta$ as listed in Table 5. Since the value for $Tc_{13}^{(1)}$ has a small influence on the temperature behavior, it therefore cannot be considered as accurate.

Table 7 lists the newly determined values for the first-order temperature coefficients of the elastic stiffnesses for alpha-quartz compared with some earlier determinations. The values listed in the columns headed "Koga et al., 1958" of Tables 7, 8, and 9 are calculated from the expressions

$$\hat{c} = \frac{c}{4}, \quad \frac{\partial \hat{c}}{\partial T}, \quad \frac{1}{2}\frac{\partial^2 \hat{c}}{\partial T^2}, \text{ and } \frac{1}{6}\frac{\partial^3 \hat{c}}{\partial T^3},$$

given in their paper. It should be mentioned that the values for the temperature coefficients of the stiffnesses given by Atanasoff and Hart [20] contain an error as they assumed that for quartz $c_{56} \neq c_{14}$ and obtained the erroneous values $Tc_{14}^{(1)} = 107 \cdot 10^{-6}$ and $Tc_{56}^{(1)} = 78 \cdot 10^{-6}$. The reason for this discrepancy is that the piezoelectric effect was not taken into account. The values for the stiffnesses given by Atanasoff and Hart [20] have been corrected by Lawson [21] resulting in $c_{56} = c_{14}$ when considering the piezoelectric effect. However, he did not correct the values for the temperature coefficients of the stiffnesses. Their value for $Tc_{56}^{(1)}$ is omitted in Table 7.

The second- and third-order temperature coefficients of the elastic stiffnesses have been determined using the experimental values for the AT and BT cuts [17] and the newly observed values for the frequency dependence of the double-rotated plates. Table 8 lists the second-order temperature coefficients of the elastic stiffnesses and Table 9 the third-order temperature coefficients of the elastic stiffnesses. Both tables contain corresponding values from earlier determinations by Mason [19], [22] and Koga, et al. [24].

The compliances $s_{\lambda\mu}$ and their first-, second-, and third-order temperature coefficients $Ts_{\lambda\mu}$ were calculated from the values of the stiffnesses $c_{\lambda\mu}$ and their temperature coefficients $Tc_{\lambda\mu}$ using the well-known relationships between the stiffnesses and compliances

$$\Sigma\, s_{\lambda\tau}\, c_{\mu\tau} = \delta_{\lambda\mu} = \begin{cases} 1, \lambda = \mu \\ 0, \lambda \neq \mu \end{cases},$$

from which the relationship

$$\sum_{\lambda=1}^{6} \sum_{p=o}^{n} c_{\lambda\mu}\, s_{\lambda\nu} \left(Tc_{\lambda\mu}^{(n-p)} + Ts_{\lambda\nu}^{(p)}\right) = \begin{cases} 0 & n > 0 \\ \delta_{\mu\nu} & n = 0 \end{cases}$$

follows.

The values for the compliances $s_{\lambda\mu}$ are given in Table 10. The first-, second-, and third-order temperature coefficients of the elastic compliances $Ts_{\lambda\mu}$, which have been calculated from the temperature coefficients of the stiffnesses as given in Tables 7, 8, and 9, are listed in Tables 11, 12, and 13. For comparison, some values from earlier determinations are shown in these tables. All new values for the temperature coefficients of the stiffnesses and compliances refer to 25°C. The values for the stiffnesses and compliances, as determined by Bechmann [9] and given in Tables 4 and 10, refer to 20°C. It should be mentioned that all "new" values for the temperature coefficients of the stiffnesses $Tc_{\lambda\mu}^{(n)}$, obtained from measurements of thickness modes, and those of the compliances calculated from the stiffnesses are values at normal constant displacement D_s. The differences between $Tc_{\lambda\mu}^{(n)E}$, the isagric values, and $Tc_{\lambda\mu}^{(n)D_s}$ are within the limits of accuracy of measurements of the temperature dependence of these plates.

APPLICATIONS TO DOUBLE-ROTATED QUARTZ PLATES

Since the temperature coefficients of the stiffnesses are known, the temperature behavior of thickness modes of any orientation can be calculated from these values. Altitude charts for the first-, second-, and third-order temperature coefficients of frequency for the C mode are given in Figs. 13, 14, and 15 respectively, and it can be seen from Fig. 13 that there is a continuous series of orientations for the thickness mode C of plates having a first-order zero temperature coefficient of frequency for all values of ϕ (0° to 30°) at both positive and negative angles of θ adjoining the AT cut at $\phi = 0°$ and $\theta = 35°$. Similar charts showing the distribution of the temperature coefficient of frequency for mode B are given in Figs. 16, 17, and 18. At negative angles of θ, mode B exhibits a continuous series of first-order zero temperature coefficients in the range $\phi = 0°$ to 14° at two angles of θ, both on the negative side adjoining the BT cut at $\phi = 0°$ and $\theta = -49°$. The curves for the first-order zero temperature coefficient of frequency for modes B and C as seen in Figs. 13 and 16 are identical with the curves shown in Figs. 19 and 20.

Fig. 19 shows the calculated locus of the first-order zero temperature coefficients of frequency for modes B and C in a rectangular coordinate system compared with some measured results. The values for the mode C are indicated by X, those for the mode B by Θ. The agreement between the calculated and measured zero angles is better than 3 percent and, taking into account the uncertainties mentioned above, the agreement is considered very satisfactory.

Figure 20 represents the locus of the first-order zero temperature coefficients of frequency in a polar coordinate system illustrating the threefold symmetry of quartz showing that, at an angle $\phi + n\,120°$ ($n = 0, 1, 2$), the elastic properties of quartz are identical with those of the angle ϕ. Mode A vibrating extensionally has a negative temperature coefficient of frequency for all orientations.

Figure 21 shows the frequency constants N of the modes B and C when $Tf^{(1)} = 0$. Figure 22 shows the second- and third-order temperature coefficients of frequency for the thickness mode C when $Tf^{(1)} = 0$ for negative angles of θ.

For mode C the second-order temperature coefficient of frequency is always negative and reaches a minimum value of about $-6.5 \cdot 10^{-9}/(°C)^2$ at $\phi = 15°$. The third-order temperature coefficient changes its sign as a function of the angle ϕ at negative θ angles but the zero angles for the first- and third-order temperature coefficients of frequency do not coincide.

At the angle $\phi = 15°$, $\theta = -34°30'$, mode C shows a first-order zero temperature coefficient of frequency, a second-order temperature coefficient of frequency of $-6.5 \cdot 10^{-9}/(°C)^2$, and a third-order temperature coefficient of $-2 \cdot 10^{-12}/(°C)^3$ (see Table 5). This cut has been proposed for practical applications and designated the RT cut [26]. Other double-rotated cuts may be useful for application at low temperatures. For example, the C mode of the cut $\phi = 10°$, $\theta = -33°$ shows a very small frequency change with temperature in the range $-160°$ to 0°C, as the three terms for the temperature behavior balance (Table 5). An experimental frequency-temperature curve is shown in Fig. 23. The disadvantage of the double-rotated cuts is that all three modes are excitable, modes B and C being rather close together. The separation between these modes is in the order of 7 percent for the RT cut and in the order of 10 percent for the IT cut. The B mode displays a large negative second-order temperature coefficient of frequency for all zero temperature coefficient cuts, including the BT cut, which for practical purposes makes mode B less useful than mode C.

APPLICATIONS TO AT- AND BT-CUT QUARTZ CRYSTALS IN AN EXTENDED TEMPERATURE RANGE

The frequency and temperature behavior of the plates (yxl)θ, the so-called rotated Y-plates, is shown in Figs. 24-27. Figure 24 gives values of the rotated stiffnesses $c_{66}' = c_{44} \sin^2\theta + c_{66}\cos^2\theta + 2c_{14}\cos\theta\sin\theta$, as a function of the angle θ in the range $\theta = -90°$ to $+90°$, derived from the values c_{66}, c_{44}, and c_{14} as given in Table 4 [9]. Figure 25 shows the frequency constant N in the same range. Figures 26 and 27 give the first-, second-, and third-order temperature coefficients respectively, calculated from the values given in Tables 7, 8, and 9, using Eqs.(9) through (11). The AT cut is described by the angle $\theta = 35°15'$, the BT cut by the angle $\theta = -49°13'$. The AT cut belongs to mode C while the BT cut belongs to mode B. The jump from mode B to mode C occurs because there is one orientation for which the secular Eq. (4) becomes degenerate, having two roots of the same value. It should be recognized that it results in a discontinuity in the other constants derived from the stiffnesses, e.g., the temperature coefficients.

For the family of cuts (yxl)θ ($\phi = 0°$) the secular Eq. (4) becomes

$$\begin{vmatrix} (\Gamma_{11}-c) & 0 & 0 \\ 0 & (\Gamma_{22}-c) & \Gamma_{23} \\ 0 & \Gamma_{23} & (\Gamma_{33}-c) \end{vmatrix} = 0 .$$

One root is $c = \Gamma_{11}$. This corresponds to mode C. The other roots are

$$c_{A,B} = \frac{\Gamma_{22} + \Gamma_{33}}{2} \pm \frac{1}{2}\sqrt{\Gamma_{22}^2 + \Gamma_{33}^2 + 4\Gamma_{23}^2 - 2\Gamma_{22}\Gamma_{33}} ,$$

where the minus sign corresponds to the smaller root (mode B). Modes B and C have a common eigenvalue at the value of θ for which

$$\Gamma_{11}^2 - \Gamma_{11}\Gamma_{22} - \Gamma_{11}\Gamma_{33} + \Gamma_{22}\Gamma_{33} - \Gamma_{23}^2 = 0 .$$

Substitution of the values for the $c_{\lambda\mu}$ and the direction cosines leads to a cubic equation with a single real root corresponding to an orientation of

$$\theta = -23°50' .$$

Physically, the mode of vibration designated B for the angle θ on one side of this value becomes mode C on the other side and vice versa. The difficulty arises because the modes are defined in such a way that mode A has the highest stiffness and mode C the lowest, where, for the region under consideration, modes B and C actually cross and mode B becomes, for positive angles, the lowest mode. For $\phi \neq 0°$ there is no ambiguity as the solutions of Eq. (4) are all distinct. The discontinuity is not apparent in the curves shown in Figs. 24 through 27.

Considering the AT and BT cuts, a maximum and minimum for the frequency-temperature curve exist as a function of the orientation angle θ following from Eqs. (8) and (8a). The behavior of the maximum and minimum can be represented by a parabola having the parabola constant b_μ (μ = max or min) for the angle considered. The calculated and observed values for T_{max} and T_{min} vs. the orientation angle θ for the AT cut in the range $\theta = 35°$ to $40°$ and for the BT cut in the range $\theta = -46°$ to $-52°$ are given in Figs. 29 and 30 respectively [17].

The inflection temperature T_i is defined by

$$\frac{\partial Tf}{\partial T} = \frac{\partial^2 f}{\partial T^2} = 0 .$$

The inflection temperature for the zero-temperature cuts depends on the angle of rotation. The inflection temperature for the AT cut is about 25°C. The inflection temperature for mode C increases when the angle ϕ on the positive side of the angle θ is increased. Figure 28* shows the inflection temperature obtained from cuts made of natural quartz when the angle ϕ is increased from 0° to 30°.

For the IT-cut ($\phi = 20°$) the inflection temperature is about 70°C. The inflection temperature T_i is given by

$$T_i - T_o = -\frac{b_o}{3\,c_o} .$$

The inflection temperatures for the AT and BT cuts, as function of the angle θ, are also shown in Figs. 29 and 30. The temperature of liquid nitrogen N is −196°C; for liquid hydrogen H is −253°C; and for liquid helium He is −269°C as indicated in these figures. The calculated values for the parabola constant b_μ as a function of the orientation angle θ, corresponding to T_{max} and T_{min} as shown in Fig. 29, are presented in Fig. 31 for the AT cut, the values corresponding to Fig. 30 are shown in Fig. 32 for the BT cut.

APPLICATIONS TO QUARTZ CUTS VIBRATING IN CONTOUR MODES

The frequencies and their temperature behavior are determined for contour modes of plates and extensional modes of bars by the elastic compliances and their temperature coefficients. Two cuts of interest exist for square plates which have one side parallel to and are rotated around the X axis at angle θ, i.e., cuts of the orientation (yxl)θ, where the first-order temperature coefficient of frequency is zero, the CT cut with an orientation angle of approximately

*Figure 28 also shows the second- and third-order temperature coefficients of frequency when $Tf^{(1)} = 0$ as a function of ϕ. At positive angles of θ, the AT cut is obtained for $\phi = 0°$, and the IT cut obtained for $\phi = 20°$.

φ = 38°, and the DT cut with an angle of approximately φ = −51°. There are three types of these cuts:

1. Square plates with one side parallel to the X axis, $Y_{\theta 0^\circ} \equiv (yxl)\varphi$.

2. Square plates with the X axis diagonal, $Y_{\theta 45^\circ} \equiv (yxlt)\theta 45^\circ$. Contour-extensional mode I of square plates [27].

3. Circular plates $Y_{\theta 0}$.

The frequencies for these three modes are given by the equation

$$f = \frac{F}{2h}\sqrt{\frac{2}{\rho s'_{55}}}, \tag{12}$$

where h is the length l of square plates or the diameter ϕ of circular plates. The expressions for F for plates $Y_{\theta 0^\circ}$ and plates $Y_{\theta 45^\circ}$ where F = 1 can be found in [27], while for circular plates $Y_{\theta 0}$ no solution has been derived. However, the value obtained experimentally on circular quartz plates is F = 1.0551 ± 1 percent.

Figure 33 gives the values for the rotated compliances $s'_{55} = s'_{44} = s_{44}\cos^2\varphi + s_{66}\sin^2\varphi - 4s_{14}\cos\varphi\sin\varphi$ as a function of the angle φ in the range φ = −90° to +90° as derived from the new values s_{66}, s_{44}, and s_{14} presented in Table 10. Figure 34 shows the frequency constants N in the same range mentioned for the three cases $Y_{\theta 0^\circ}$, $Y_{\theta 45^\circ}$, and $Y_{\theta 0}$. Figure 35 gives the first-, second-, and third-order temperature coefficients of frequency calculated from the new values given in Tables 11, 12, and 13.

It may be mentioned that the two zero angles of the temperature coefficient of frequency, first-order, are slightly dependent (in the order of ±1°) on the configuration, the thickness of the plating, and the mounting of the plate. Table 14 gives the observed and calculated values of the frequency constants and the temperature coefficients of frequency for the CT cut. Table 15 presents the same information for the DT cut. The experimental values given in Tables 14 and 15 for the zero angles are obtained from earlier investigations where the electrodes were sprayed and baked [28]. According to Eq. (12), the values for the temperature coefficients of frequency of the three modes are equal, as F is a constant determined by boundary conditions and therefore all three modes should have identical angles for their first-order zero temperature coefficients of frequency.

The calculated maximum and minimum for the frequency-temperature curve as a function of the orientation angle φ are shown in Fig. 36 for the CT cut. In this curve the experimental values for T_{min}, assumed to be linear in [28], are also presented by dashed lines. The theoretical and experimental values are in very good agreement. The calculated values for the parabola constant b_μ for this cut as a function of the orientation angle φ, corresponding to Fig. 36, are exhibited in Fig. 37. Similarly, the calculated temperature of the zero temperature coefficient of frequency vs the orientation angle φ for the DT cut is shown in Fig. 38. The calculated values for the parabola constant b_μ for the DT cut as a function of the orientation φ, corresponding to the zero coefficient temperature curve of Fig. 38, are shown in Fig. 39.

REFERENCES

1. G. Green, Trans. Cambridge Phil. Soc., vol. 7; 1839.

2. E. B. Christoffel, "Ueber die Fortpflanzung von Stössen durch elastische feste Körper," *Ann. di Matematica Milano*, vol. 8, pp. 193-243; 1877.

3. I. Koga, "Thickness Vibrations of Piezoelectric Oscillating Crystals," *Physics*, vol. 3, pp. 70-80; August 1932.

4. R. D. Mindlin, "Thickness-Shear and Flexural Vibrations of Crystal Plates," J. Appl. Phys., vol. 22, pp. 316-323; March 1951.

5. R. Bechmann, "Über die Temperatur-Koeffizienten der Eigenschwingungen piezoelektrischer Quarzplatten und Stäbe," *Hochfrequenz. und Elektroak.*, vol. 44, pp. 145-160; November 1934.

6. J. Laval, "Élasticité des Cristaux," *Compt. rend. Acad. Sci., (Paris)*, vol. 232, pp. 1947-1948; 21 May 1951.
"Sur l'élasticité du milieu cristallin, L'état solide," Congres Solvay, Stoops, Bruxelles, pp. 273-313; 1952.

7. H. Jaffe and C. S. Smith, "Elastic Constants of Ammonium Dihydrogen Phosphate and the Laval Theory of Crystal Elasticity," *Phys. Rev.*, vol. 121, pp. 1604-1607; 15 March 1961.

8. V. G. Zubov and M. M. Firsova, "On the Measurement and New Computation of the Dynamic Elastic Constants of Quartz," *Kristallografiya*, vol. 1, pp. 546-556; May 1956. (In Russian.)

9. R. Bechmann, "Elastic and Piezoelectric Constants of Alpha-Quartz," *Phys. Rev.*, vol. 110, pp. 1060-1061; 1 June 1958.

10. R. D. Mindlin, Letter-type Report, U.S. Signal Corps Contract DA36-039 SC-87414; 29 March 1961. (Unpublished.)

11. W. G. Cady, "Piezoelectricity," McGraw-Hill Book Co., New York, N.Y., London, England; 1946.
J. A. Schouten, "Tensor Analysis for Physicists," Clarendon Press, Oxford, England; 1951.
J. P. Musgrave, "The Propagation of Elastic Waves in Crystals and Other Anisotropic Media," *Repts. Progr. Phys.*, vol. 22, pp. 74-96; 1959, Physical Soc., London, England; 1959.

12. K. Heegner, "Gekoppelte selbsterregte elektrische Kreise und Kristalloszillatoren," *Elektr. Nachrichtentech*, vol. 15, pp. 359-368; December 1938.

13. "IRE Standards on Piezoelectric Crystals, 1949," Proc. IRE, vol. 37, pp. 1378-1395; December 1949.

14. W. R. Ives, "A New Zero Temperature Coefficient Quartz Oscillator Plate," M.S. thesis, Colorado A & M College, Ft. Collins, Colorado; March 1951.

15. R. D. Mindlin and D. C. Gazis, "Strong Resonances of Rectangular AT-cut Quartz Plates," Report, U.S. Signal Corps Contract DA36-039 SC-87414; July 1961.

16. J. L. Saunders and D. L. Hammond, "Design and Development of Extended Temperature Range CR-(XA-21)/U Crystal Units," Wright Air Dev. Ctr., Wright Patterson AF Base, Ohio, Final Rept. AF 33(600)33889, 16 September 1956-26 June 1959.

17. R. Bechmann, "Frequency-Temperature-Angle Characteristics of AT- and BT-Type Quartz Oscillators in an Extended Temperature Range," Proc. IRE, vol. 48, p. 1494; August 1960.

18. R. Bechmann, "Influence of the Order of Overtone on the Temperature Coefficient of Frequency of AT-Type Quartz Resonators," Proc. IRE, vol. 43, pp. 1667-1668; November 1955.

19. W. P. Mason, "Low Temperature Coefficient Quartz Crystals," *Bell System Tech. J.*, vol. 19, pp. 74-93; January 1940.

20. J. V. Atanasoff and P. J. Hart, "Dynamical Determination of the Elastic Constants and their Temperature Coefficients for Quartz," *Phys. Rev.*, Vol. 59, pp. 85-96; 1 January 1941.

21. A. W. Lawson, "Comment on the Elastic Constants of Alpha-Quartz," *Phys. Rev.*, vol. 59, pp. 838-839; May 1941.

22. W. P. Mason, "Zero Temperature Coefficient Quartz Crystals for Very High Temperatures," *Bell System Tech. J.*, vol. 30, pp. 366-380; April 1951.

23. R. Bechmann and S. Ayers, "The Shear Elastic Constants of Quartz and their Behaviour with Temperature," Post Office Res. Sta., Engrg. Dept., London, Dollis Hill, England, Res. Rept. No. 13524; December 1951.

24. I. Koga, M. Aruga and Y. Yoshinaka, "Theory of Plane Elastic Waves in a Piezoelectric Crystalline Medium and Determination of Elastic and Piezoelectric Constants of Quartz," *Phys. Rev.*, vol. 109, pp. 1467-1473; March 1958.

25. E. Giebe and E. Blechschmidt, "Über Drillungsschwingungen von Quarzstäben und ihre Benützung für Frequenznormale," *Hochfrequenz. und Elektroak.*, vol. 56, pp. 65-87; March 1940.

26. R. Bechmann, "Thickness-Shear Mode Quartz Cut with Small Second- and Third-Order Temperature Coefficients of Frequency (RT Cut)," Proc. IRE, vol. 49, p. 1454; September 1961. USASRDL Docket No. 12831 (19 August 1960).

27. "IRE Standards on Piezoelectric Crystals: Determination of the Elastic, Piezoelectric, and Dielectric Constants -- The Electromechanical Coupling Factor, 1958," Proc. IRE, vol. 46, pp. 764-778; April 1958.

28. R. Bechmann, "Quarzoszillatoren und Resonatoren im Bereich von 50 bis 300 kHz.," *Hochfrequenz. und Elektroak.*, vol. 61, pp. 1-12; January 1943.

29. R. Bechmann, "Zur Festlegung der Orientierung von Kristallplatten und die zugehorige Koordinatentransformation," Archiv d. elektr. Übertragung, 7, 305-307; 1953.

TABLE 1

FREQUENCY TEMPERATURE BEHAVIOR OF AT, BT, CT, DT, AND RT CUTS

CUT	ANGLE ϕ	ANGLE θ	a $10^{-6}/°C$	b $10^{-9}/(°C)^2$	c $10^{-12}/(°C)^3$
AT	0°	35°15′	0	0.4	109.5
AT Opt. Angle	0°	35°20′	−0.40	−0.02	109.3
BT	0°	−49°12′	0	−40	−128
CT	0°	36°20′	0	−58	−151
DT	0°	−50°40′	0	−17	52
RT	15°	−34°30′	0	−6	−2

TABLE 2

GENERAL EXPRESSIONS FOR THE CHRISTOFFEL STIFFNESSES Γ_{ik}, THE PIEZOELECTRIC STRESS CONSTANTS Ξ_i, AND THE DIELECTRIC PERMITTIVITY ϵ_s

	α_1^2	α_2^2	α_3^2	$\alpha_2\alpha_3$	$\alpha_3\alpha_1$	$\alpha_1\alpha_2$
Γ_{11}	c_{11}	c_{66}	c_{55}	$2c_{65}$	$2c_{51}$	$2c_{16}$
Γ_{22}	c_{66}	c_{22}	c_{44}	$2c_{24}$	$2c_{46}$	$2c_{62}$
Γ_{33}	c_{55}	c_{44}	c_{33}	$2c_{43}$	$2c_{35}$	$2c_{54}$
Γ_{23}	c_{65}	c_{24}	c_{43}	$c_{23}+c_{44}$	$c_{45}+c_{63}$	$c_{64}+c_{25}$
Γ_{13}	c_{51}	c_{46}	c_{35}	$c_{45}+c_{36}$	$c_{31}+c_{55}$	$c_{56}+c_{41}$
Γ_{12}	c_{16}	c_{62}	c_{54}	$c_{64}+c_{52}$	$c_{56}+c_{14}$	$c_{12}+c_{66}$
Ξ_1	e_{11}	e_{26}	e_{35}	$e_{25}+e_{36}$	$e_{31}+e_{15}$	$e_{16}+e_{21}$
Ξ_2	e_{16}	e_{22}	e_{34}	$e_{24}+e_{32}$	$e_{36}+e_{14}$	$e_{12}+e_{26}$
Ξ_3	e_{15}	e_{24}	e_{33}	$e_{23}+e_{34}$	$e_{35}+e_{13}$	$e_{14}+e_{25}$
ϵ_s	ϵ_{11}	ϵ_{22}	ϵ_{33}	$2\epsilon_{23}$	$2\epsilon_{13}$	$2\epsilon_{12}$

TABLE 3

EXPRESSIONS FOR THE CHRISTOFFEL STIFFNESSES Γ_{ik}, THE PIEZOELECTRIC STRESS CONSTANTS Ξ_i AND THE DIELECTRIC PERMITTIVITY ϵ_s FOR THE TRIGONAL CRYSTAL CLASS D_3, e.g., ALPHA-QUARTZ

	a_1^2	a_2^2	a_3^2	a_2a_3	a_3a_1	a_1a_2
Γ_{11}	c_{11}	c_{66}	c_{44}	$2c_{14}$	0	0
Γ_{22}	c_{66}	c_{11}	c_{44}	$-2c_{14}$	0	0
Γ_{33}	c_{44}	c_{44}	c_{33}	0	0	0
Γ_{23}	c_{14}	$-c_{14}$	0	$c_{13}+c_{44}$	0	0
Γ_{31}	0	0	0	0	$c_{13}+c_{44}$	$2c_{14}$
Γ_{12}	0	0	0	0	$2c_{14}$	$c_{12}+c_{66}$
Ξ_1	e_{11}	$-e_{11}$	0	$-c_{14}$	0	0
Ξ_2	0	0	0	0	e_{14}	$-2e_{11}$
Ξ_3	0	0	0	0	0	0
ϵ_3	ϵ_{11}	ϵ_{11}	ϵ_{33}	0	0	0

TABLE 4

ELASTIC STIFFNESSES $c_{\lambda\mu}$ IN 10^9 Nm^{-2} FOR ALPHA-QUARTZ AT 20°C

$\lambda\mu$	STIFFNESSES OF QUARTZ Bechmann (9)		STIFFNESSES OF QUARTZ Mindlin and Gazis (15)
	$c_{\lambda\mu}^{E\sigma}$	$c_{\lambda\mu}^{D\sigma}$	$c_{\lambda\mu}$
11	86.74	87.49	86.75
33	107.2	107.2	107.2
12	6.99	6.23	5.95
13	11.91	11.91	11.91
44	57.94	57.98	57.8
66	39.88	40.63	40.4
14	−17.91	−18.09	−17.8

TABLE 5

MEASURED AND CALCULATED FIRST-, SECOND- AND THIRD-ORDER TEMPERATURE COEFFICIENTS OF FREQUENCY a, b, c FOR THE THICKNESS MODES A, B, AND C OF SOME SELECTED QUARTZ PLATES

TEMPERATURE COEFFICIENTS, MODE A

	ORIENTATION		$T_{(MAX)}$	OBSERVED VALUES			CALCULATED VALUES		
	ϕ	θ	°C	$a \times 10^{-6}/°C$	$b \times 10^{-9}/(°C)^2$	$c \times 10^{-12}/(°C)^3$	$a \times 10^{-6}/°C$	$b \times 10^{-9}/(°C)^2$	$c \times 10^{-12}/(°C)^3$
	10°	−28°	>−160°	−76.5			−78.4	−111.0	−62.2
	10°	−38°	>−160°	−94.7			−85.6	−128.0	−94.9
*	12°30′	−34°	>−160°	−81.0	−129.0	−58.9	−78.6	−118.0	−86.5
*	15°	−33°	>−160°	−75.0	−110.0	+82.5	−72.0	−111.0	−90.0
*	15°	−35°	>−160°	−72.0	−88.3	+90.3	−73.0	−114.0	−94.0
*	20°	−36°	>−160°	−70.0	−93.2	+266.0	−66.6	−110.0	−106.0
X CUT	30°	0°	>−160°	−20.5	−53.2	−36.6	−20.5	−52.0	−36.9
*	30°	±10°	>−160°	−29.3	−67.0	−58.3	−29.8	−64.3	−68.6
*	30°	±20°	>−160°	−42.0	−86.0	−92.7	−41.4	−80.7	−95.4
*	30°	±30°	>−160°	−54.8	−105.0	−119.0	−51.7	−96.0	−113.0
				TEMPERATURE COEFFICIENTS, MODE B					
	0°	−40°	>+160°	+20.7	−15.2	−112.6	+19.9	−21.3	−116.0
	0°	−45°	+125°	+10.7	−32.0	−128.0	+9.1	−31.6	−123.0
BT CUT	0°	−49°13′	+25°	0.0	−40.0	−128.0	0.0	−39.6	−128.0
	0°	−50°	−10°	−1.3	−44.4	−130.0	−1.3	−42.0	−129.0
	0°	−55°	>−160°	−13.7	−71.7	−171.9	−12.3	−51.4	−133.0
	0°	−60°	>−160°	−24.5	−75.0	−134.8	−22.8	−60.9	−136.0

*Denotes cuts for which complete data on A, B, and C Modes are available.

TABLE 5 (Continued)

TEMPERATURE COEFFICIENTS, MODE B (Continued)

	ORIENTATION		$T_{(MAX)}$	OBSERVED VALUES			CALCULATED VALUES		
	ϕ	θ	°C	$a \times 10^{-6}$/°C	$b \times 10^{-9}/(°C)^2$	$c \times 10^{-12}/(°C)^3$	$a \times 10^{-6}$/°C	$b \times 10^{-9}/(°C)^2$	$c \times 10^{-12}/(°C)^3$
	5°	−43°	> +160°	+35.7	−9.5	+195.8	+9.2	−33.7	−123.0
	5°	−45°	+50°	+3.2	−44.6	−169.6	+5.4	−36.5	−125.0
	5°	−47°	+10°	−0.9	−41.1	−118.0	+1.7	−39.8	−127.0
	5°	−48°	+10°	−1.5	−43.1	−122.6	−0.17	−41.5	−128.0
	5°	−49°	−40°	−5.1	−53.5	−156.0	−2.1	−43.1	−129.0
	10°	−24°	>160°	+18.2	−34.0	−124.0	−0.10	−10.2	−39.2
	10°	−26°	>160°	+16.6	−43.0	−148.0	+6.5	+21.5	+13.2
	10°	−30°	+140°	+10.0	−27.0	−103.0	+16.0	−33.9	−106.0
	10°	−32°	+110°	+9.8	−33.8	−197.3	+13.6	−36.4	−112.0
	10°	−33°	+85°	+7.5	−39.9	−168.5	+12.5	−37.3	−114.0
	10°	−34°	+80°	+5.7	−41.5	−141.7	+11.4	−38.0	−115.0
	10°	−35°	+75°	+5.4	−42.9	−50.8	+10.3	−38.7	−117.0
	10°	−38°	+40°	+1.1	−39.0	−91.3	+6.8	−40.7	−120.0
	10°	−40°	−5°	−2.4	−41.9	−115.4	+4.3	−42.2	−122.0
	10°	−42°	−60°	−5.9	−47.5	−81.2	+1.9	−43.6	−123.0
	12°30′	−30°	+70°	+2.22	−27.2	−74.95	+8.4	−39.0	−100.7
	12°30′	−31°	+60°	+2.5	−32.3	−89.2	+7.6	−40.8	−104.0
	12°30′	−32°	+50°	+2.1	−33.8	−88.3	+7.9	−41.9	−107.0
	12°30′	−33°	+45°	+1.8	−34.9	−90.5	+6.0	−42.7	−108.0
	12°30′	−33°30′	0°	−1.3	−43.4	−118.5	+5.6	−43.1	−109.0
*	12°30′	−34°	0°	−2.1	−44.7	−75.6	+5.1	−43.5	−110.0

*Denotes cuts for which complete data on A, B, and C Modes are available.

TABLE 5 (Continued)

TEMPERATURE COEFFICIENTS, MODE B (Continued)

	ORIENTATION		$T_{(MAX)}$	OBSERVED VALUES			CALCULATED VALUES		
	ϕ	θ	°C	a × 10^{-6}/°C	b × 10^{-9}/(°C)^2	c × 10^{-12}/(°C)^3	a × 10^{-6}/°C	b × 10^{-9}/(°C)^2	c × 10^{-12}/(°C)^3
	15°	−31°	>−160°	−11.2	−21.7	−26.4	+0.75	−44.4	−98.7
	15°	−32°	>−160°	−8.8	−39.1	−88.8	+0.64	−45.6	−101.0
*	15°	−33°	>−160°	−7.5	−33.2	−64.8	+0.23	−46.5	−103.0
	15°	−34°	>−160°	−7.3	−37.4	−80.3	−0.37	−47.1	−104.0
	15°	−34°30′	>−160°	−7.4	−28.1	−39.7	−0.67	−47.4	−105.0
*	15°	−35°	>−160°	−7.45	−33.5	−58.8	−0.98	−47.7	−106.0
	15°	−35°30′	>−160°	−8.5	−39.3	−75.1	−1.34	−48.0	−107.0
*	20°	−36°	>−160°	−19.9	−30.5	+20.3	−9.7	−51.4	−95.2
*	30°	+10°	>−160°	−14.9	−42.5	−86.0	−14.7	−33.7	−73.6
*	30°	+20°	>−160°	−9.3	−21.8	−34.4	−9.3	−20.4	−37.6
*	30°	+30°	>−160°	−19.1	−24.5	−28.9	−18.2	−27.0	−33.9
	30°	+40°	>−160°	−22.2	−39.3	−46.5	−19.5	−50.9	−77.9
	30°	+50°	>−160°	−28.0	−43.9	−33.1	−24.2	−58.8	−99.2

TEMPERATURE COEFFICIENTS, MODE C

	0°	+50°	>−160°	−71.5	−82.6		−66.2	−67.8	+46.8
	0°	+40°	>−160°	−17.5	−16.0		−24.0	−22.4	+95.8
AT CUT	0°	+35°30′	25°	0.0	+0.40	+109.5	0.0	−0.4	+109.0
	0°	+10°	>+160°	+96.3			+90.5	+64.1	+53.4
Y CUT	0°	0°	>+160°	+97.1			+92.5	+57.5	+5.8
	0°	−10°	>+160°	+89.7			+81.2	+41.4	−36.8
	0°	−20°	>+160°	+65.8			+62.9	+21.1	−71.2

*Denotes cuts for which complete data on A, B, and C Modes are available.

TABLE 5 (Continued)

TEMPERATURE COEFFICIENTS, MODE C (Continued)

	ORIENTATION		$T_{(MAX)}$	OBSERVED VALUES			CALCULATED VALUES		
	ϕ	θ	°C	$a \times 10^{-6}/°C$	$b \times 10^{-9}/(°C)^2$	$c \times 10^{-12}/(°C)^3$	$a \times 10^{-6}/°C$	$b \times 10^{-9}/(°C)^2$	$c \times 10^{-12}/(°C)^3$
	5°	−24°	> +160°	+33.1	−58.5	−334.0	+27.8	−67.8	−253
	5°	−25°	+15°	−0.57	−82.2	−60.0	−3.2	−63.4	+12.0
	5°	−26°	> −160°	−6.0	−28.3	−66.2	−6.4	−28.4	−79.2
	5°	−28°	> −160°	−1.7	−16.4	−51.6	−3.0	−20.8	−58.6
	10°	−28°	+70°	+3.3	−40.0	−48.0	−2.4	−23.0	−57.6
	10°	−30°	+55°	+0.8	−11.5	−30.0	−1.1	−16.0	−40.3
	10°	−31°	+40°	+0.61	−10.7	−34.2	−1.2	−14.4	−34.4
	10°	−32°	+30°	+0.26	−9.8	−32.4	−1.5	−13.0	−29.3
	√10°	−33°	−40°	−0.87	−7.81	−21.5	−1.9	−12.5	−25.0
	10°	−34°	> −160°	−1.7	−6.3	−10.5	−2.7	−12.0	−20.7
	10°	−35°	> −160°	−0.2	−5.8	−7.2	−3.5	−11.8	−16.8
	10°	−36°	> −160°	−3.4	−6.0	−5.0	−4.6	−11.9	−13.3
	10°	−38°	> −160°	−5.5	−5.9	+1.7	−7.2	−12.6	−6.9
	10°	−40°	> −160°	−8.8	−6.5	+13.5	−10.4	−14.3	−1.5
	10°	−48°	> −160°	−27.4	−19.6	+40.0	−29.0	−29.0	+8.8
	12°30′	−25°	+140°	+12.1	−35.6	−94.0	+13.5	−46.6	−110.0
	12°30′	−26°	+130°	+12.3	−37.9	−115.0	+12.9	−50.2	−122.0
	12°30′	−27°	+130°	+12.5	−38.6	−98.0	+13.2	−69.8	−150.0
	12°30′	−28°	+140	+14.6	−39.7	−132.0	+3.24	−37.3	−62.8
	12°30′	−31°	+124°	+2.7	−10.5	−28.0	−0.34	−13.9	−29.6
	12°30′	−31°30′	+120°	+2.0	−9.3	−10.0	−0.65	−13.3	−27.2
	12°30′	−32°	+108°	+1.9	−8.8	−23.1	−0.95	−12.8	−24.9
	12°30′	−32°30′	+90	+1.4	−8.7	−24.9	−1.28	−12.5	−22.8
	12°30′	−33°	+62	+0.8	−7.6	−19.6	−1.62	−12.1	−20.7
	12°30′	−33°30′	0	−0.4	−7.4	−14.0	−2.07	−11.9	−18.8
*	12°30′	−34°	+16°	−0.01	−7.5	−18.0	−2.54	−11.7	−16.9

*Denotes cuts for which complete data on A, B, and C Modes are available.

TABLE 5 (Continued)

TEMPERATURE COEFFICIENTS, MODE C (Continued)

	ORIENTATION		$T_{(MAX)}$	OBSERVED VALUES			CALCULATED VALUES		
	ϕ	θ	°C	$a \times 10^{-6}$/°C	$b \times 10^{-9}/(°C)^2$	$c \times 10^{-12}/(°C)^3$	$a \times 10^{-6}$/°C	$b \times 10^{-9}/(°C)^2$	$c \times 10^{-12}/(°C)^3$
	15°	−30°	>160°	+13.3	−21.1	−47.8	+3.2	−15.3	−25.8
	15°	−31°	>160°	+11.3	−13.7	−39.2	+1.2	−13.3	−22.4
	15°	−32°	>160°	+6.6	−9.7	−19.2	0.00	−12.2	−18.8
*	15°	−33°	>160°	+4.7	−7.2	−17.5	−1.1	−11.7	−15.3
	15°	−34°	+154°	+1.8	−7.16	−1.3	−2.29	−11.6	−12.1
RT CUT	15°	−34°30′	+100°	+1.3	−7.3	−6.6	−2.9	−11.55	−10.5
*	15°	−35°	+11°	−0.2	−7.02	−2.6	−3.48	−11.5	−8.86
	15°	−35°30′	−15.2°	−0.6	−7.3	−4.7	−3.64	−11.7	−7.4
	17°30′	−34°30′	> +160°	+2.49	−8.24	−4.41	−2.2	−11.4	−3.2
	17°30′	−35°	+30°	+0.2	−8.3	+2.37	−3.34	−11.35	−3.27
	17°30′	−35°30′	+100°	+1.34	−8.4	−3.36	−4.0	−11.41	−3.38
	17°30′	−36°	−30°	−1.02	−8.9	+2.9	−4.89	−11.48	−3.5
IT CUT	20°	+34°20′	+15°	−0.06	−8.9	+52.0	−0.5	−10.5	+62
	20°	−28°	+80°	+4.0	−32.6	−28.1	+7.1	−39.5	−57.9
	20°	−30°	+93°	+4.6	−30.3	−29.4	+10.6	−18.4	−14.1
	20°	−32°	+149°	+7.1	−24.9	−19.4	+3.7	−11.4	+0.02
	20°	−34°	>160°	+7.0	−13.8	+0.6	−1.2	−11.1	+1.6
*	20°	−36°	>160°	+2.7	−10.5	+15.1	−4.9	−11.9	+5.2
	20°	−37°	−6°	−0.7	−9.9	+13.2	−6.8	−12.6	+7.1
	20°	−38°	−115°	−4.1	−11.45	+12.8	−8.7	−13.5	+8.9
	20°	−39°	−165°	−6.2	−11.32	+19.9	−10.7	−14.6	+10.6

*Denotes cuts for which complete data on A, B, and C Modes are available.

TABLE 5 (Continued)

TEMPERATURE COEFFICIENTS, MODE C (Continued)

ORIENTATION		$T_{(MAX)}$	OBSERVED VALUES			CALCULATED VALUES		
ϕ	θ	°C	a × 10^{-6}/°C	b × 10^{-9}/(°C)^2	c × 10^{-12}/(°C)^3	a × 10^{-6}/°C	b × 10^{-9}/(°C)^2	c × 10^{-12}/(°C)^3
25°	−26°	+120°	+4.3	−23.2	−11.8	+3.4	−37.7	−28.0
25°	−28°	+105°	+3.7	−23.15	−13.7	+4.2	−35.9	−28.2
25°	−30°	+90°	+3.5	−24.2	−12.8	+6.4	−27.8	−15.8
25°	−34°	>150°	+4.9	−18.0	−5.6	+0.83	−12.2	+17.8
30°	±10°	>+160°	+13.3	−7.9	+34.4	+11.5	−21.8	+43.0
30°	±20°	>+160°	+7.0	−16.9	−0.4	+6.3	−28.5	+14.1
30°	±30°	>+160°	+5.0	−20.5	−12.4	+5.1	−25.2	+5.7
30°	±32°	>+160°	+4.3	−14.9	+11.6	+4.3	−18.4	+20.4
30°	±34°	+60°	+0.75	−12.96	+17.4	+0.26	−14.3	+31.5
30°	±36°	−100°	−4.55	−14.3	+20.6	−5.4	−14.4	+34.4
30°	±40°	>−160°	−14.9	−19.8	+27.0	−16.8	−19.8	+34.7
30°	±50°	>−160°	−46.4	−50.1	+44.5	−46.2	−47.0	+21.6
30°	±60°	>−160°	−72.8	−101.7		−73.1	−80.0	−14.4

TABLE 6

VALUES FOR $Tc_{44}^{(1)}$, $Tc_{66}^{(1)}$, $Tc_{14}^{(1)}$ IN $10^{-6}/°C$ USING TWO DIFFERENT ZERO ANGLES OF THE AT AND BT CUTS

	ZERO ANGLE AT: $\theta = 35°15'$ BT: $\theta = -49°13'$	ZERO ANGLE AT: $\theta = 35°22'$ BT: $\theta = -49°40'$	Δ PERCENT
$Tc_{44}^{(1)}$	−177.4	−175.6	1.02
$Tc_{66}^{(1)}$	177.6	179.3	0.96
$Tc_{14}^{(1)}$	101.3	103.9	2.55

TABLE 7

VALUES FOR THE FIRST-ORDER TEMPERATURE COEFFICIENTS OF THE STIFFNESSES FOR ALPHA-QUARTZ IN $10^{-6}/°C$

	BECHMANN [5] 1934	MASON [19] 1940	ATANASOFF[20] AND HART 1941	MASON [22] 1951	GPO[23] RESEARCH REPORT No. 13524 1951	KOGA [24] et al. 1958	NEW VALUES 1961
		$T_o = 20°$	$T_o = 35°$	$T_o = 50°$	$T_o = 20°$	$T_o = 20°$	$T_o = 25°$
$Tc_{11}^{(1)}$	−48	−54	−49.7	−53.5	———	−44.3	−48.5
$Tc_{33}^{(1)}$	−208	−251	−213	−165	———	−188	−160
$Tc_{12}^{(1)}$	−2115	−2350	−3000	−3030	———	−2930	−3000
$Tc_{13}^{(1)}$	−530	−687	−580	−510	———	−492	−550
$Tc_{44}^{(1)}$	−151	−160	−169	−171	−169	−172	−177
$Tc_{66}^{(1)}$	144	161	170.1	168	168	180	178
$Tc_{14}^{(1)}$	82	96	107	90	94	98	101

TABLE 8

VALUES FOR THE SECOND-ORDER TEMPERATURE COEFFICIENTS OF THE STIFFNESSES FOR ALPHA-QUARTZ IN $10^{-9}/(°C)^2$

	MASON [22] 1951	GPO [23] RESEARCH REPORT No. 13524 1951	KOGA, et al. [24] 1958	NEW VALUES 1961
	T_o = 50° C	T_o = 20° C	T_o = 20° C	T_o = 25°C
$Tc_{11}^{(2)}$	−75	———	−407	−107
$Tc_{33}^{(2)}$	−187	———	−1412	−275
$Tc_{12}^{(2)}$	−1500	———	−7245	−3050
$Tc_{13}^{(2)}$	−2000	———	−596	−1150
$Tc_{44}^{(2)}$	−212	−233	−225	−216
$Tc_{66}^{(2)}$	−5	193	201	118
$Tc_{14}^{(2)}$	−270	−82	−13	−48

TABLE 9

VALUES FOR THE THIRD-ORDER TEMPERATURE COEFFICIENTS OF THE STIFFNESSES FOR ALPHA-QUARTZ IN $10^{-12}/(°C)^3$

	MASON [22] 1951	KOGA et al [24] 1958	NEW VALUES 1961
	T_o = 50° C	T_o = 20° C	T_o = 25° C
$Tc_{11}^{(3)}$	−15	−371	−70
$Tc_{33}^{(3)}$	−410	−243	−250
$Tc_{12}^{(3)}$	1910	4195	−1260
$Tc_{13}^{(3)}$	600	−5559	−750
$Tc_{44}^{(3)}$	−65	−190	−216
$Tc_{66}^{(3)}$	−167	−777	21
$Tc_{14}^{(3)}$	−630	−625	−590

TABLE 10

ELASTIC COMPLIANCES $s_{\lambda\mu}$ FOR ALPHA-QUARTZ

AT 20°C IN 10^{-12} m^2N^{-1}

	COMPLIANCES OF QUARTZ According to R. Bechmann [9]		COMPLIANCES OF QUARTZ Calculated from Mindlin and Gazis [15] Using their Values $c_{\lambda\mu}$
$\lambda\mu$	$s_{\lambda\mu}^{E\sigma}$	$s_{\lambda\mu}^{D\sigma}$	$s_{\lambda\mu}$
11	12.77	12.64	12.71
33	9.60	9.60	9.60
12	−1.79	−1.66	−1.61
13	−1.22	−1.22	−1.23
44	20.04	20.03	20.017
66	29.12	28.58	28.64
14	4.50	4.46	4.41

TABLE 11

VALUES FOR THE FIRST-ORDER TEMPERATURE COEFFICIENTS OF THE COMPLIANCES FOR ALPHA-QUARTZ IN $10^{-6}/°C$

	BECHMANN [5] 1934	GIEBE AND BLECHSCHMIDT [25] 1940	MASON [19] 1940	MASON [22] 1951	GPO [23] RESEARCH REPORT No. 13524 1951	NEW VALUES 1961
		$T_o = 20° C$		$T_o = 50° C$	$T_o = 20° C$	$T_o = 25° C$
$Ts_{11}^{(1)}$	11.5	———	12	16.5	———	15.5
$Ts_{33}^{(1)}$	180	———	213	134.5	———	140
$Ts_{12}^{(1)}$	−1125	———	−1265	−1270	———	−1370
$Ts_{13}^{(1)}$	−148	———	−238	−678	———	−166
$Ts_{44}^{(1)}$	175	175.9	189	201	200	210
$Ts_{66}^{(1)}$	−119	−128.9	−133.5	−138	−134	−145
$Ts_{14}^{(1)}$	113	———	123	139.5	125	134

TABLE 12

VALUES FOR THE SECOND-ORDER TEMPERATURE COEFFICIENTS OF THE COMPLIANCES FOR ALPHA-QUARTZ IN $10^{-9}/(°C)^2$

	GIEBE [25] AND BLECHSCHMIDT 1940	MASON [22] 1951	GPO [23] RESEARCH REPORT No. 13524 1951	NEW VALUES 1961
		$T_o = 50°C$	$T_o = 20°C$	$T_o = 25°C$
$Ts_{11}^{(2)}$		58.5		85.3
$Ts_{33}^{(2)}$		144		247
$Ts_{12}^{(2)}$		−575		−1385
$Ts_{13}^{(2)}$		−2110		−718
$Ts_{44}^{(2)}$	298	200	272	262
$Ts_{66}^{(2)}$	−118	−18	−83	−85
$Ts_{14}^{(2)}$		40	83	93

TABLE 13

VALUES FOR THE THIRD-ORDER TEMPERATURE COEFFICIENTS OF THE COMPLIANCES FOR ALPHA-QUARTZ IN $10^{-12}/(°C)^3$

	MASON [29] 1951	NEW VALUES 1961
	$T_o = 50°C$	$T_o = 25°C$
$Ts_{11}^{(3)}$	33	38.3
$Ts_{33}^{(3)}$	570	300
$Ts_{12}^{(3)}$	−215	−1460
$Ts_{13}^{(3)}$	610	−823
$Ts_{44}^{(3)}$	−26	162
$Ts_{66}^{(3)}$	3	−135
$Ts_{14}^{(3)}$	−54	−465

TABLE 14

MEASURED AND CALCULATED VALUES FOR FREQUENCY CONSTANTS N AND FIRST-, SECOND-, AND THIRD-ORDER TEMPERATURE COEFFICIENTS FOR THE CT CUT VIBRATING IN CONTOUR MODE

		OBSERVED			CALCULATED		
		$Y_{\theta 0°}$	$Y_{\theta 45°}$	$Y_{\theta O}$	$Y_{\theta 0°}$	$Y_{\theta 45°}$	$Y_{\theta O}$
(yxl) ϑ Angle	θ	37°40′		36°15′		36°20′	
kc-mm	N	3087	3583	3766	3145	3594	3793
10^{-6}/°C	a		0			0	
$10^{-9}/(°C)^2$	b		−58			−58	
$10^{-12}/(°C)^3$	c		−151			−161	
10^{-6}/°C	$\frac{\partial a}{\partial \theta}$					5.28	
$10^{-9}/(°C)^2$	$\frac{\partial b}{\partial \theta}$					4.75	
$10^{-12}/(°C)^3$	$\frac{\partial c}{\partial \theta}$					2.10	
°C	T_m		25°			25°	
°C	$\frac{\partial T_m}{\partial \theta}$		45°			See Fig. 36	

TABLE 15

MEASURED AND CALCULATED VALUES FOR FREQUENCY CONSTANTS N AND FIRST-, SECOND-, AND THIRD-ORDER TEMPERATURE COEFFICIENTS FOR THE DT CUT VIBRATING IN CONTOUR MODE

		OBSERVED			CALCULATED		
		$Y_{\theta 0°}$	$Y_{\theta 45°}$	$Y_{\theta O}$	$Y_{\theta 0°}$	$Y_{\theta 45°}$	$Y_{\theta O}$
(yxl) θ Angle	θ	−51°50′		−51°10′		−50°40′	
kc-mm	N	2073	2341	2471	2085	2356	2486
10^{-6}/°C	a		0			0	
10^{-9}/(°C)^2	b		−17			−19.4	
10^{-12}/(°C)^3	c		52			75.6	
10^{-6}/°C	$\frac{\partial a}{\partial \theta}$					−2.30	
10^{-9}/(°C)^2	$\frac{\partial b}{\partial \theta}$					−2.01	
10^{-12}/(°C)^3	$\frac{\partial C}{\partial \theta}$					−1.06	
°C	T_m		25°			25°	
°C	$\frac{\partial T_m}{\partial \theta}$		−75°				

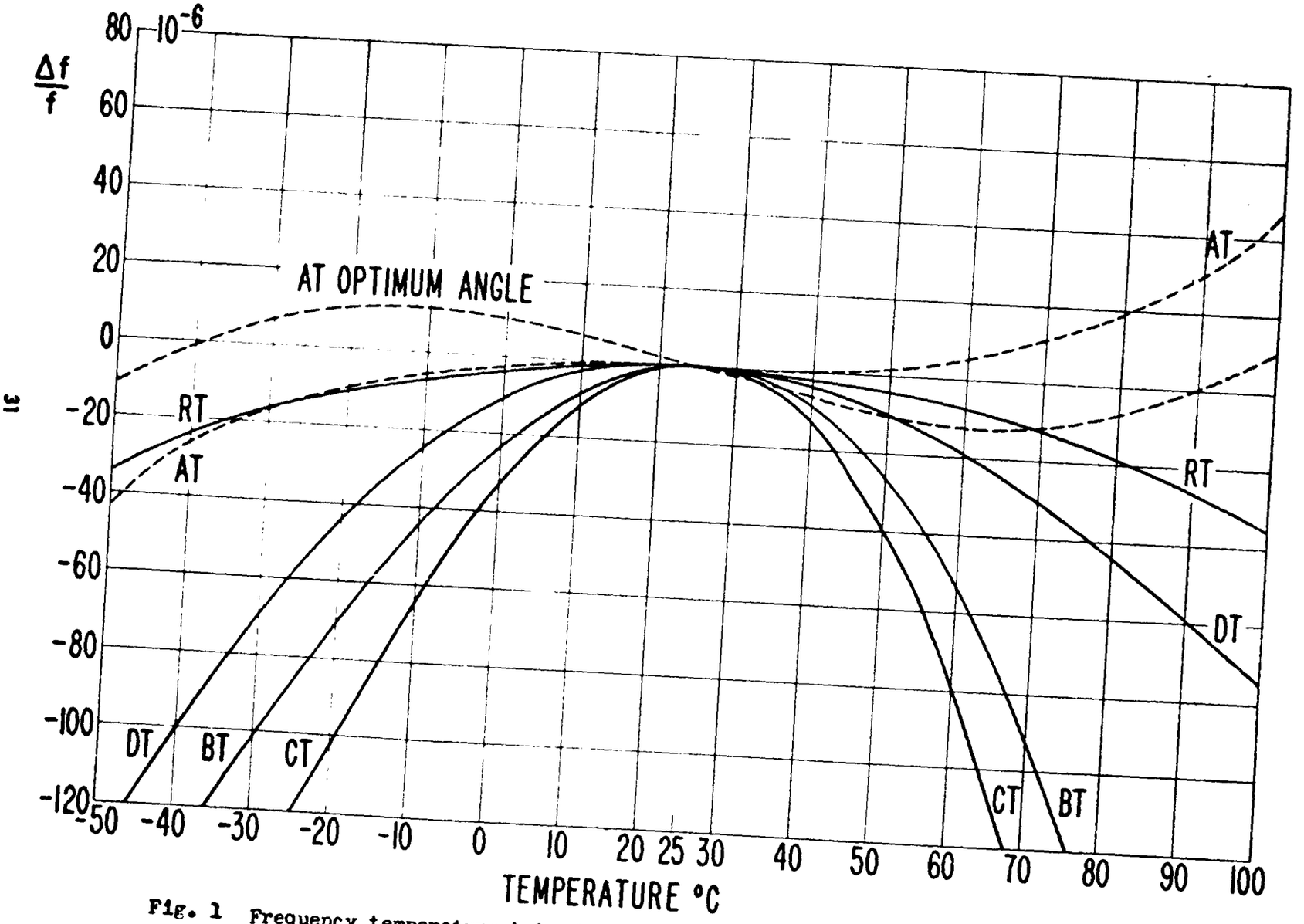

Fig. 1 Frequency temperature behavior of the AT, BT, CT, DT, and RT cuts.

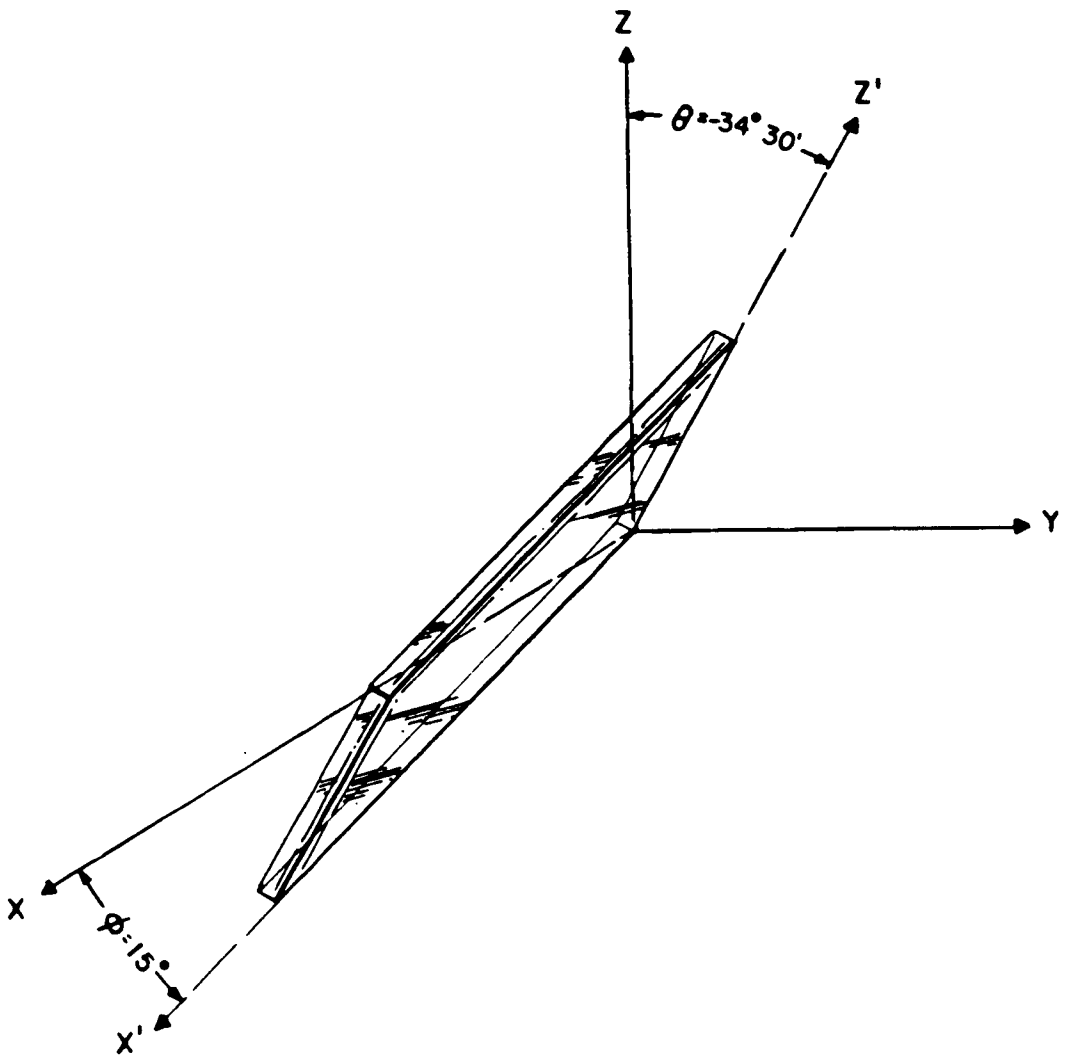

Fig. 2. Orientation of a quartz plate described by the angles ϕ and θ: Plate $\phi = 15°$, $\theta = -34°30'$.

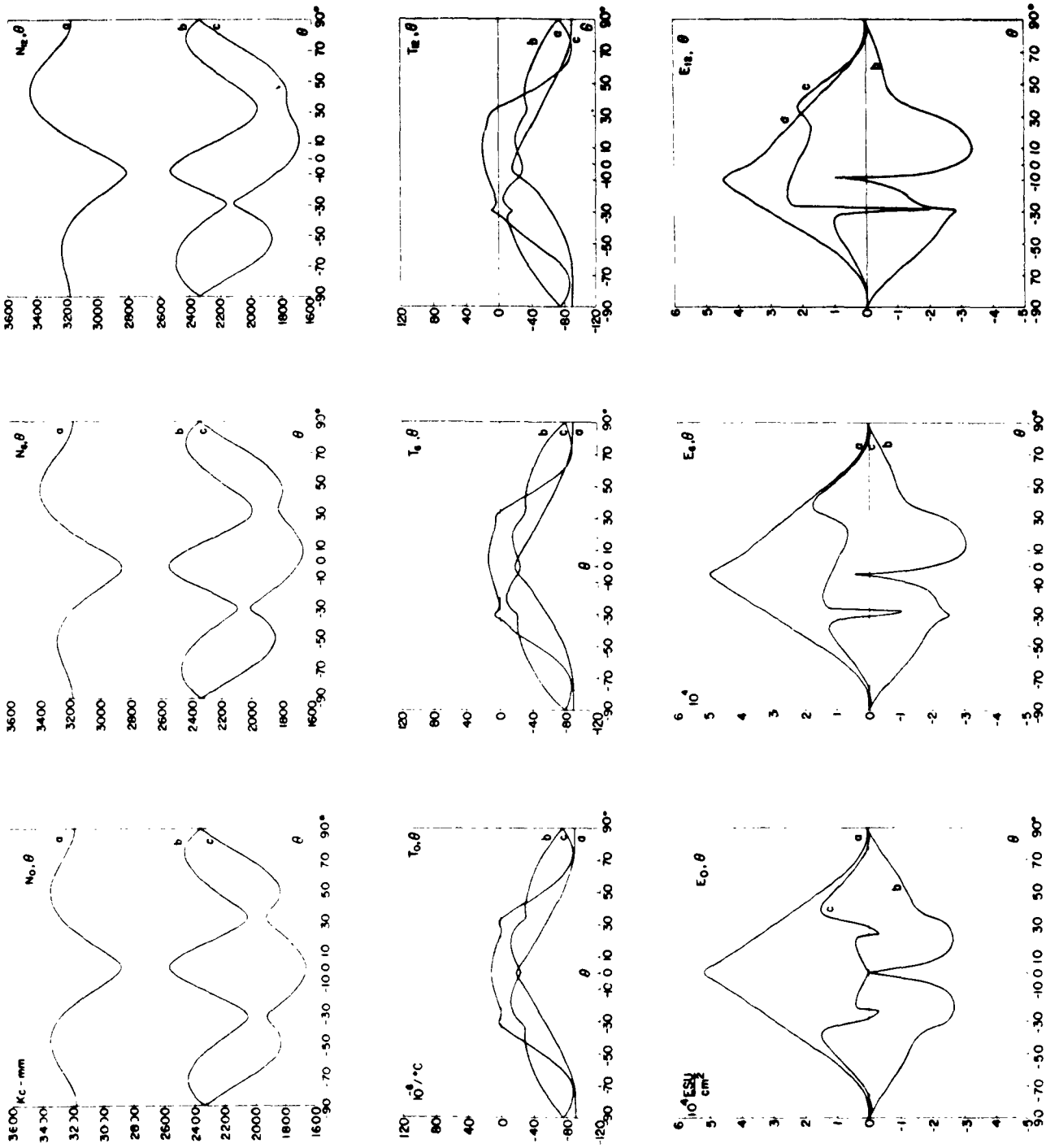

Fig. 3a Frequency constant N, piezoelectric constant e, and temperature coefficient of frequency (first order) Tf for quartz plates of different orientations vibrating in thickness modes.

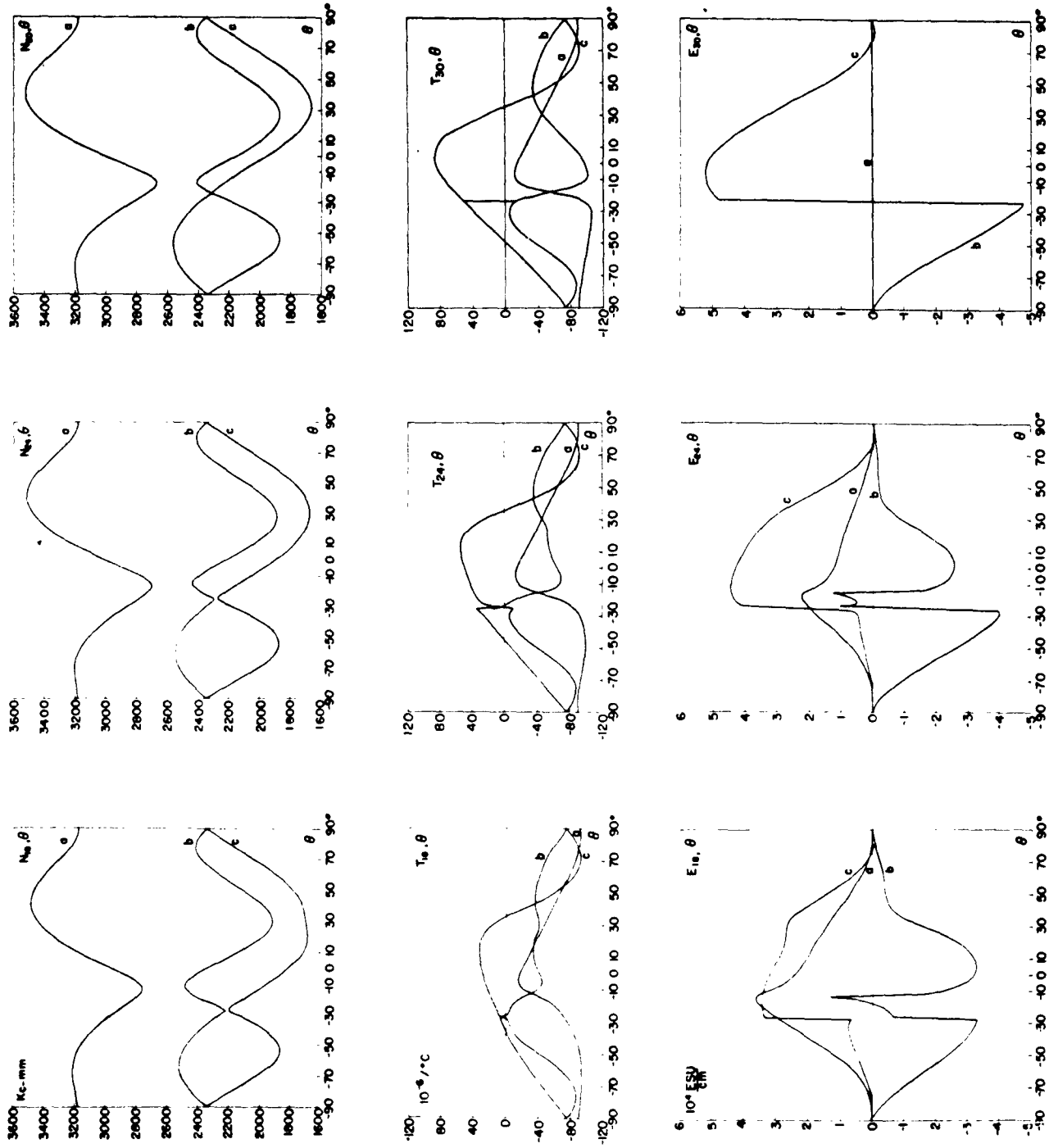

Fig. 3b Frequency constant N, piezoelectric constant e, and temperature coefficient of frequency (first order) Tf for quartz plates of different orientations vibrating in thickness modes.

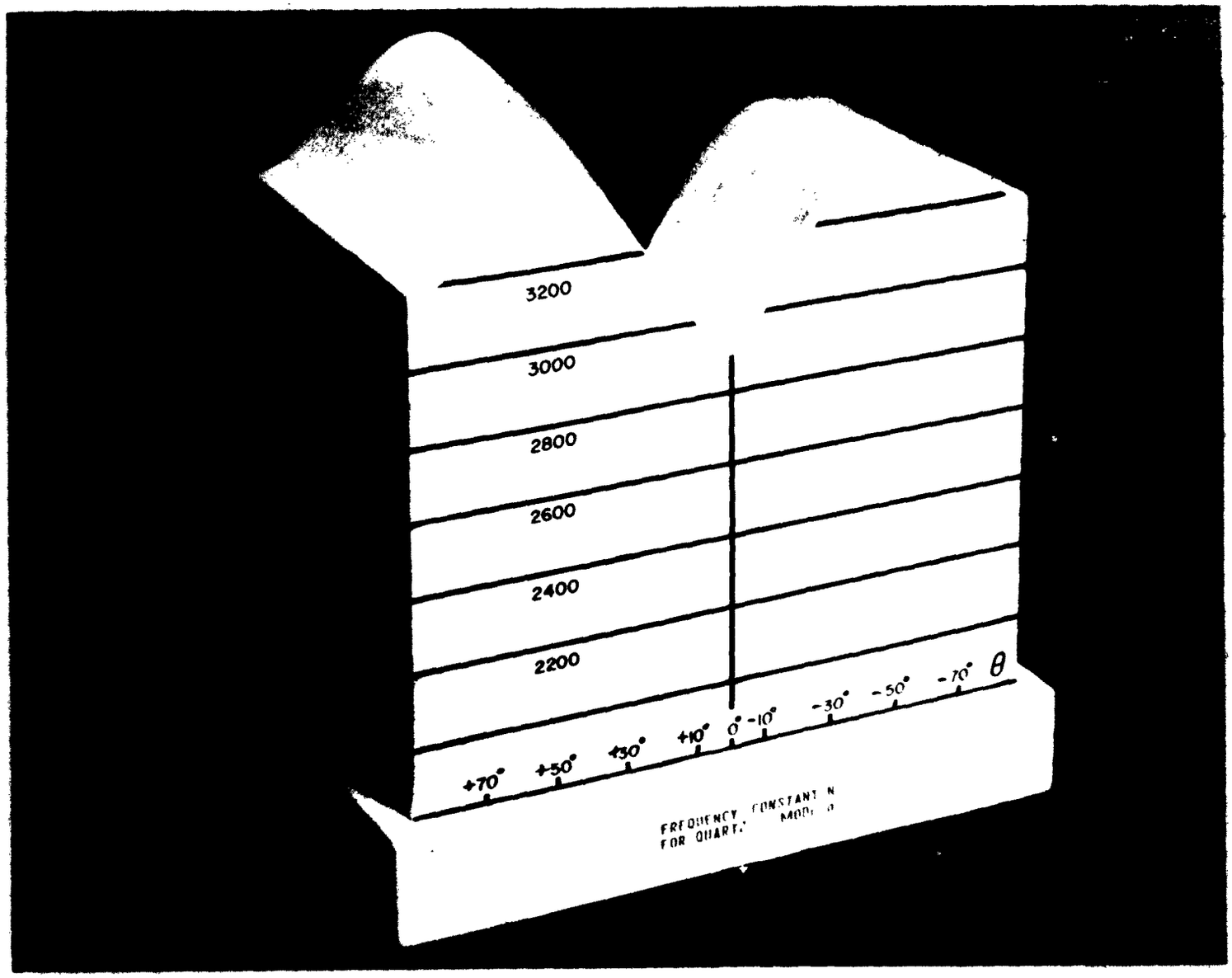

Fig. 4 Model of the frequency constant N for quartz plates of different orientations vibrating in the thickness mode A (Photograph)

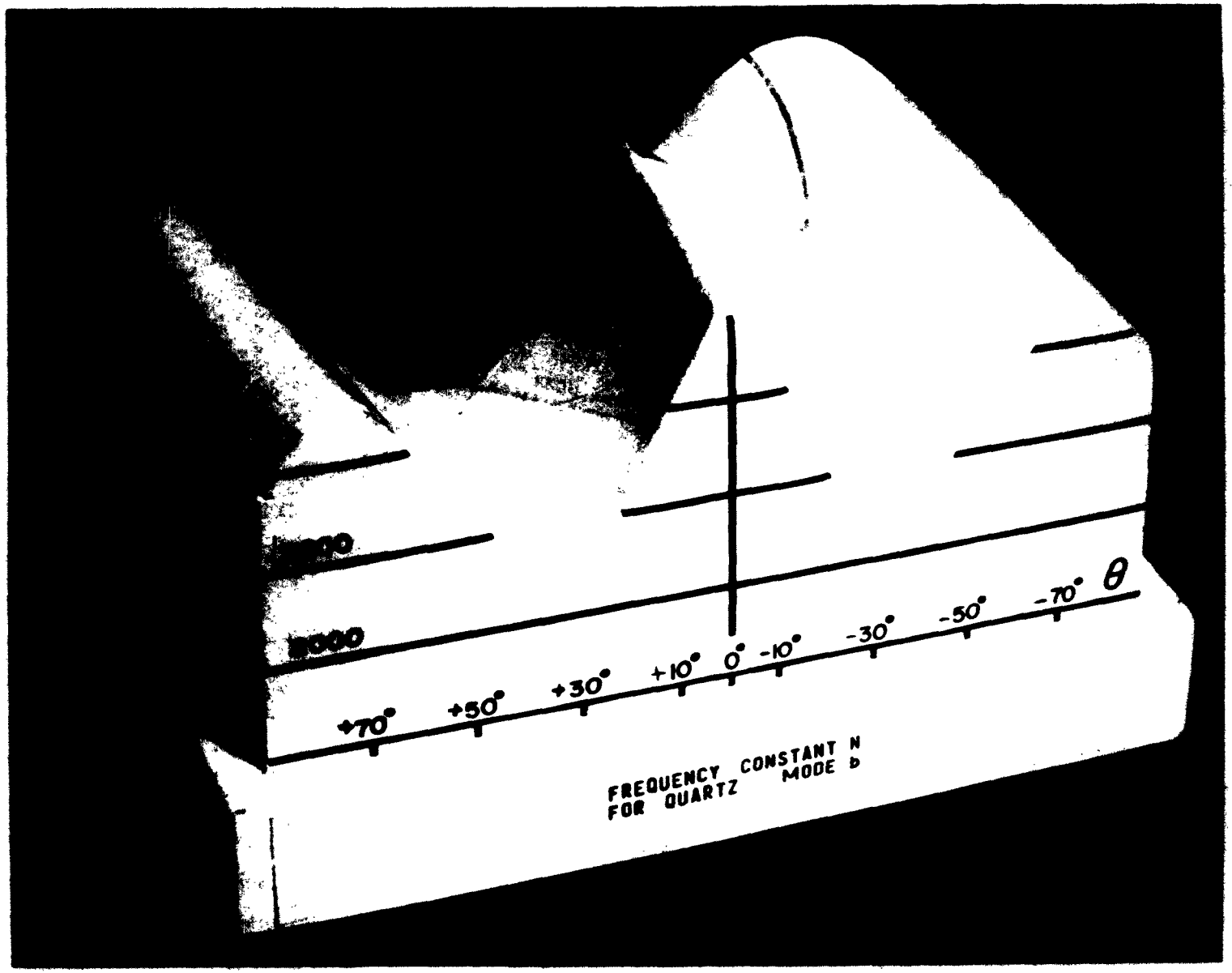

Fig. 5 Model of the frequency constant N for quartz plates of different orientations vibrating in the thickness mode B (Photograph)

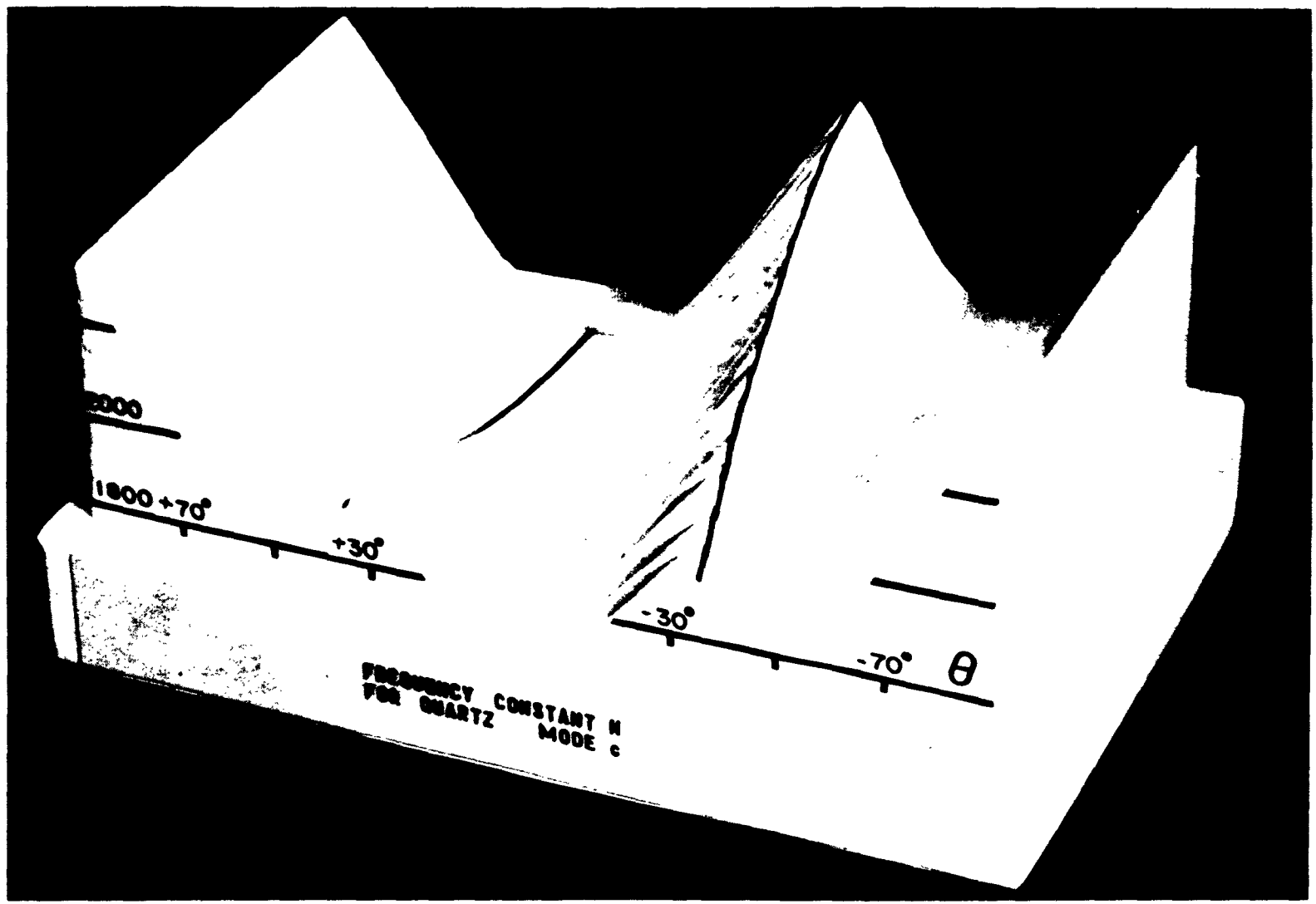

Fig. 6 Model of the frequency constant N for quartz plates of different orientations vibrating in the thickness mode C (Photograph)

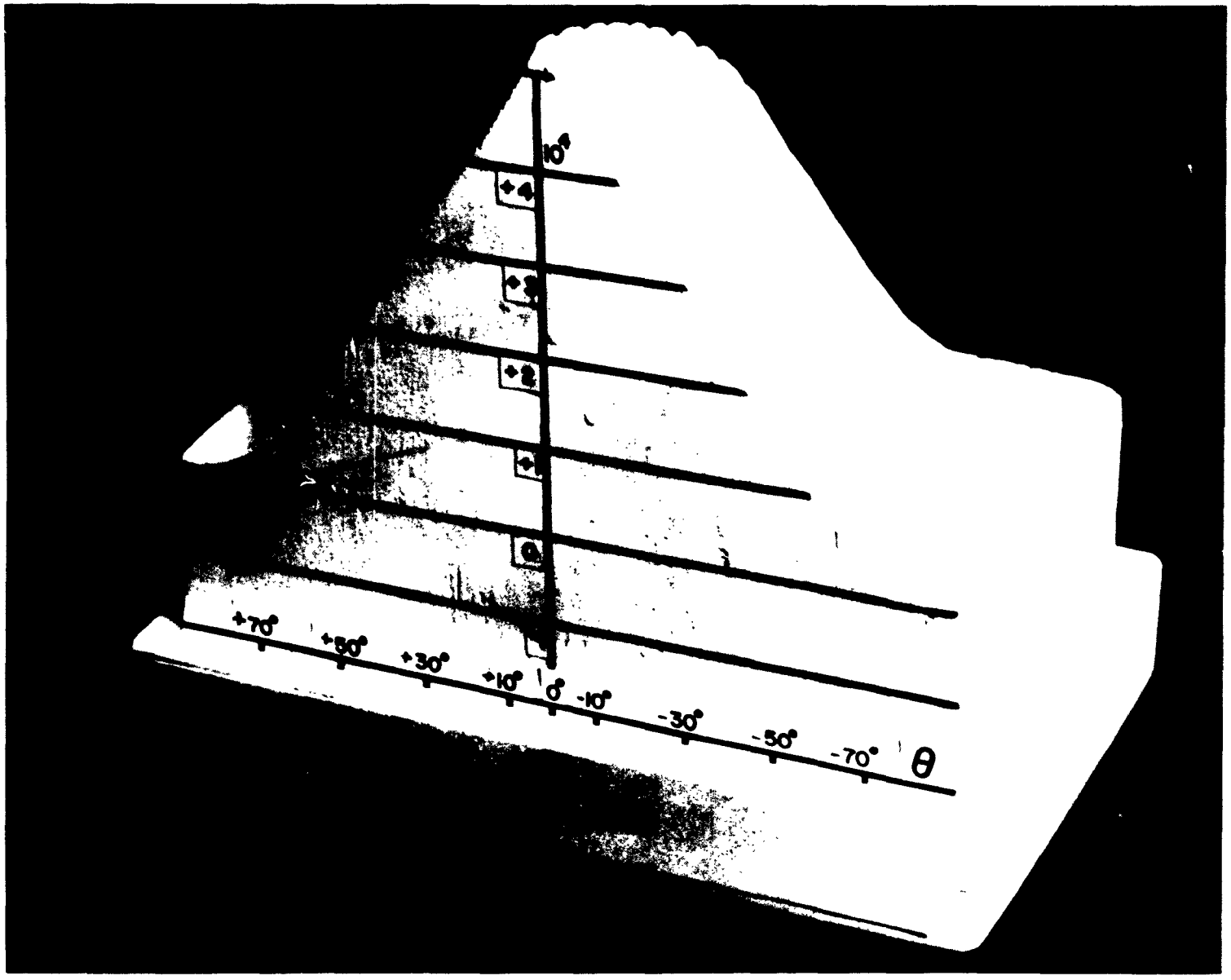

Fig. 7 Model of the piezoelectric constant e for quartz plates of different orientations viratin, in the thickness mode A (Photograph)

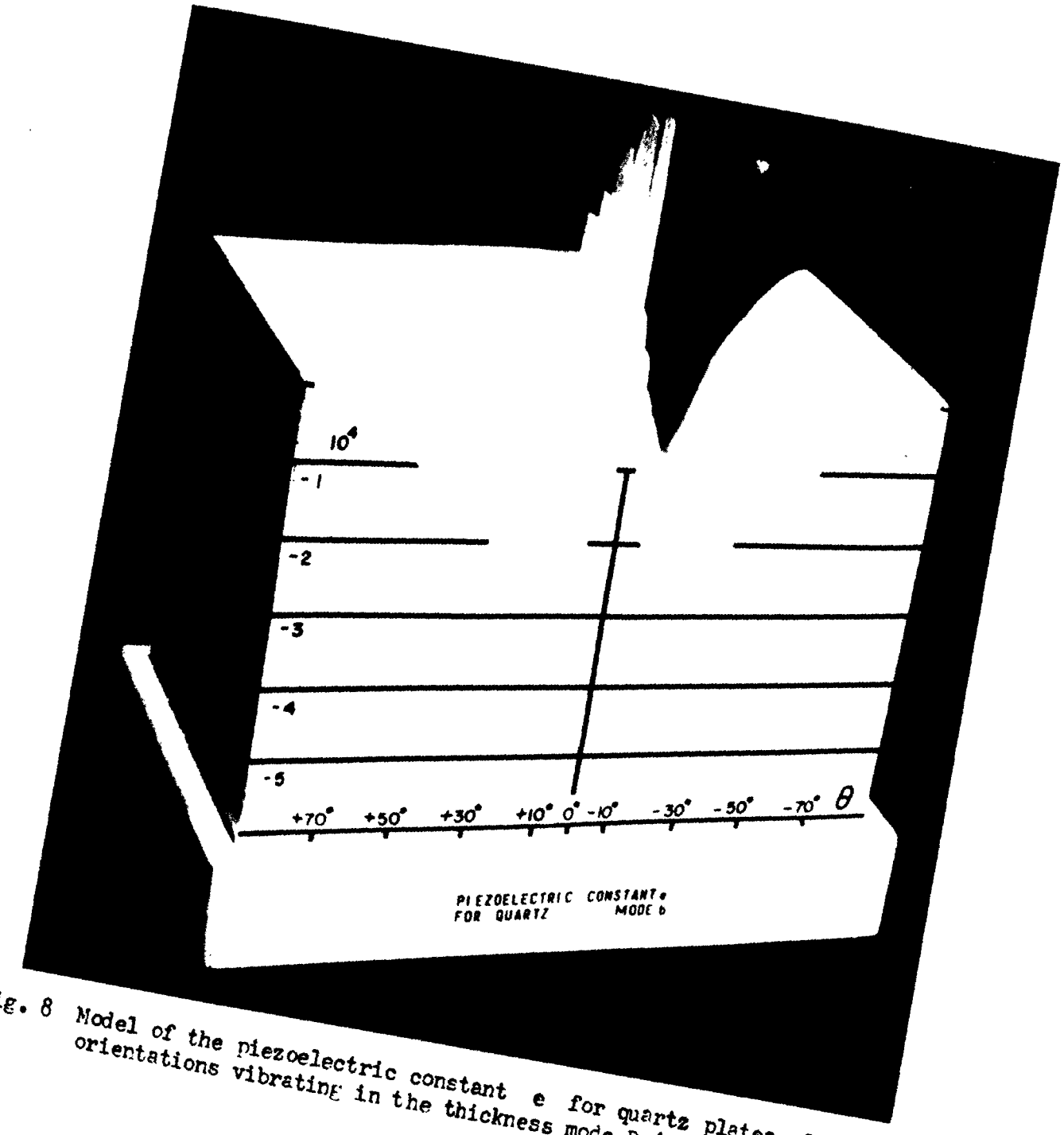

Fig. 8 Model of the piezoelectric constant e for quartz plates of different orientations vibrating in the thickness mode B (Photograph)

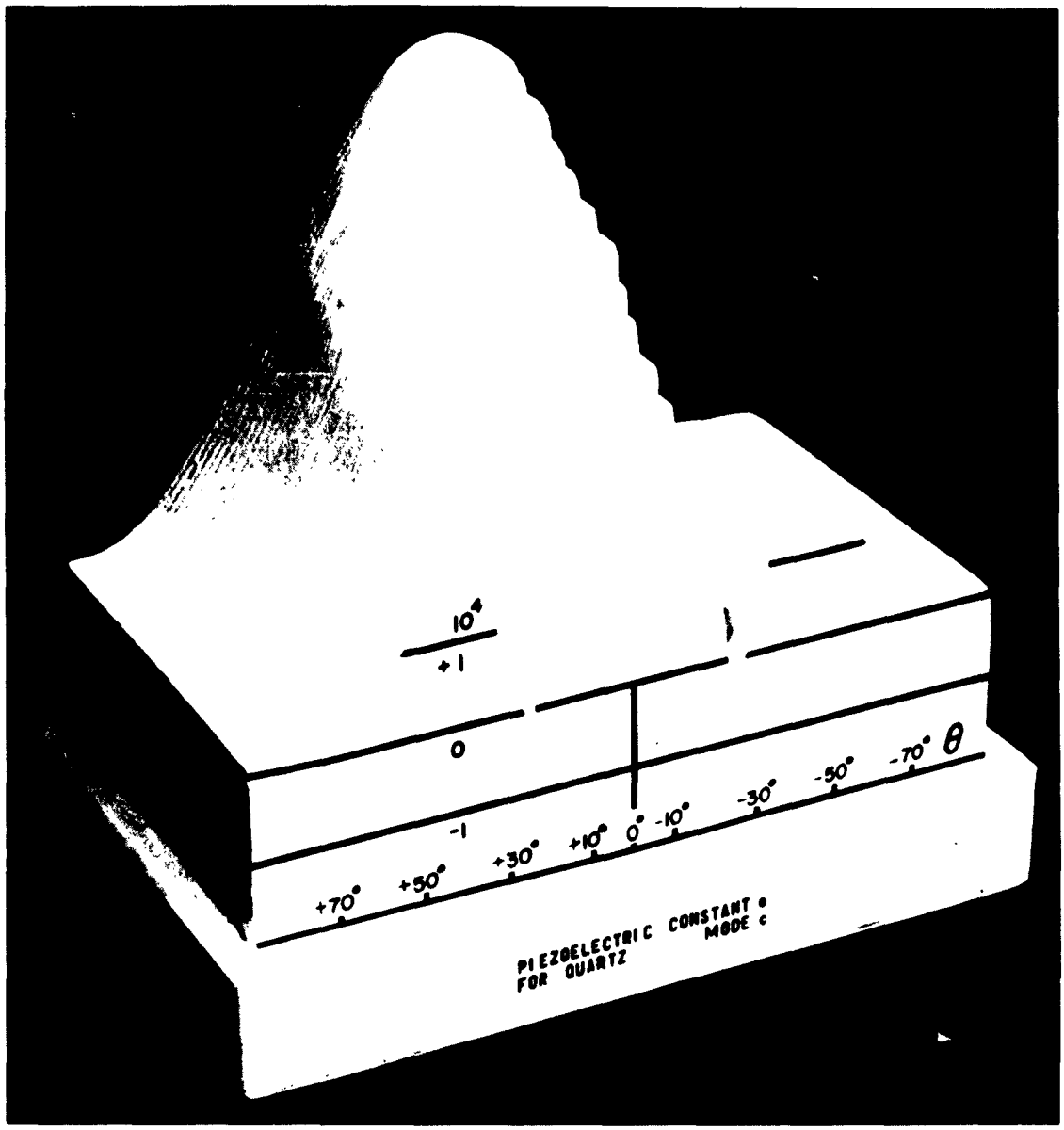

Fig. 9 Model of the piezoelectric constant e for quartz plates of different orientations vibrating in the thickness mode C (Photograph)

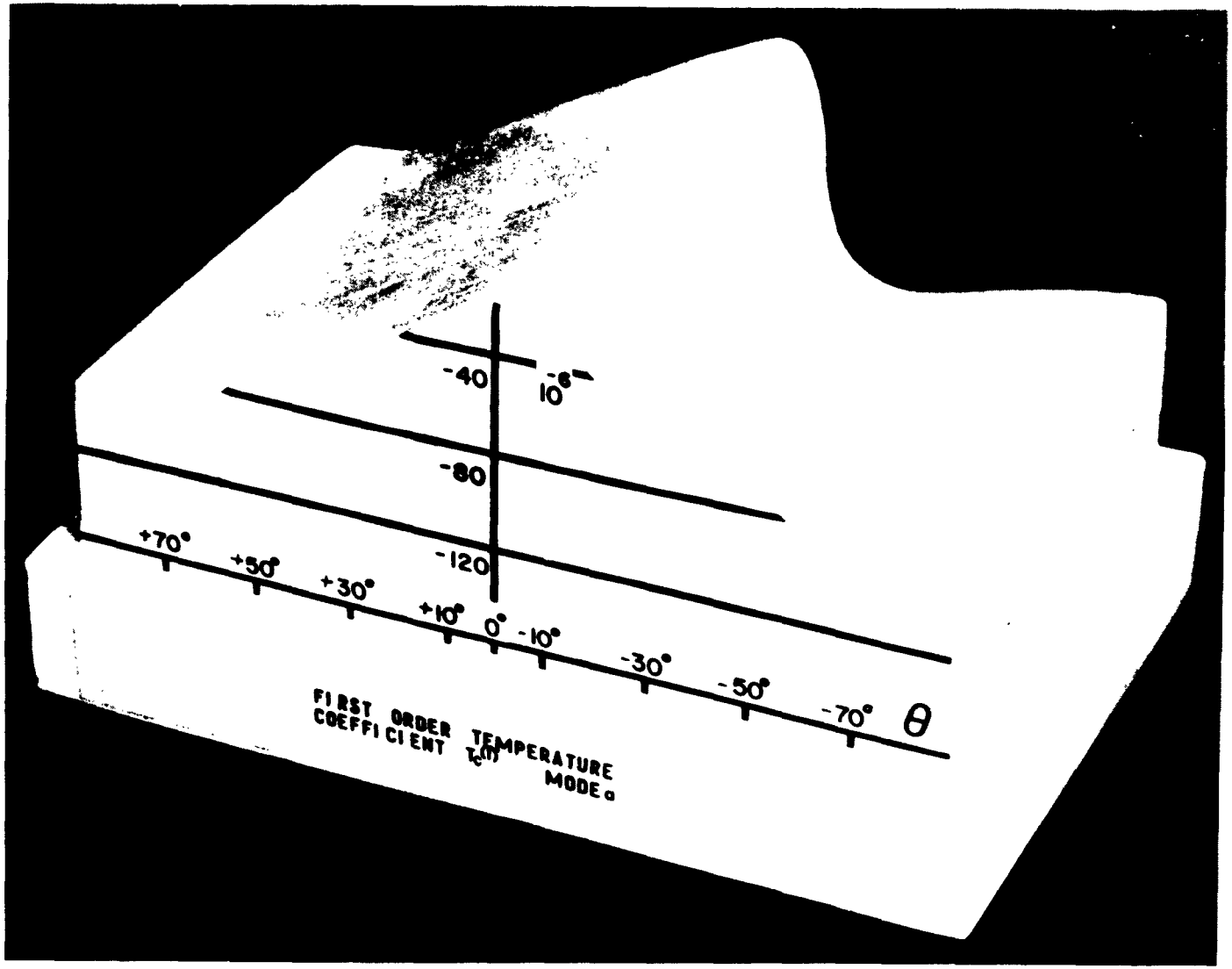

Fig. 10 Model of the temperature coefficient of frequency first order $T_c^{(1)}$ for quartz plates of different orientations vibrating in the thickness mode A (Photograph)

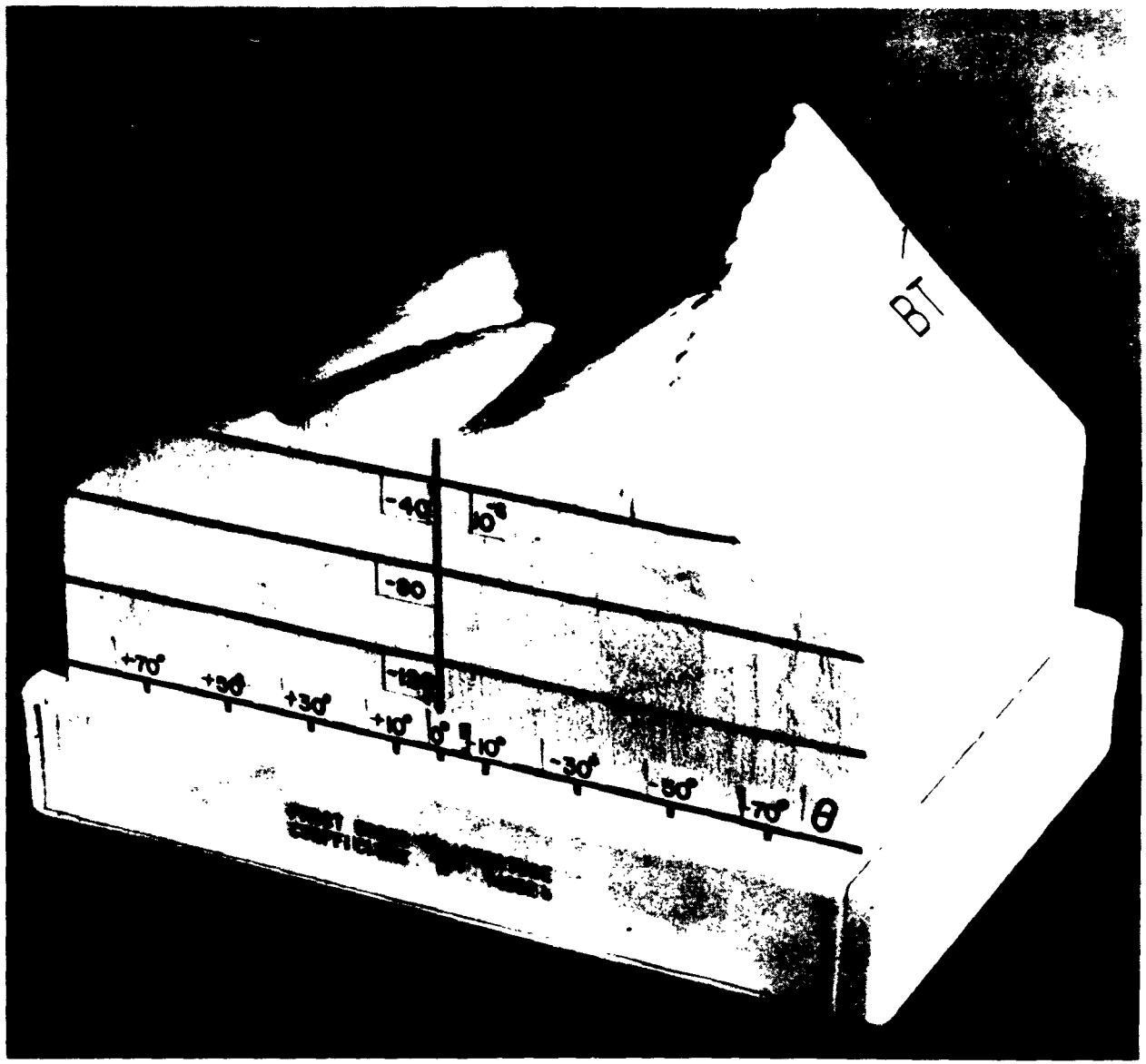

Fig. 11 Model of the temperature coefficient of frequency first order $T_c^{(1)}$ for quartz plates of different orientations vibrating in the thickness mode B (Photograph)

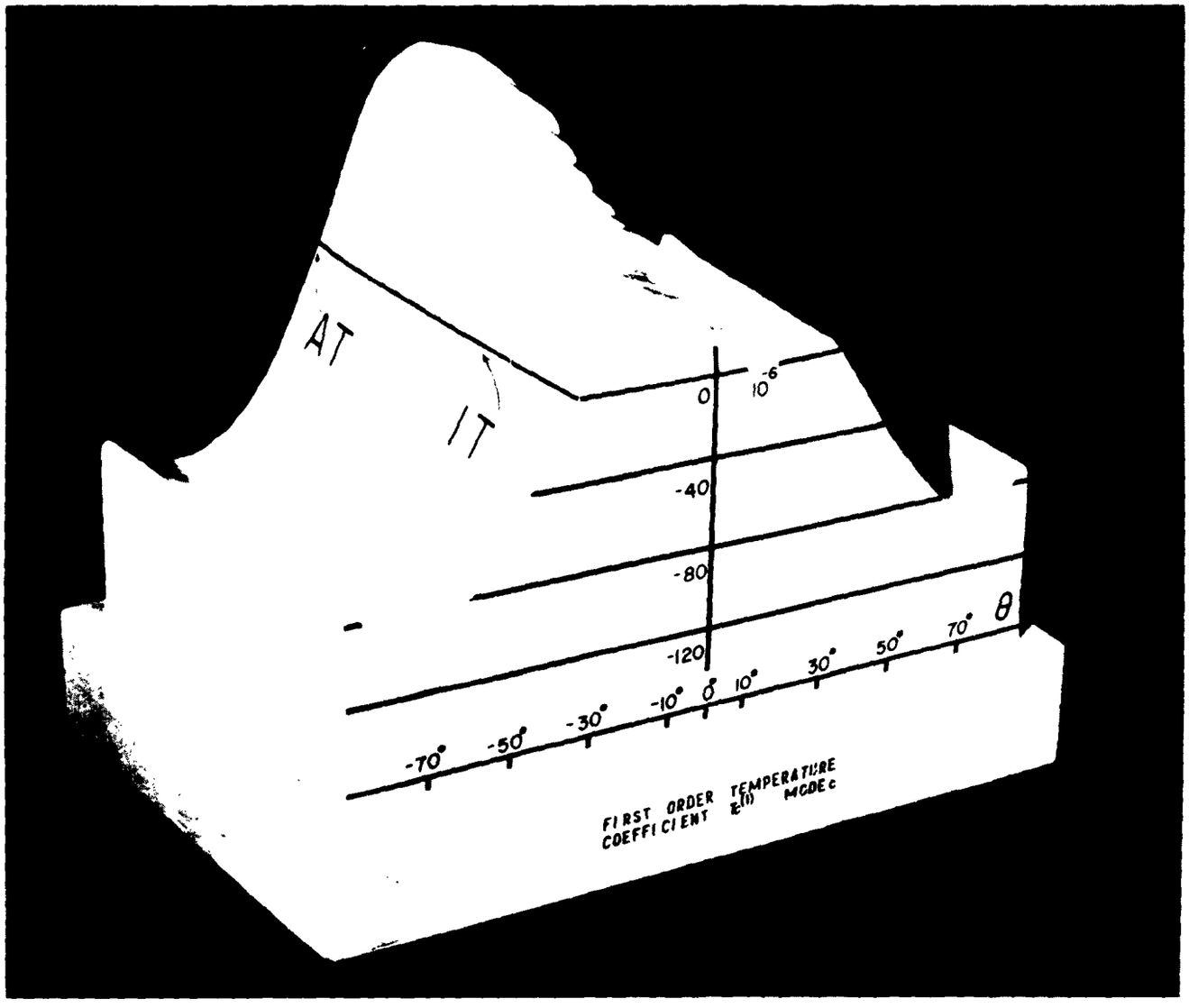

Fig. 12 Model of the temperature coefficient of frequency first order $T_c^{(1)}$ for quartz plates of different orientations vibrating in the thickness mode C (Photograph)

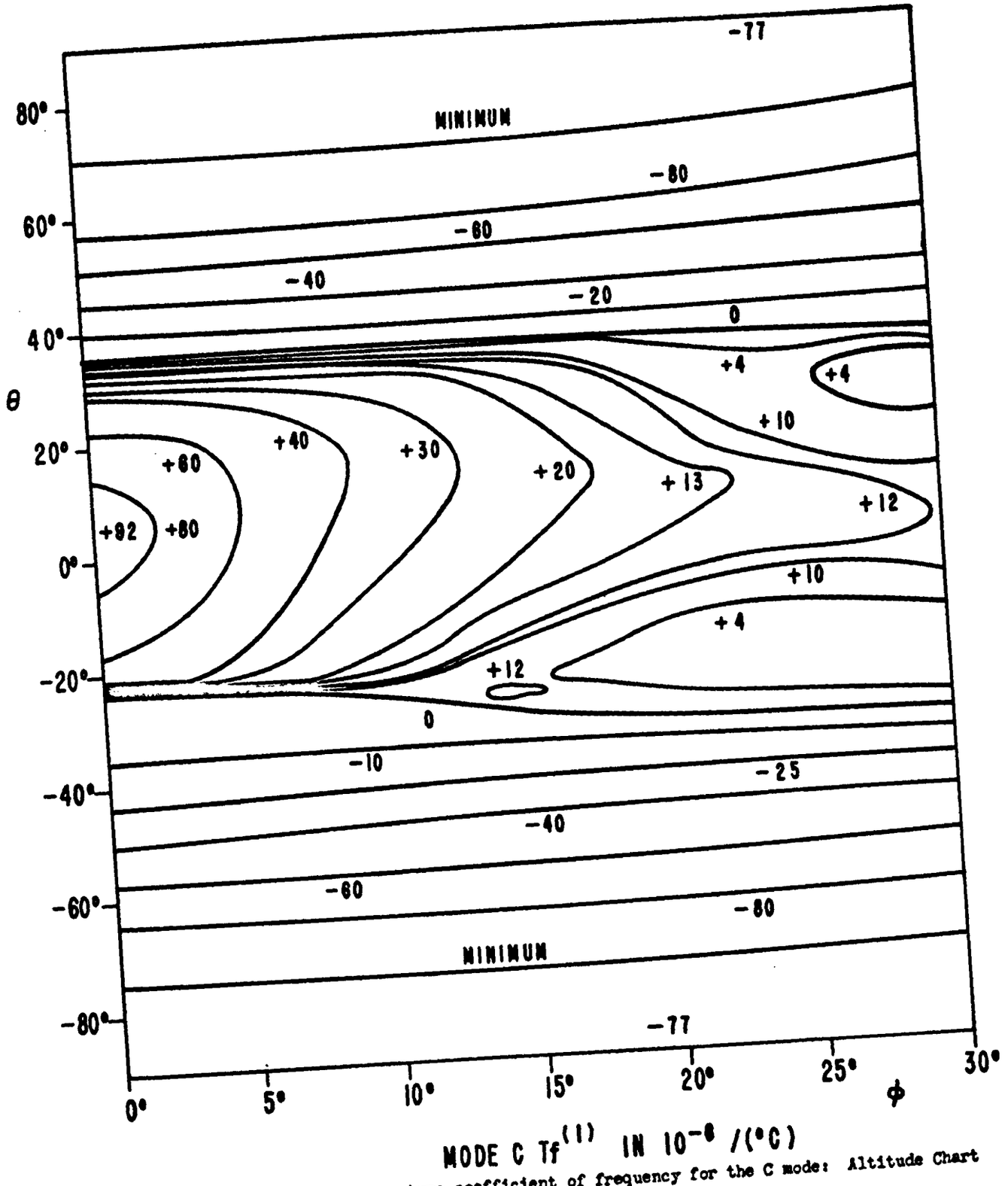

Fig. 13 First-order temperature coefficient of frequency for the C mode: Altitude Chart

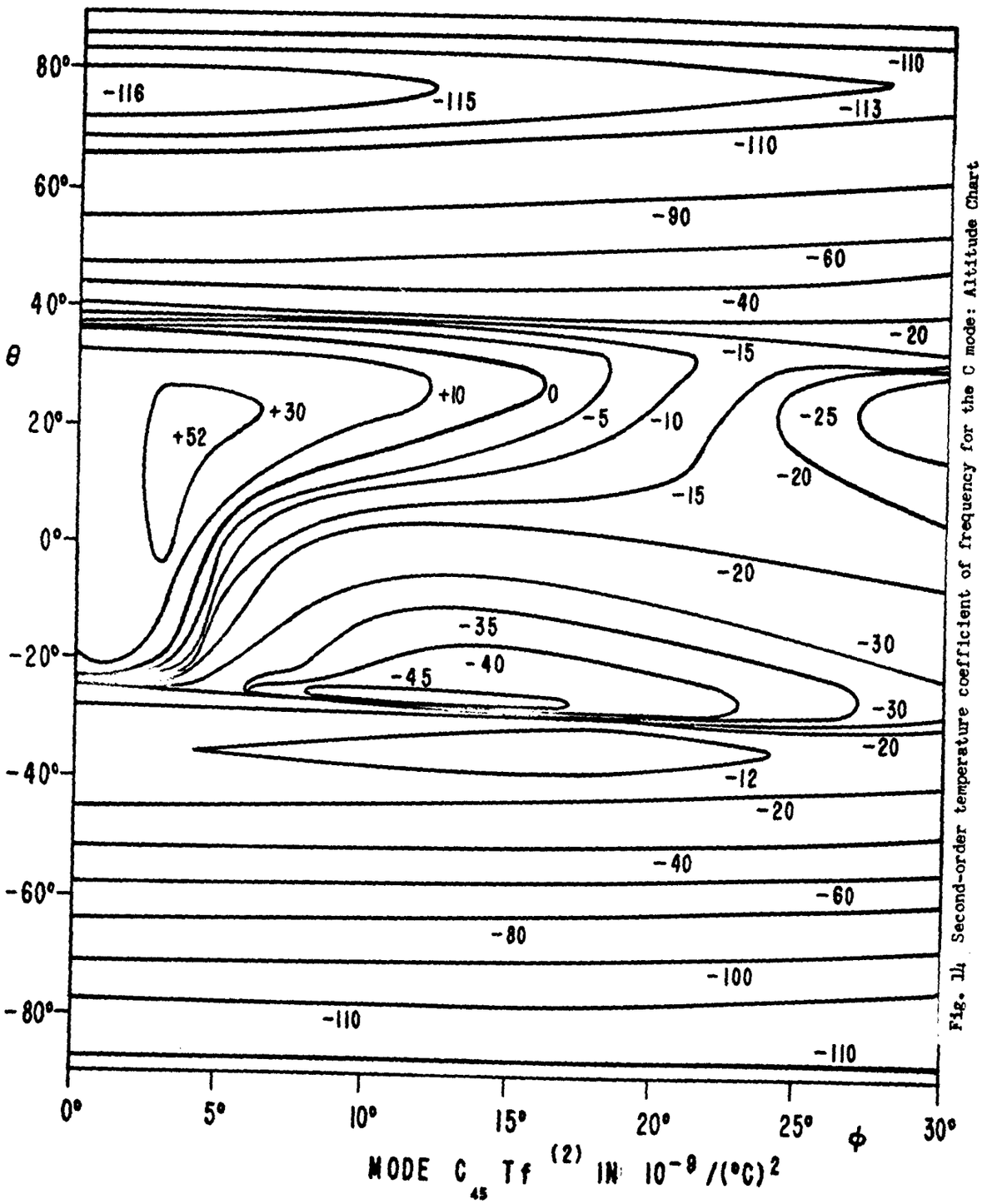

Fig. 14 Second-order temperature coefficient of frequency for the C mode: Altitude Chart

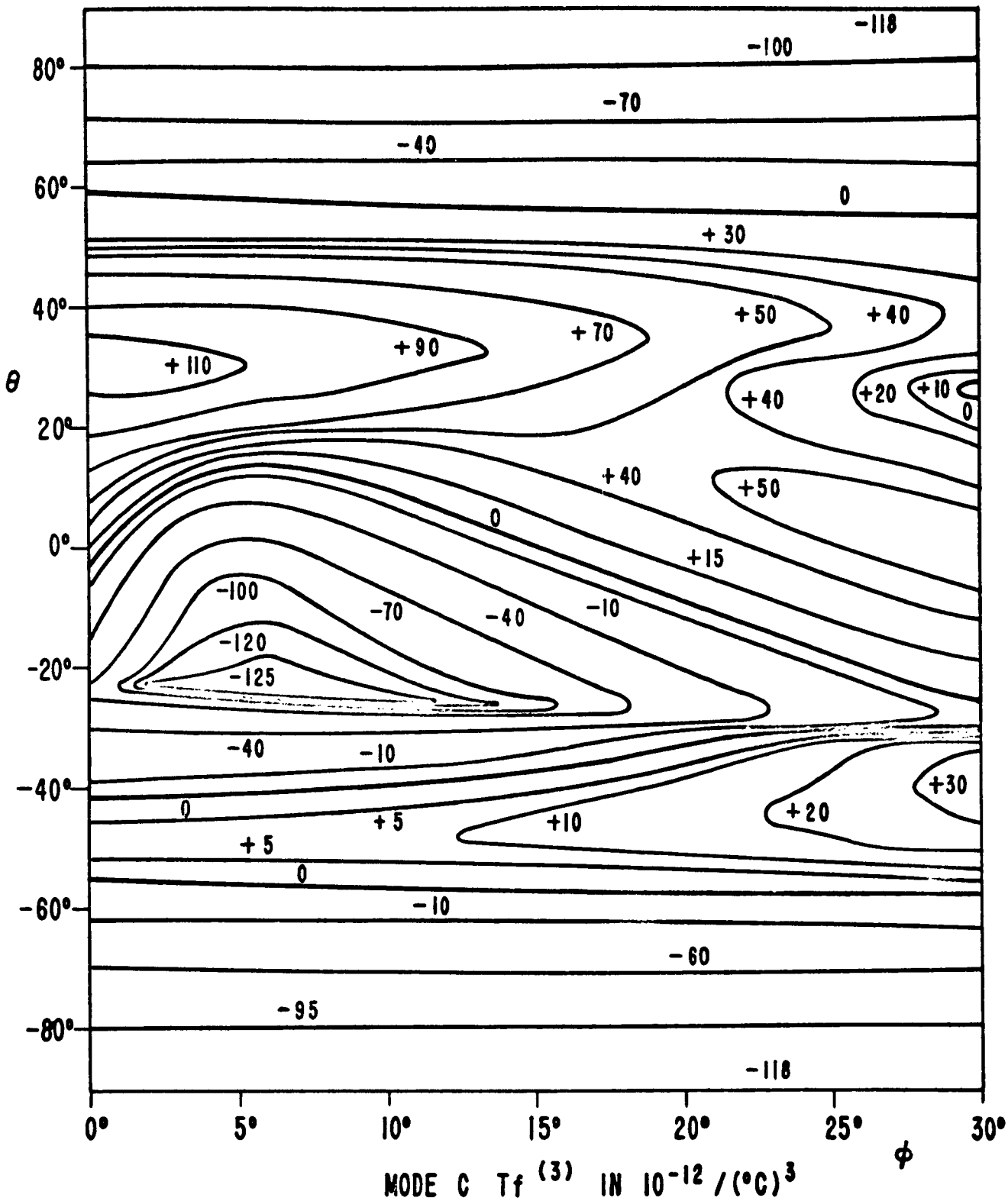

Fig. 15 Third-order temperature coefficient of frequency for the C mode: Altitude Chart

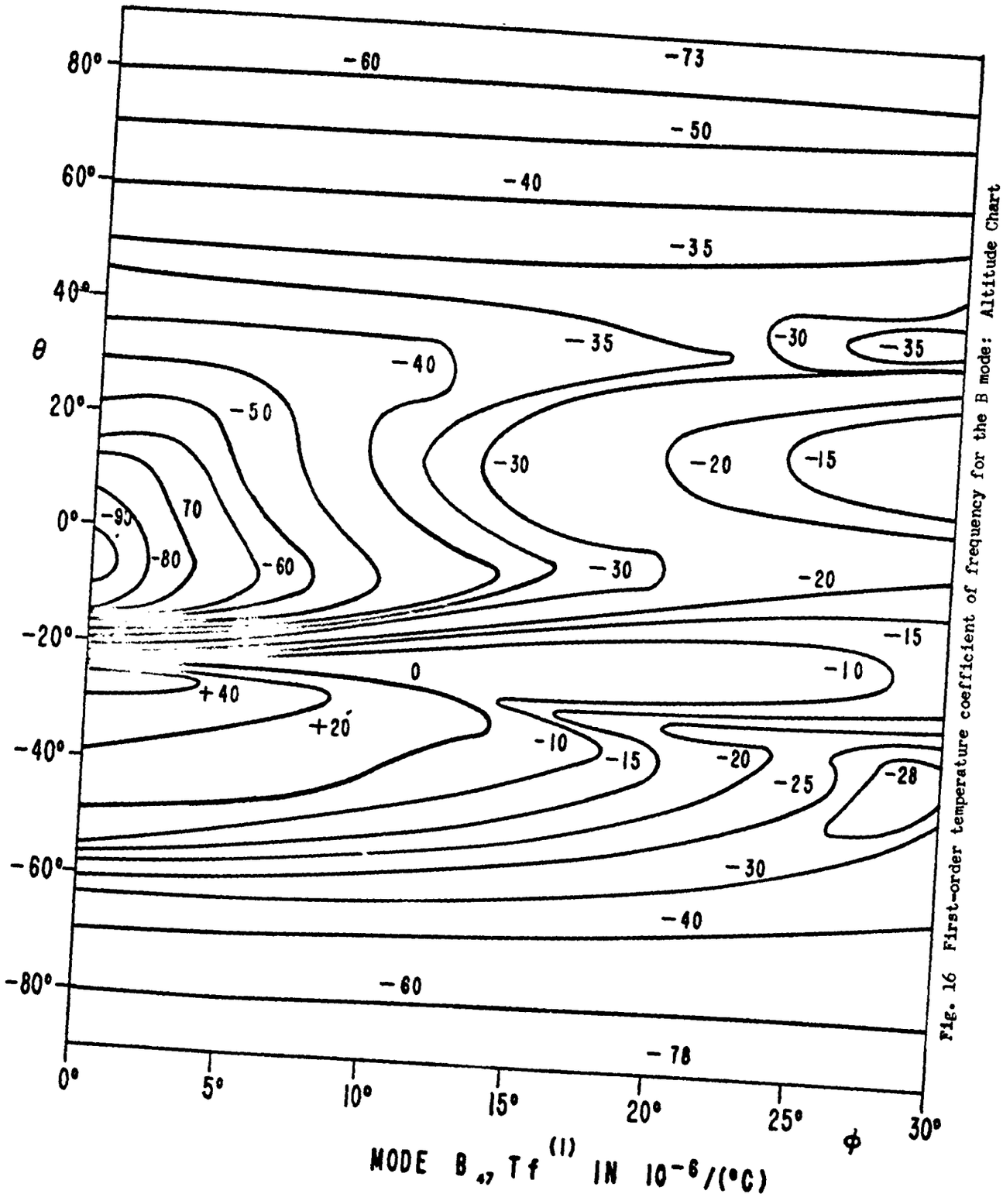

Fig. 16 First-order temperature coefficient of frequency for the B mode: Altitude Chart

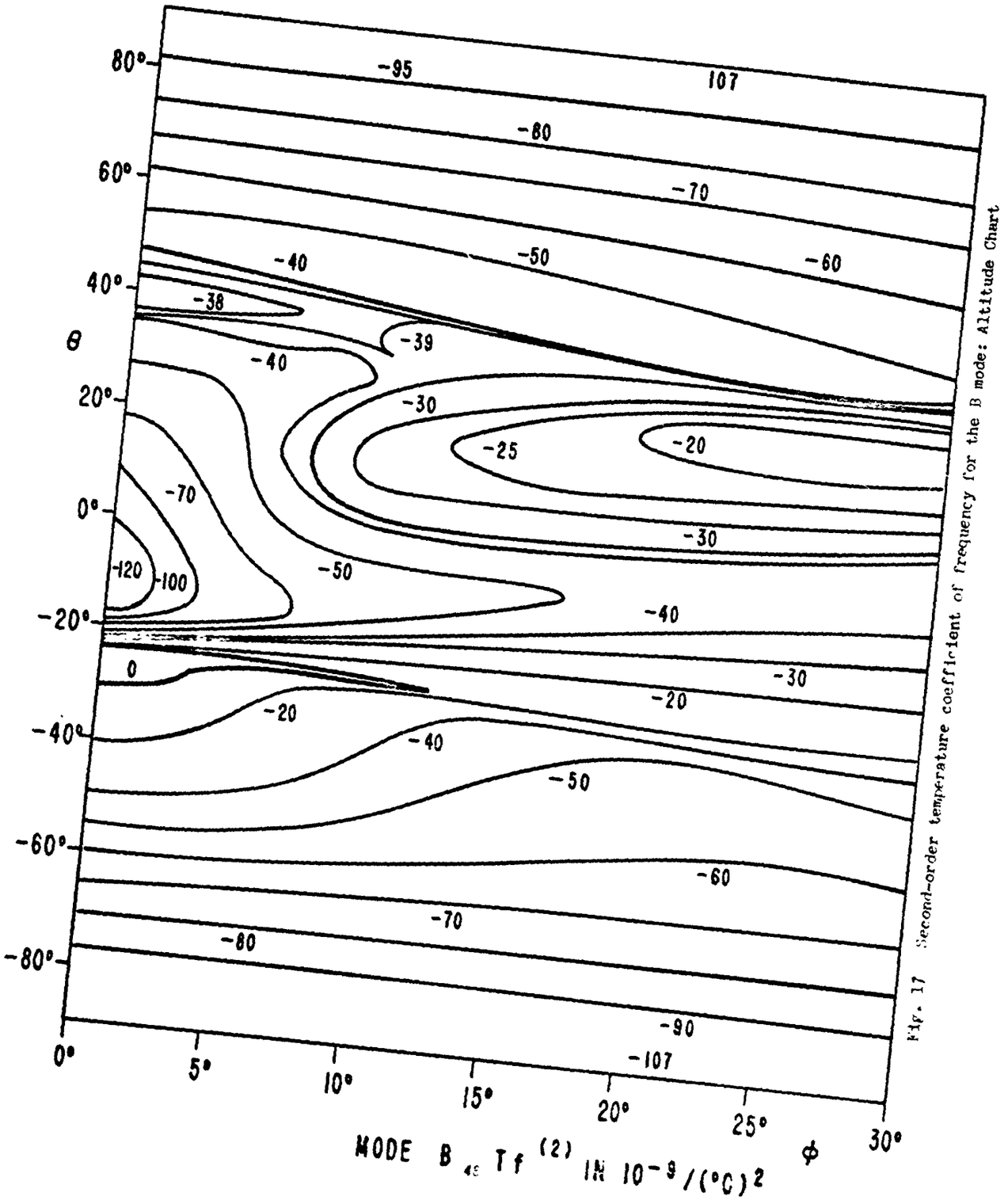

Fig. 17 Second-order temperature coefficient of frequency for the B mode: Altitude Chart

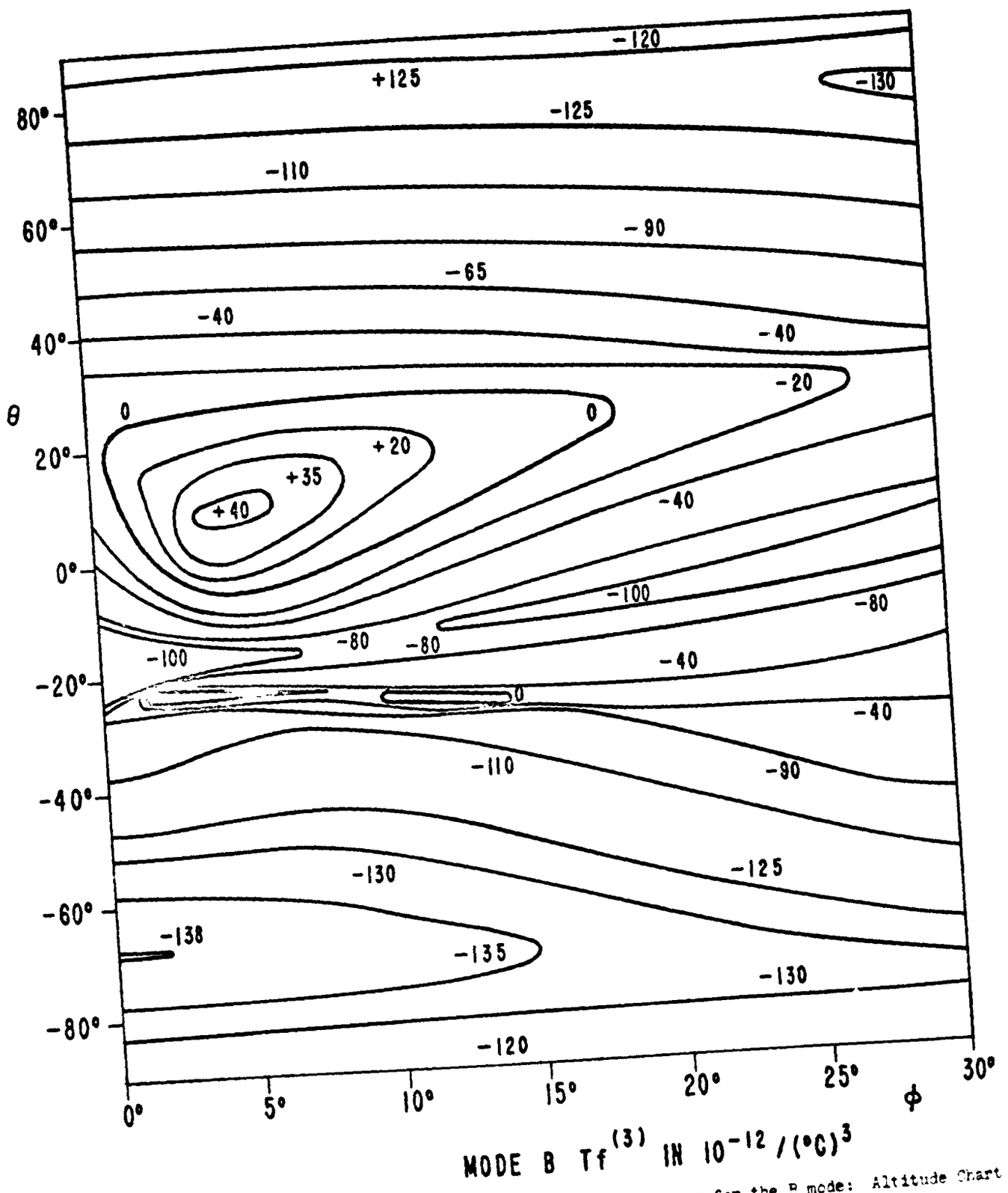

Fig. 15 Third-order temperature coefficient of frequency for the B mode: Altitude Chart

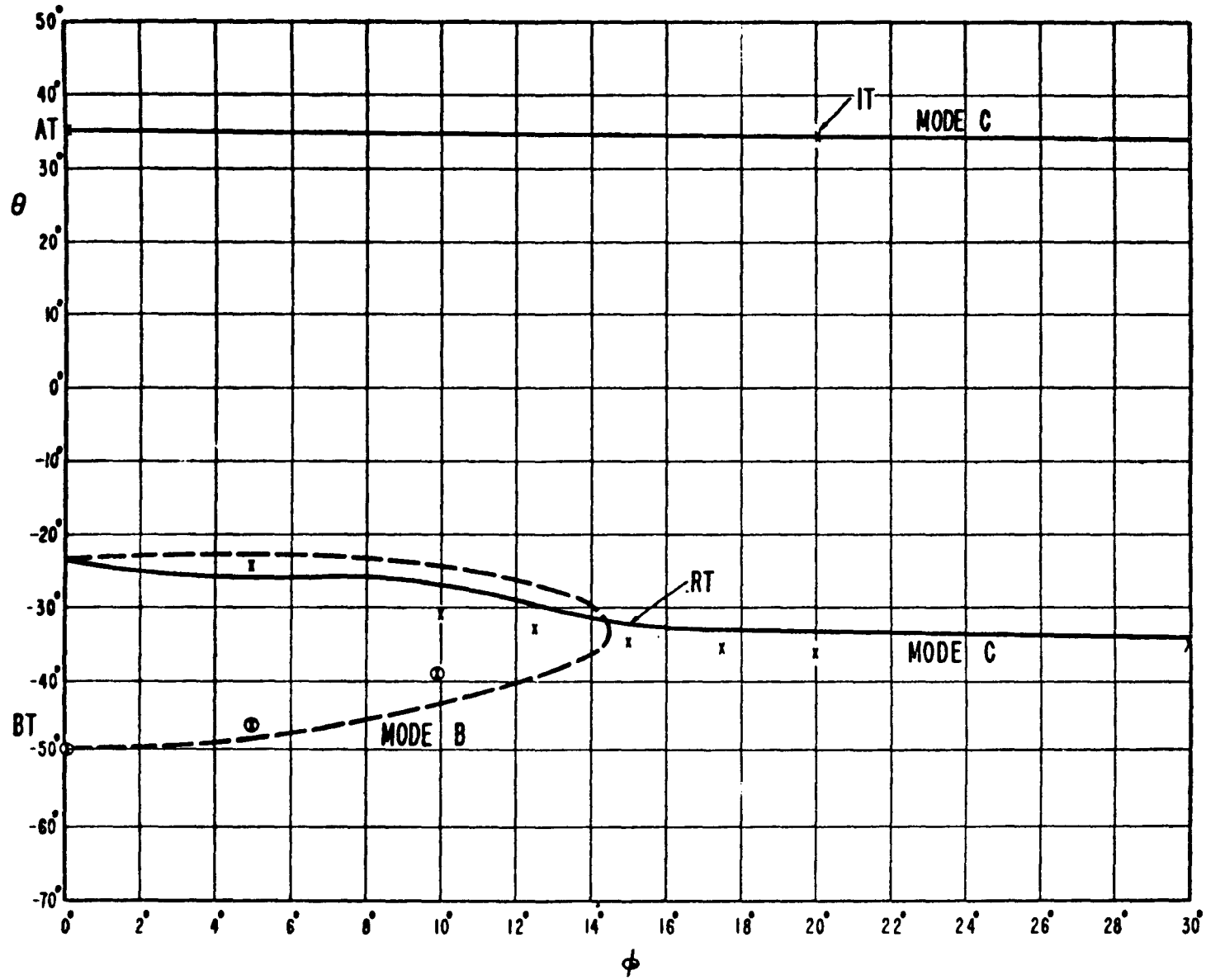

Fig. 19. Locus of $Tf^{(1)} = 0$ for the thickness modes B and C of quartz plates as a function of the angles θ and ϕ in a rectangular coordinate system.

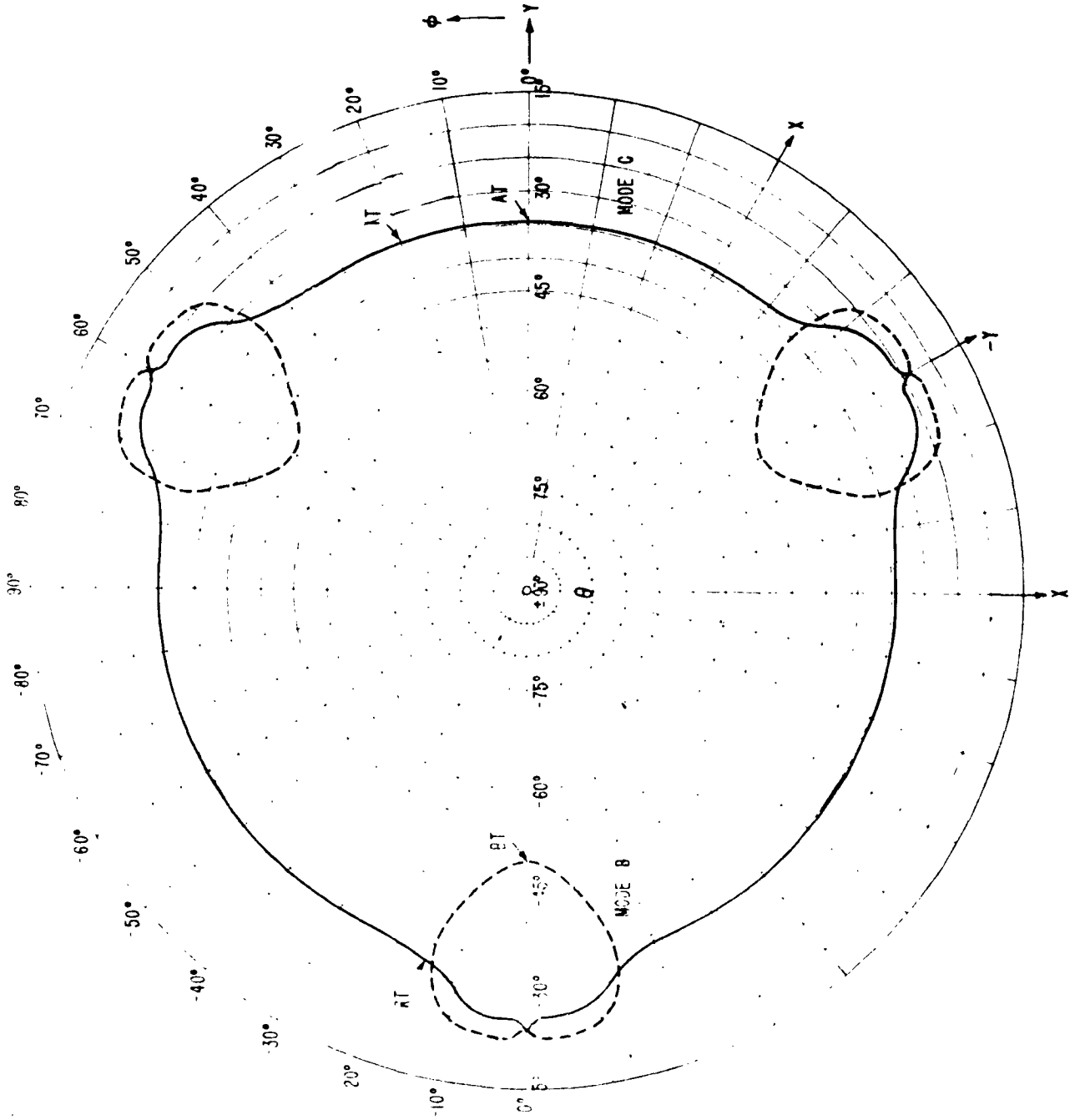

Fig. 20. Locus of $Tf^{(1)} = 0$ for the thickness modes B and C of quartz plates as a function of the angles θ and φ in a polar coordinate system.

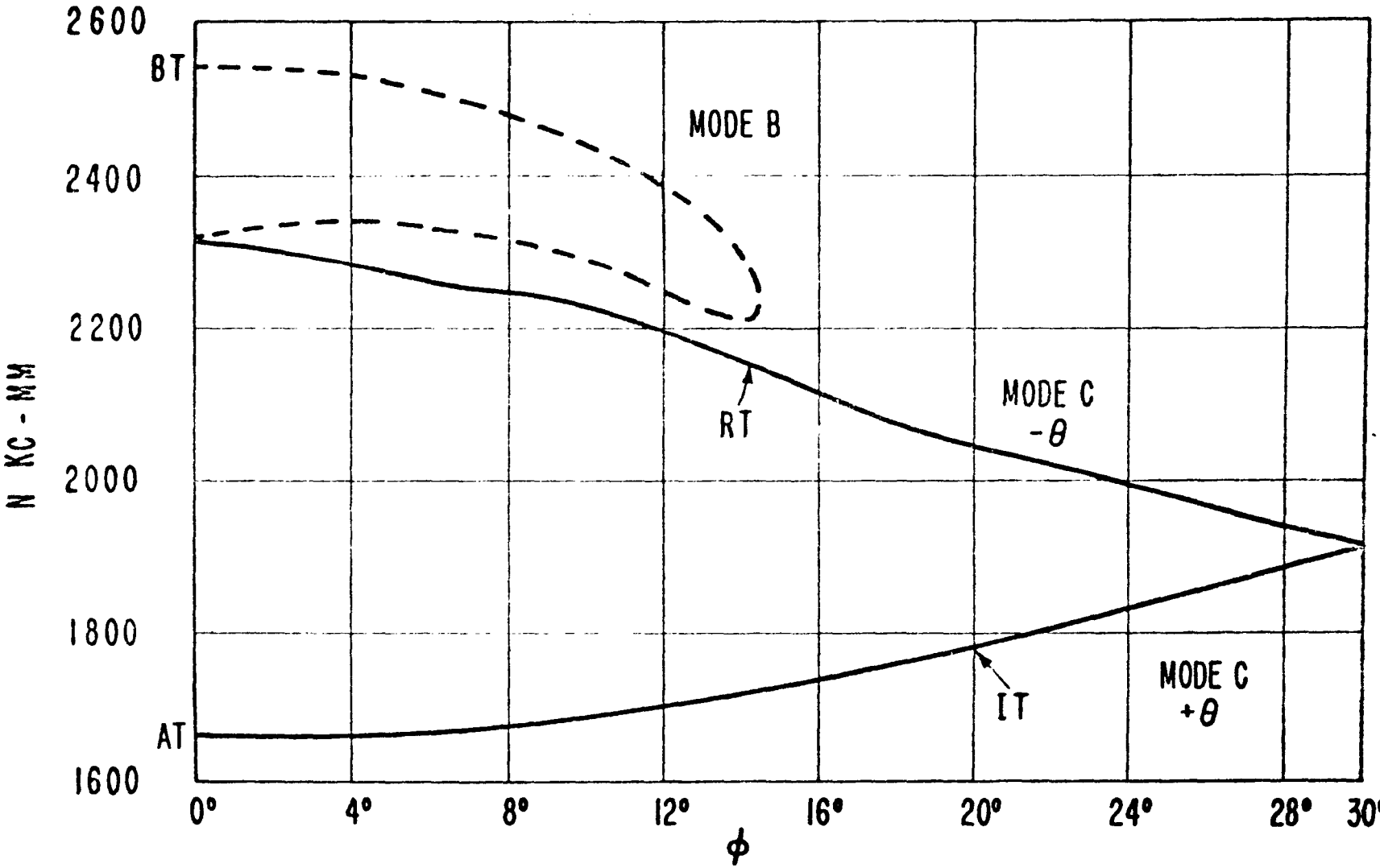

Fig. 21 Frequency constants of modes B and C when $Tf^{(1)} = 0$.

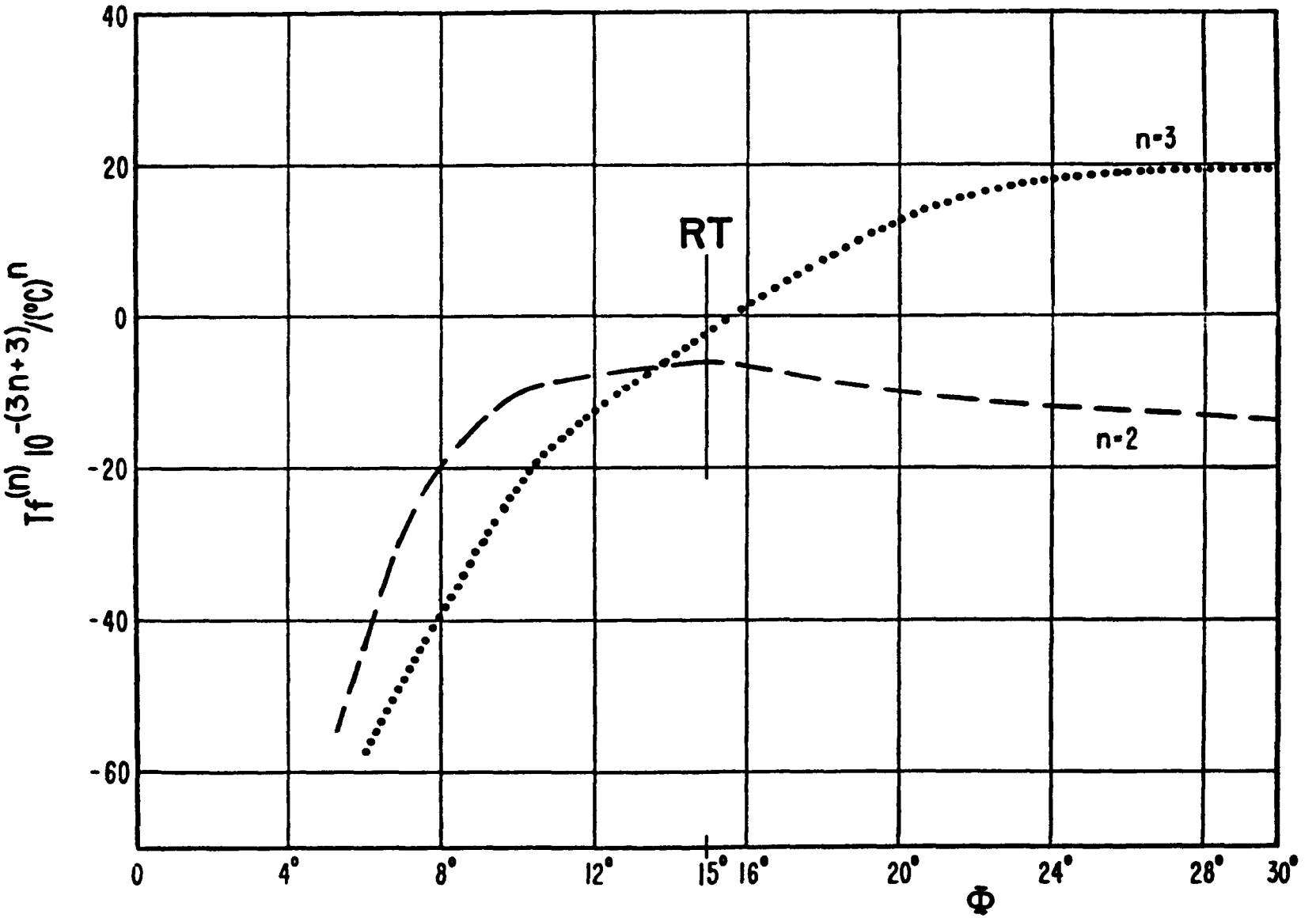

Fig. 22. Second- and third-order temperature coefficients of frequency for the thickness mode C when $Tf^{(1)} = 0$ for negative angles of θ.

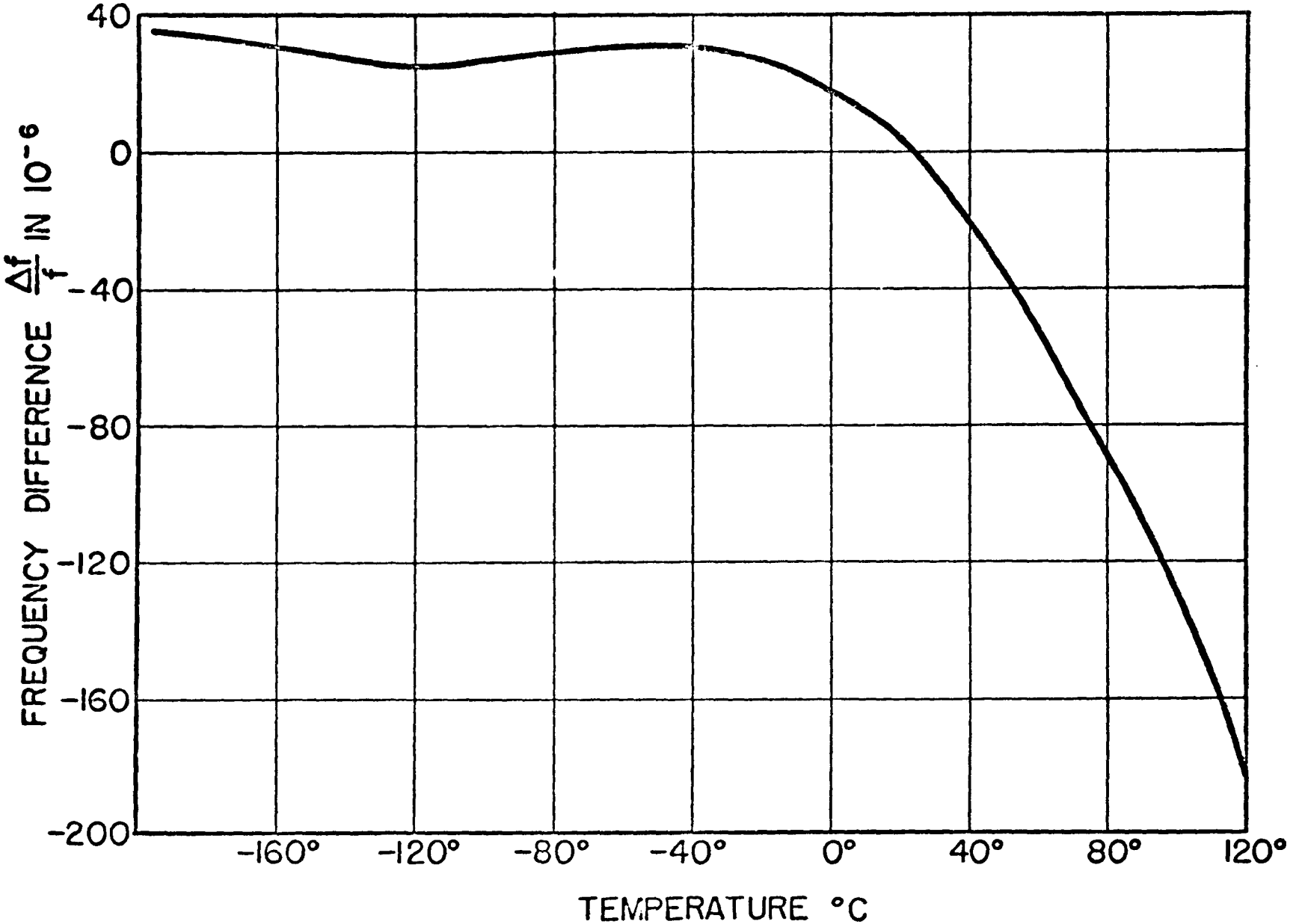

Fig. 23. Quartz cut (yxw ℓ) 10°, −32° having a small temperature dependence in the temperature range −200°C to 0°C.

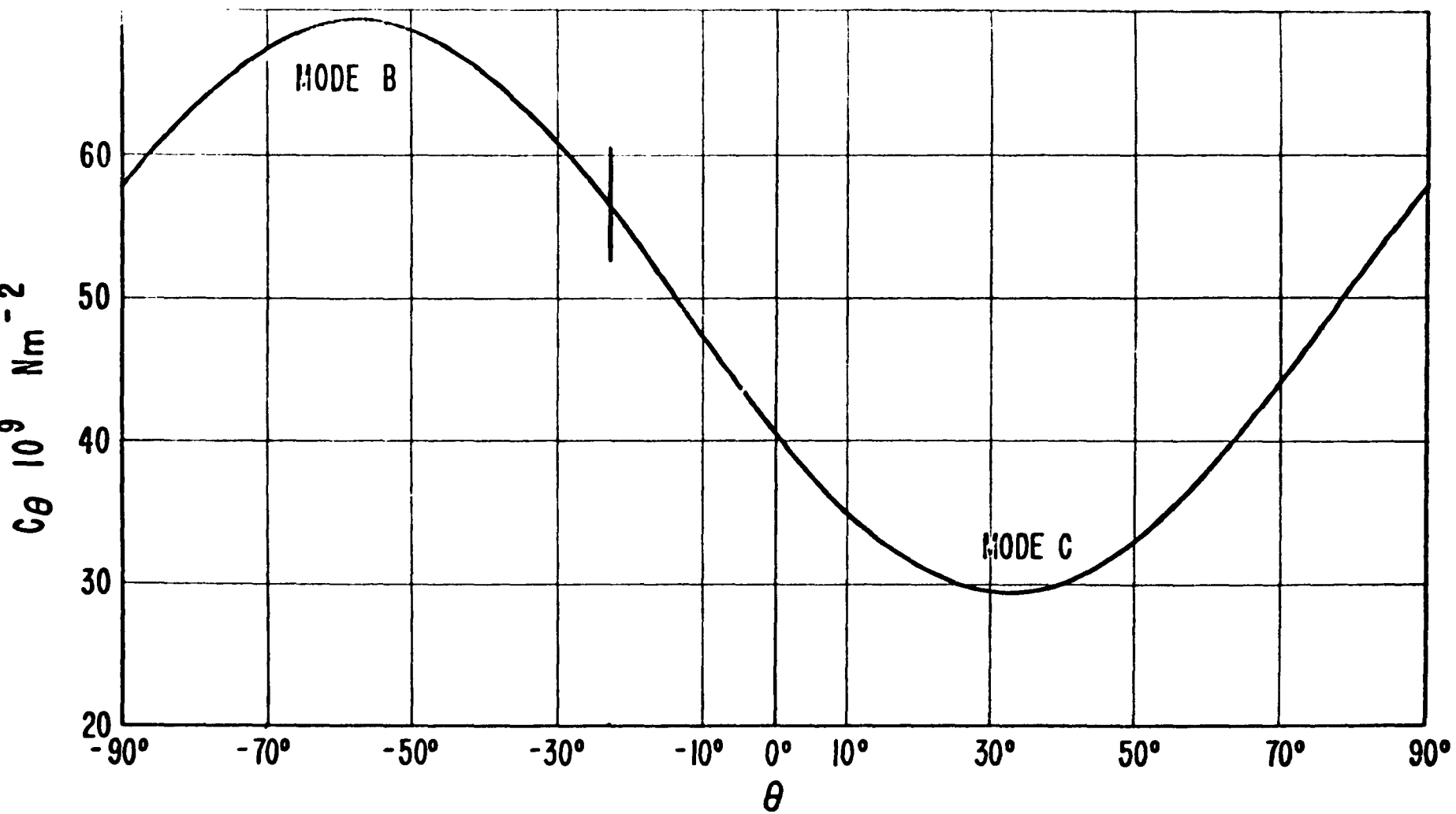

Fig. 24. Elastic stiffnesses c'_{55} (c'_{44}) for rotation (yxℓ) θ as a function of the angle θ.

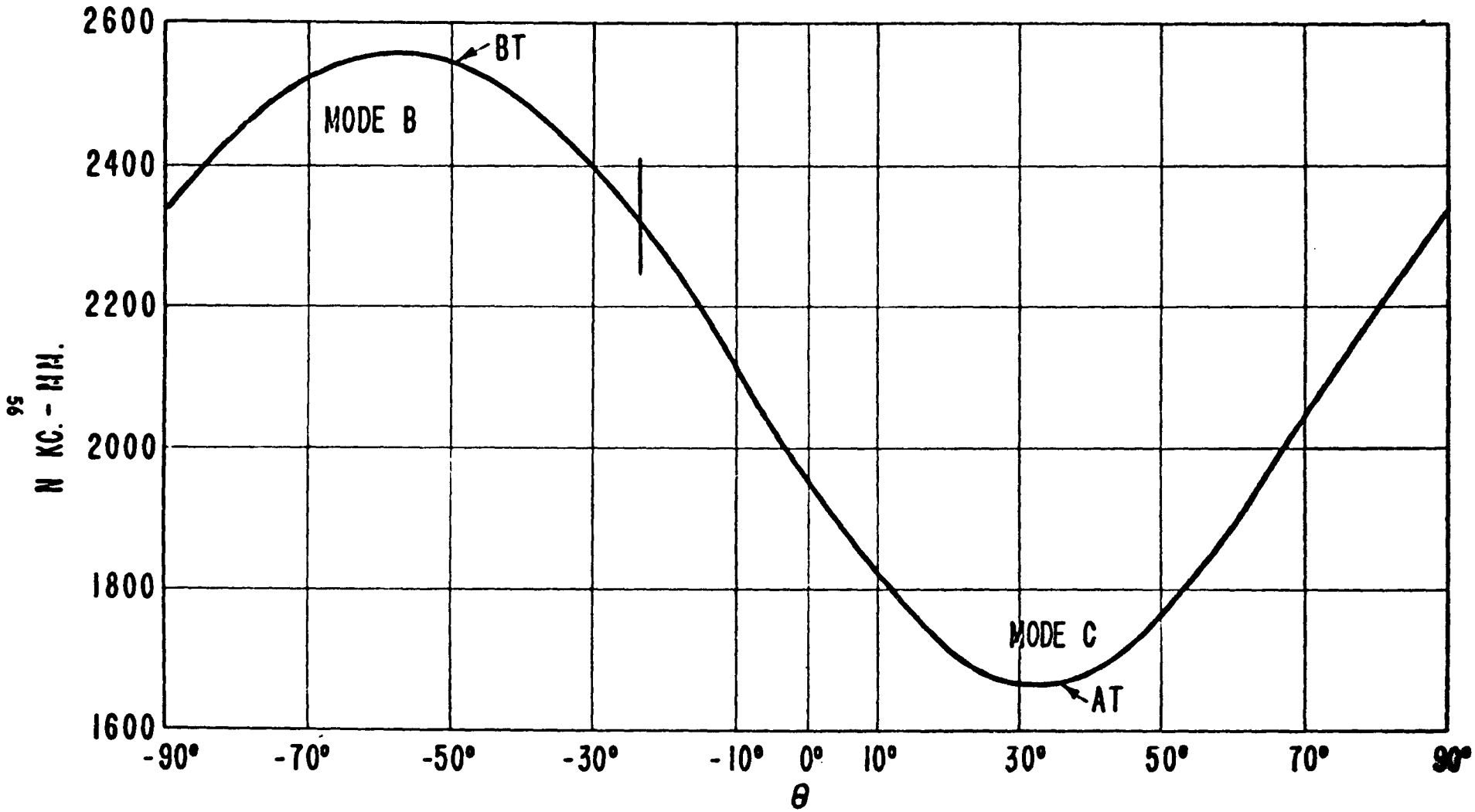

Fig. 25. Frequency constant N of the thickness-shear mode of the plate (yx ℓ) θ as a function of the angle θ.

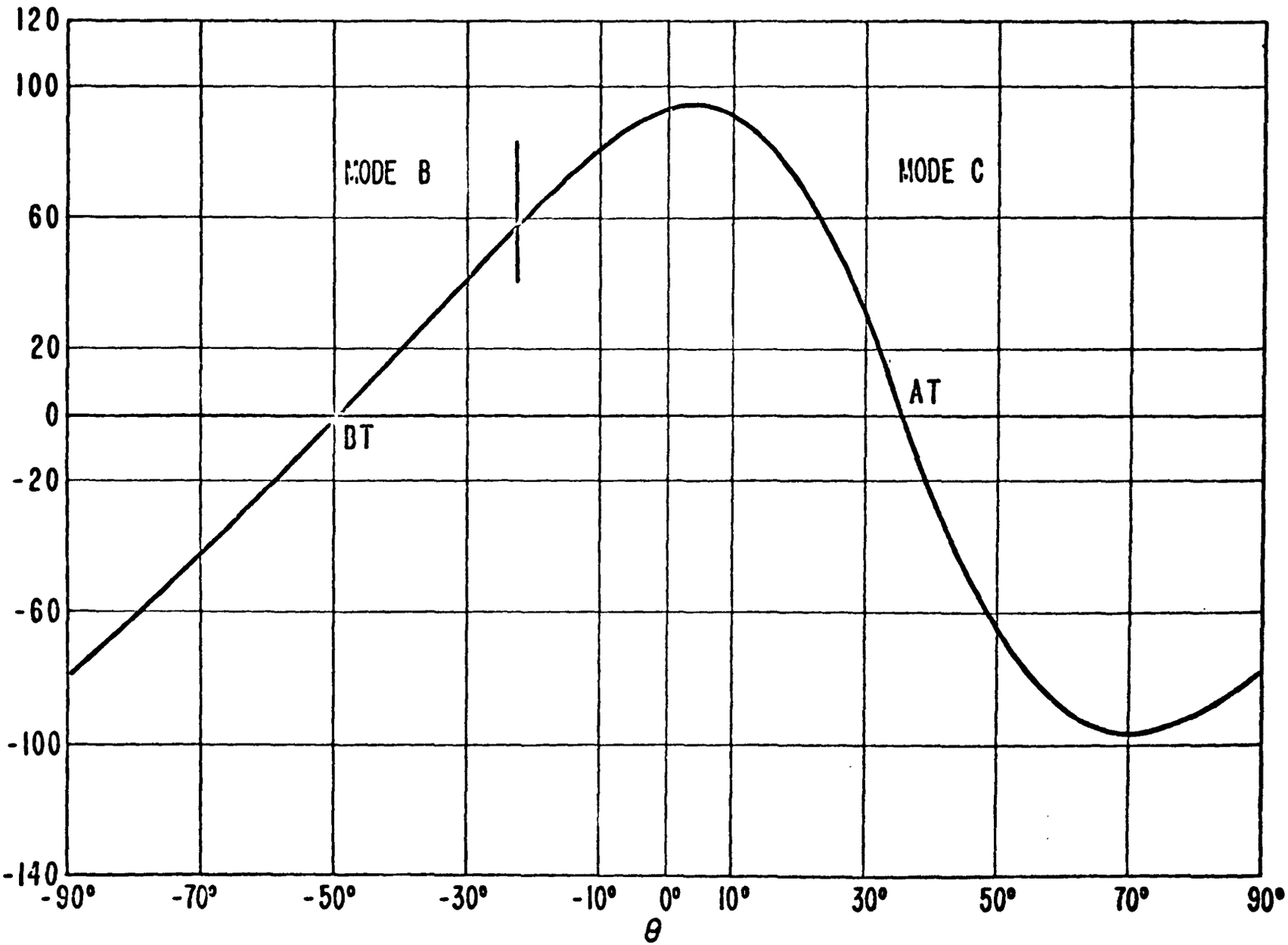

Fig. 26. First-order temperature coefficient of frequency for the plate (yx ℓ) θ

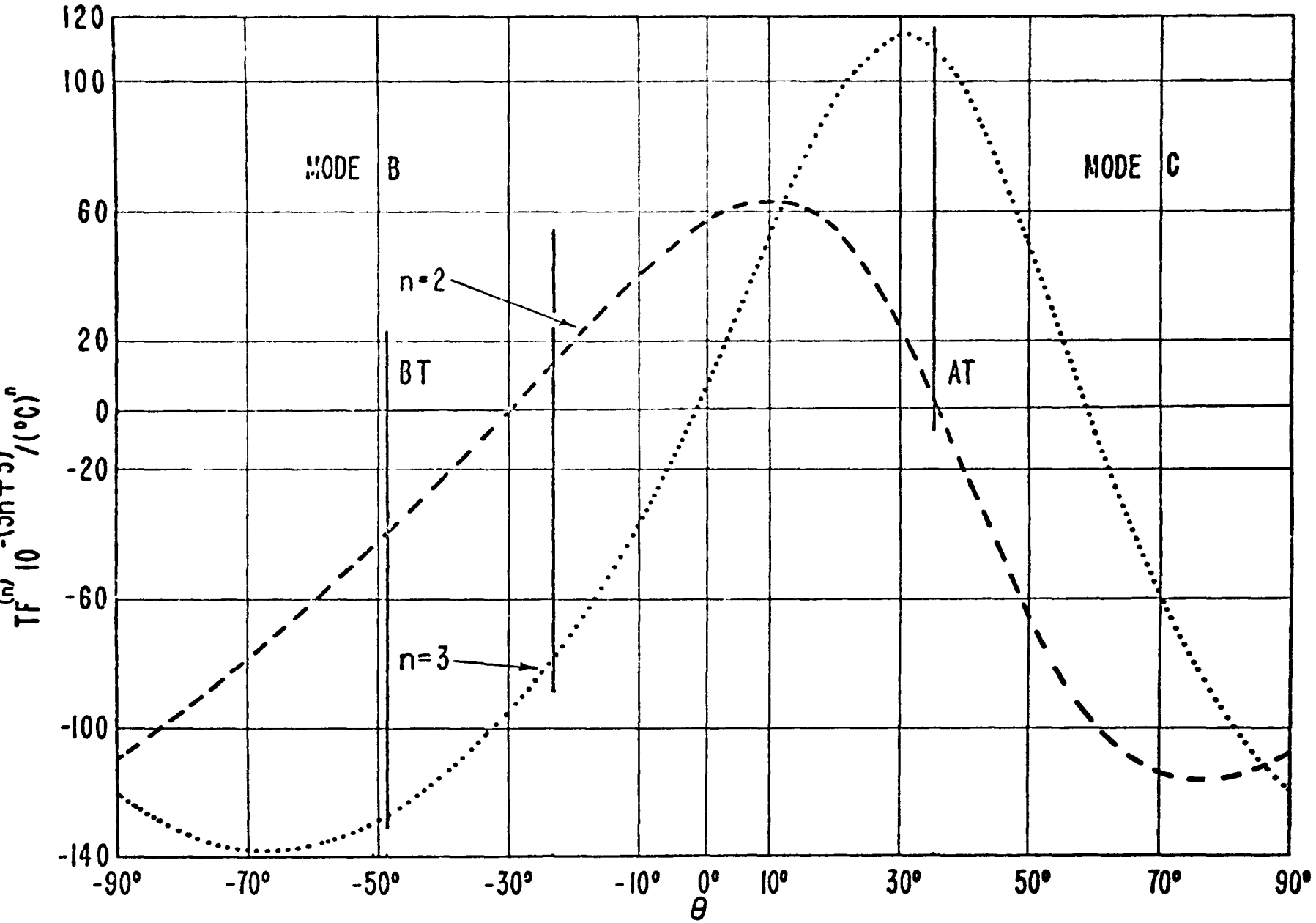

Fig. 27. Second- and third-order temperature coefficients of frequency for the plate (yxℓ) θ vibrating in thickness modes as a function of the angle θ.

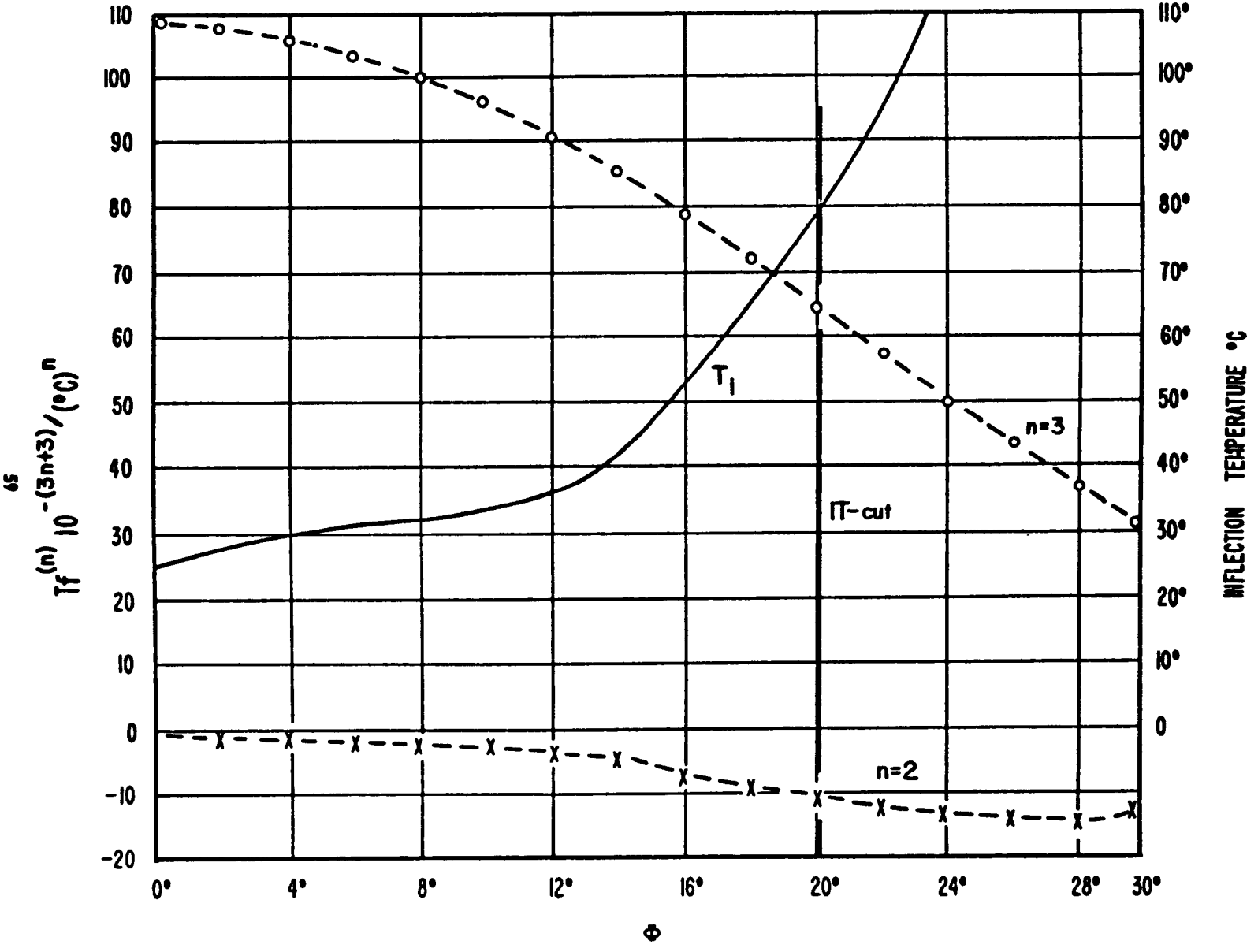

Fig. 28. Second- and third-order temperature coefficients of frequency when $Tf^{(1)} = 0$

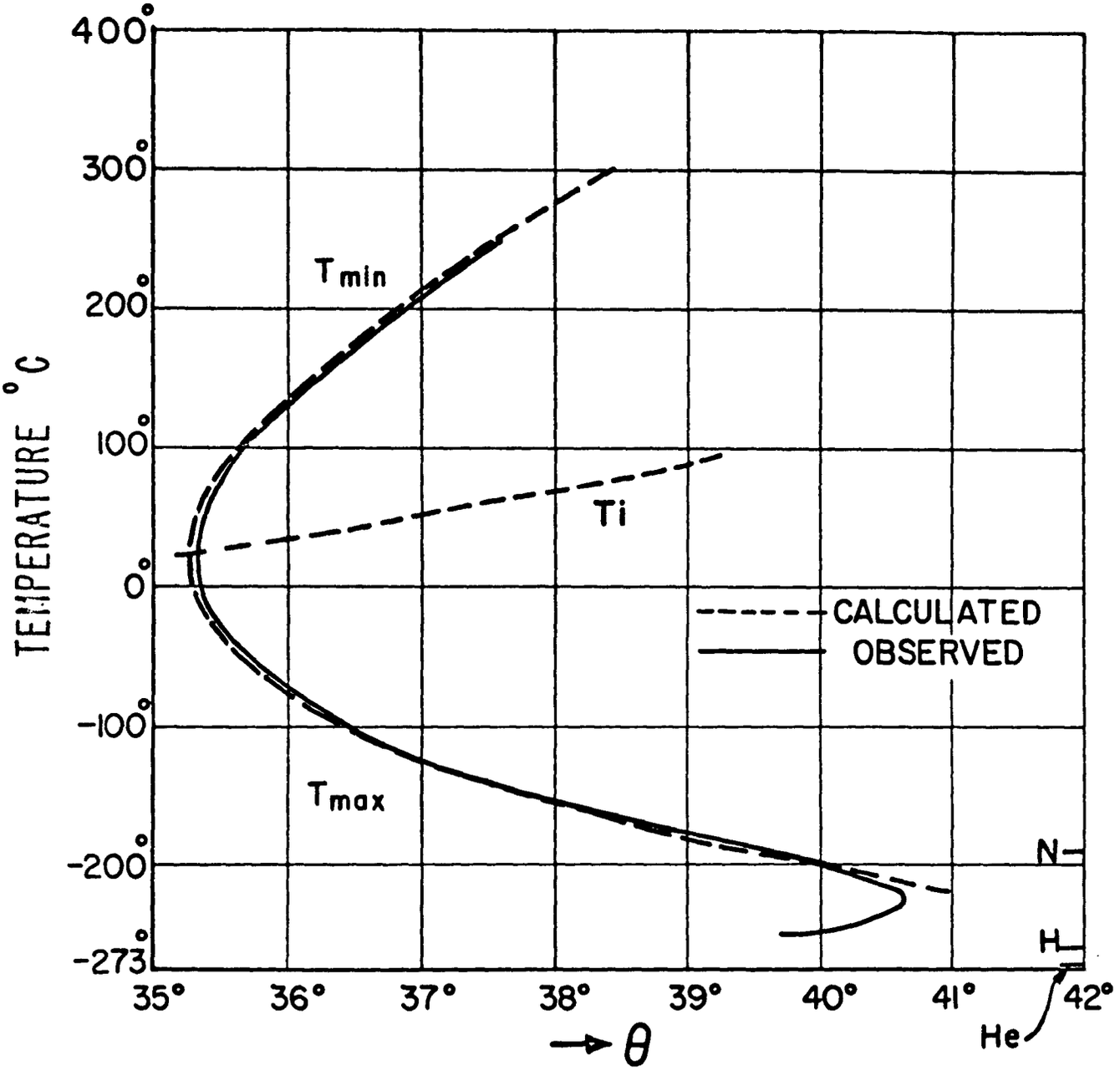

Fig. 29. Observed and calculated temperature of zero temperature coefficient of frequency vs the orientation angle φ for the AT cut.

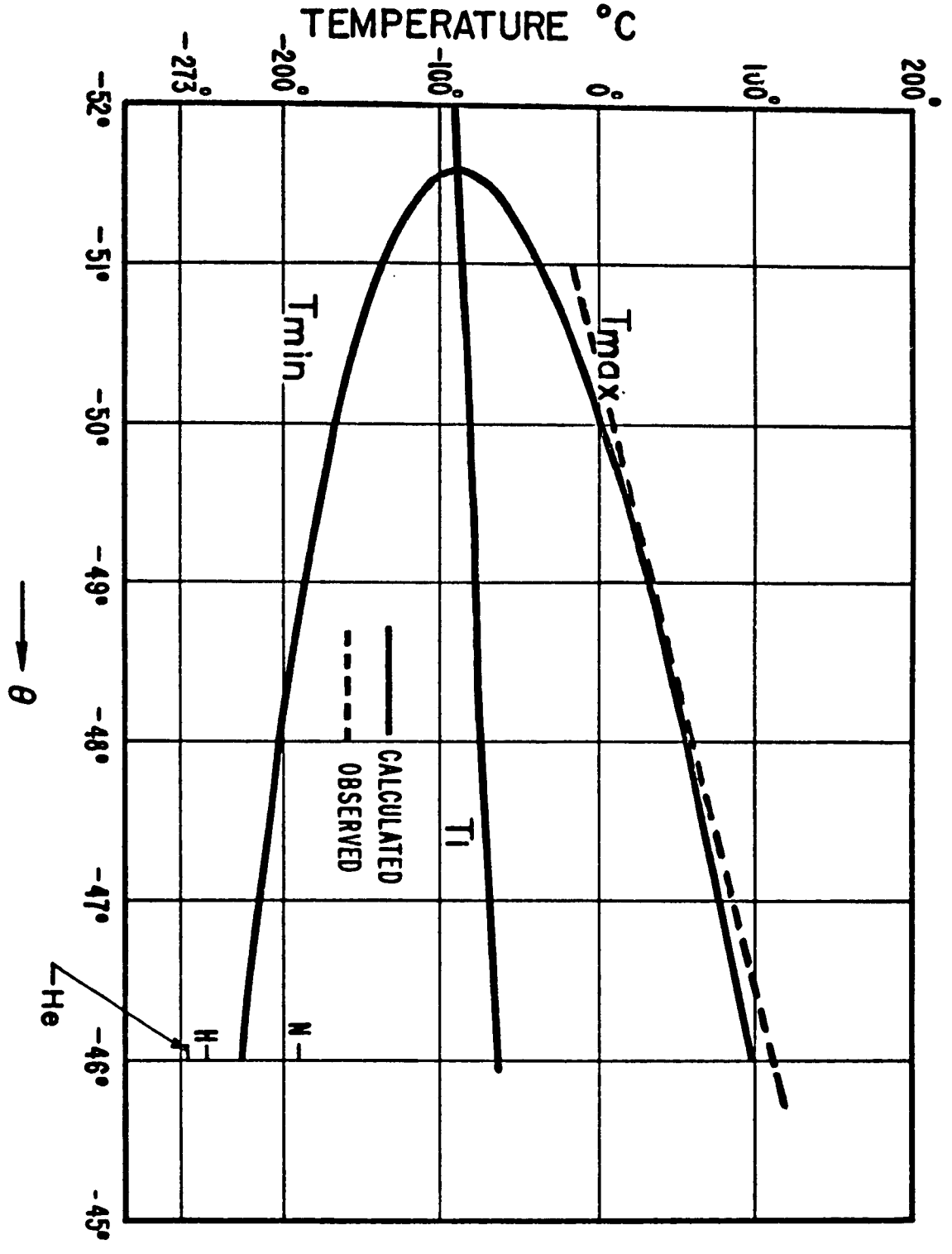

Fig. 30. Observed and calculated temperature of zero temperature coefficient of frequency vs the orientation angle θ for the BT cut.

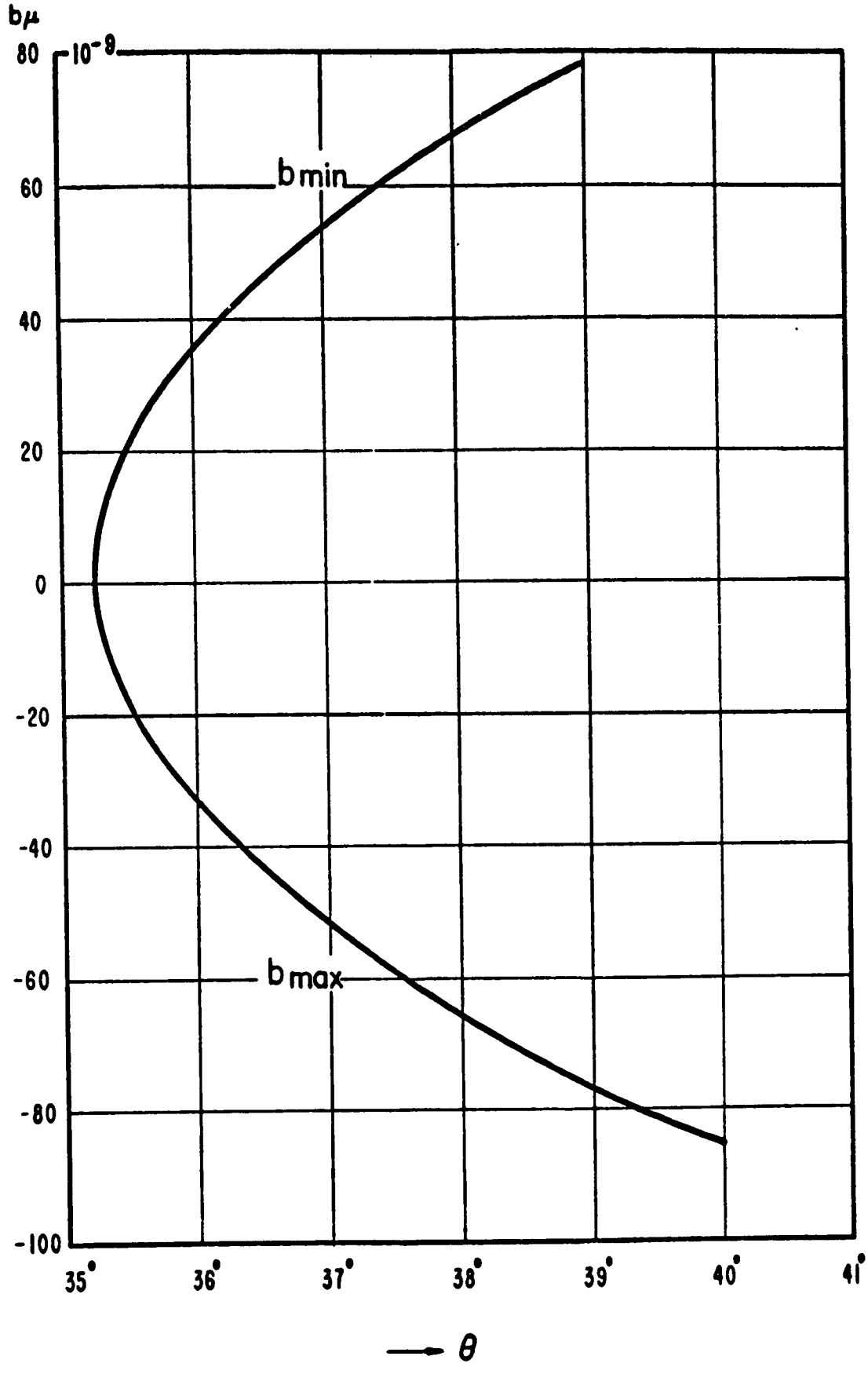

Fig. 31. Calculated values of the parabola constant b_μ in 10^{-9} $(°C)^2$ for the AT cut as a function of the orientation θ corresponding to the zero temperature coefficient curve of Fig. 26.

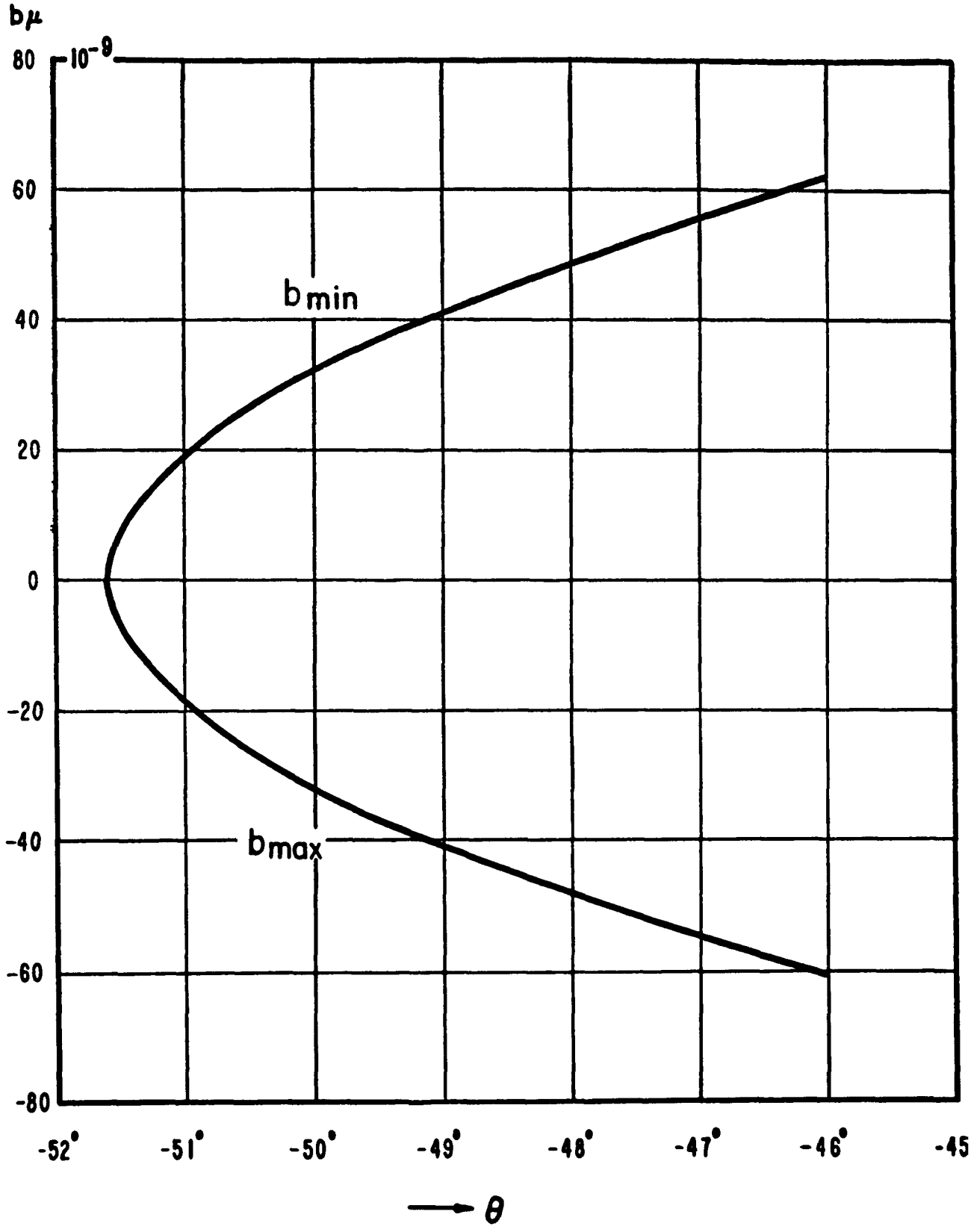

Fig. 32. Calculated values of the parabola constant b_μ in $10^{-9}/(°C)^2$ for the BT cut as a function of the orientation θ corresponding to the zero temperature coefficient curve of Fig. 26.

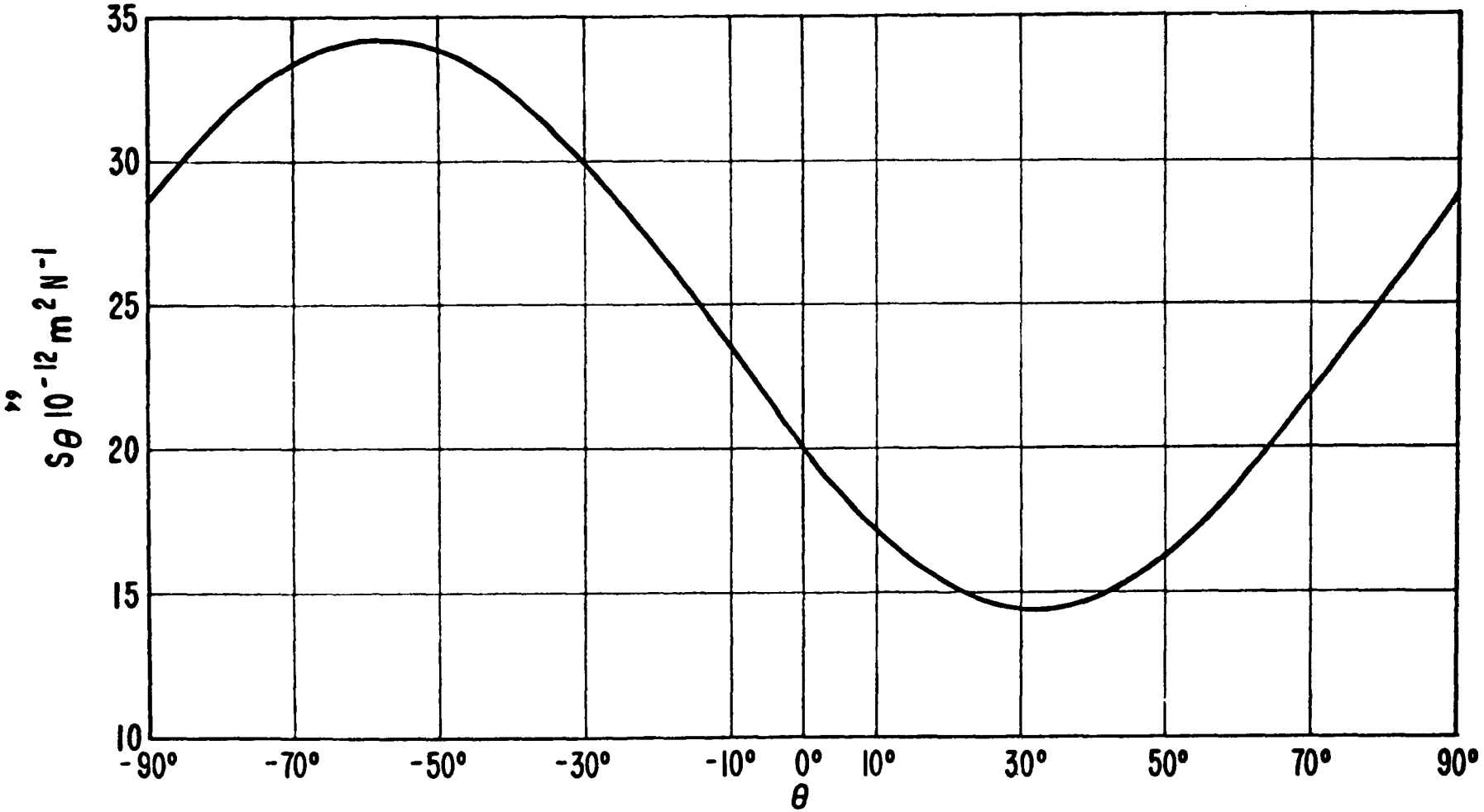

Fig. 33. Elastic compliance s'_{55} ($= s'_{44}$) for rotation (yx ℓ) θ as a function of the angle θ.

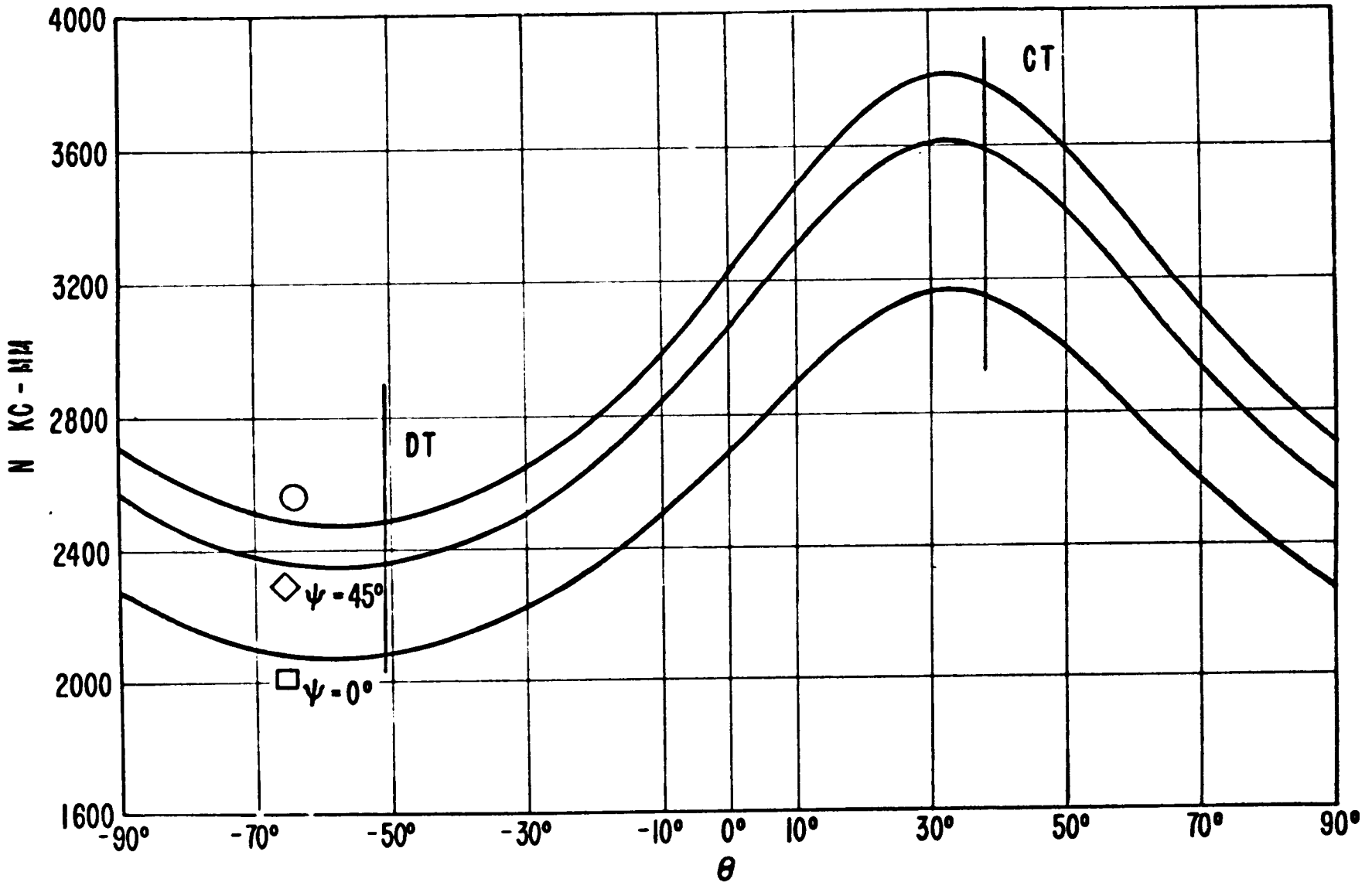

Fig. 34. Frequency constants N for the contour modes $Y_{\theta 0°}$, $Y_{\theta 45°}$, $Y_{\theta O}$ for plates (yx ℓ) θ as a function of the angle θ.

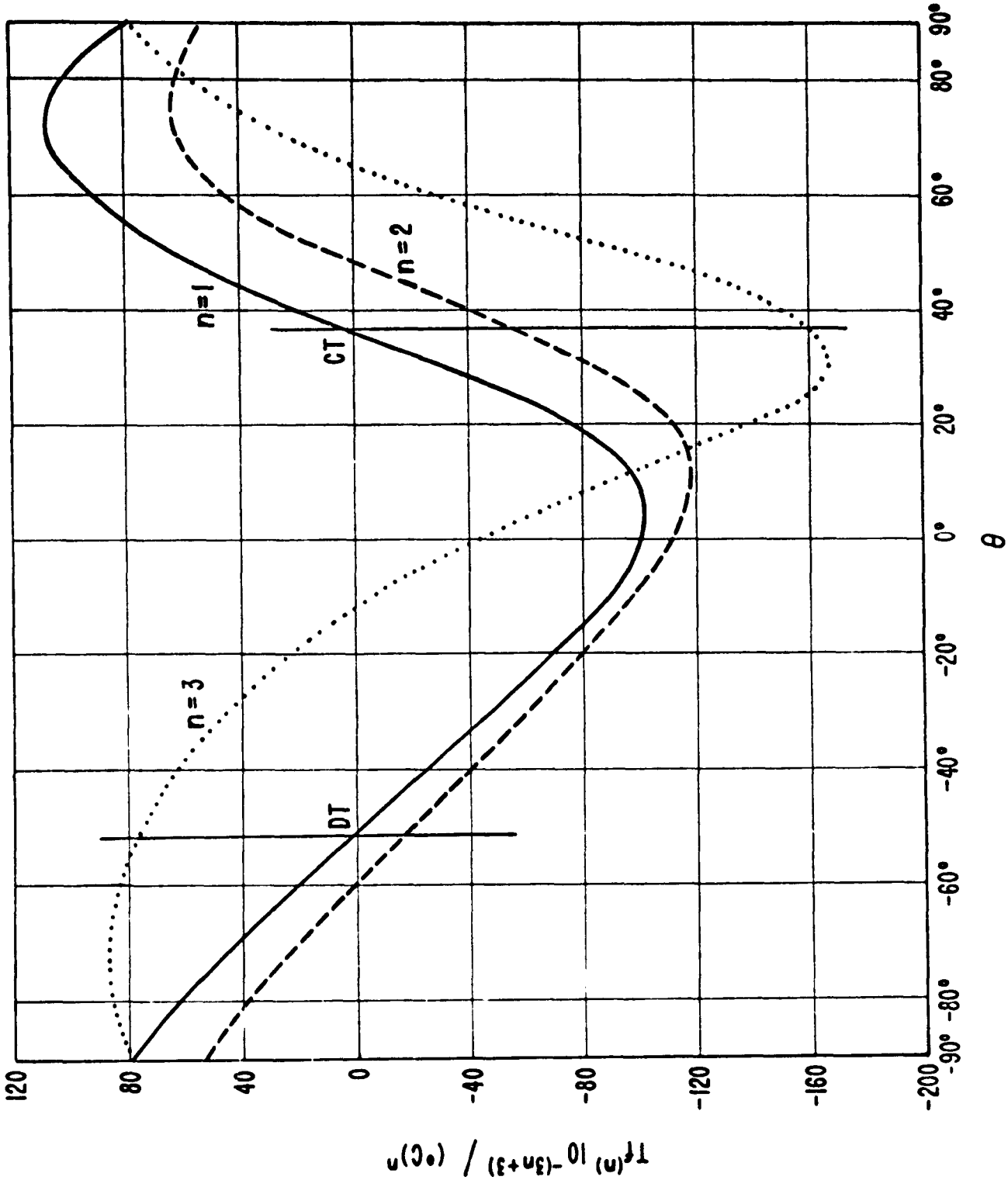

Fig. 35 First-, second- and third-order temperature coefficients of frequency for the plates (yx ℓ) θ vibrating in contour modes as a function of the angle θ

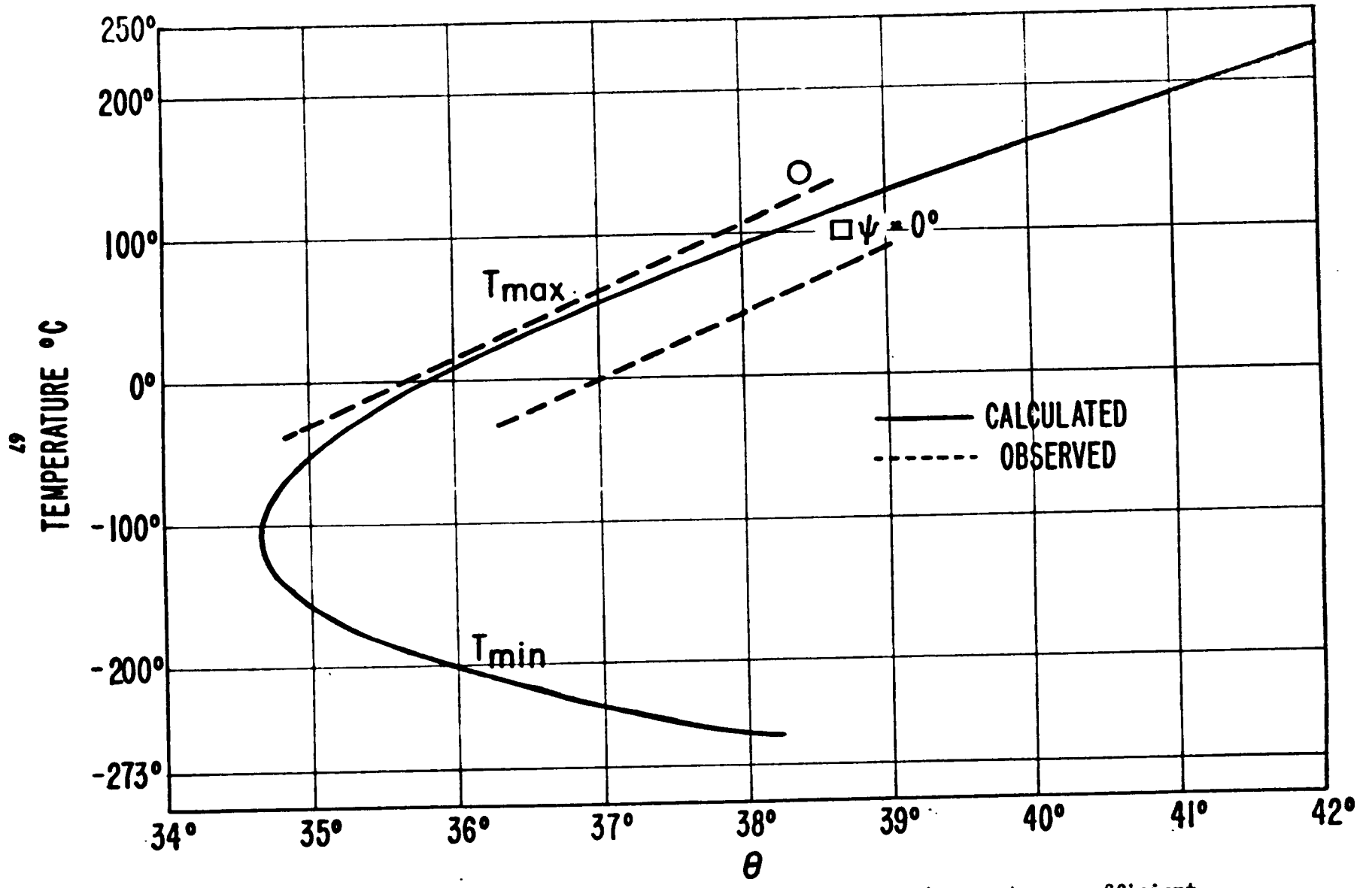

Fig. 36 Observed and calculated temperature of the zero temperature coefficient of frequency first order vs. the orientation angle θ for the CT-cut

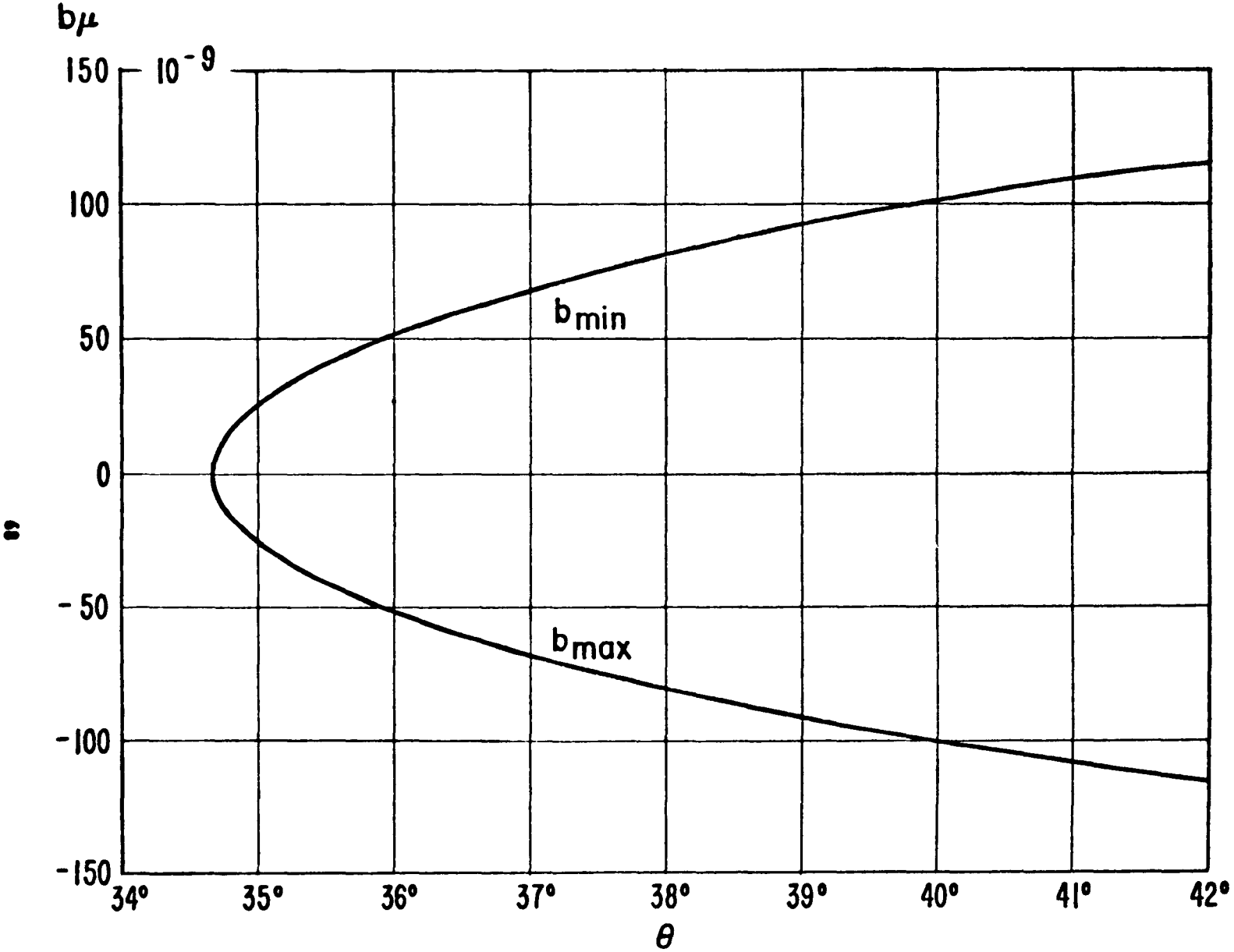

Fig. 37. Calculated values for the parabola constant b_μ in $10^{-9}/(°C)^2$ for the CT cut as a function of the orientation θ corresponding to the zero coefficient curve of Fig. 35.

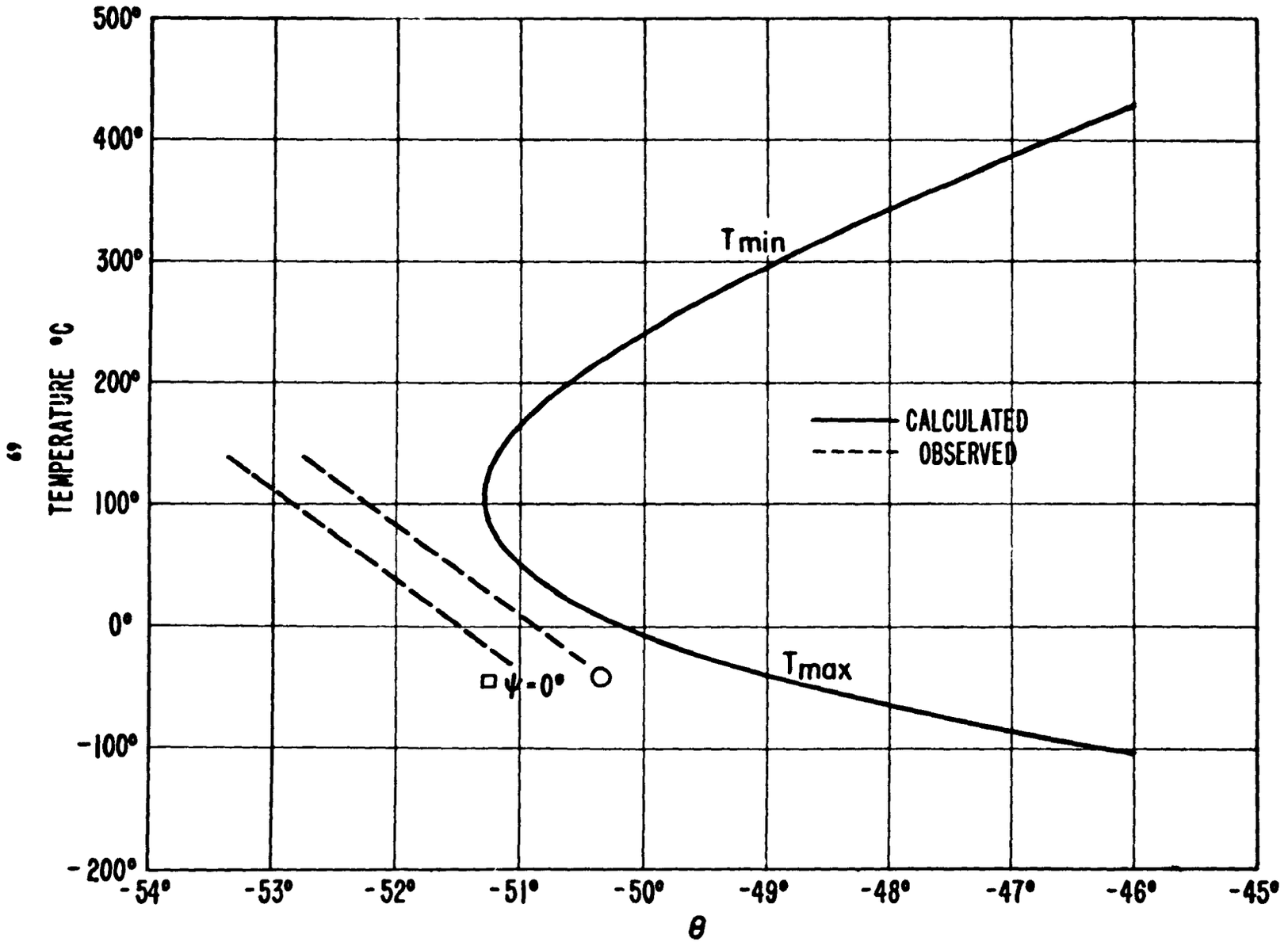

Fig. 38. Calculated temperature of zero temperature coefficient of frequency vs the orientation

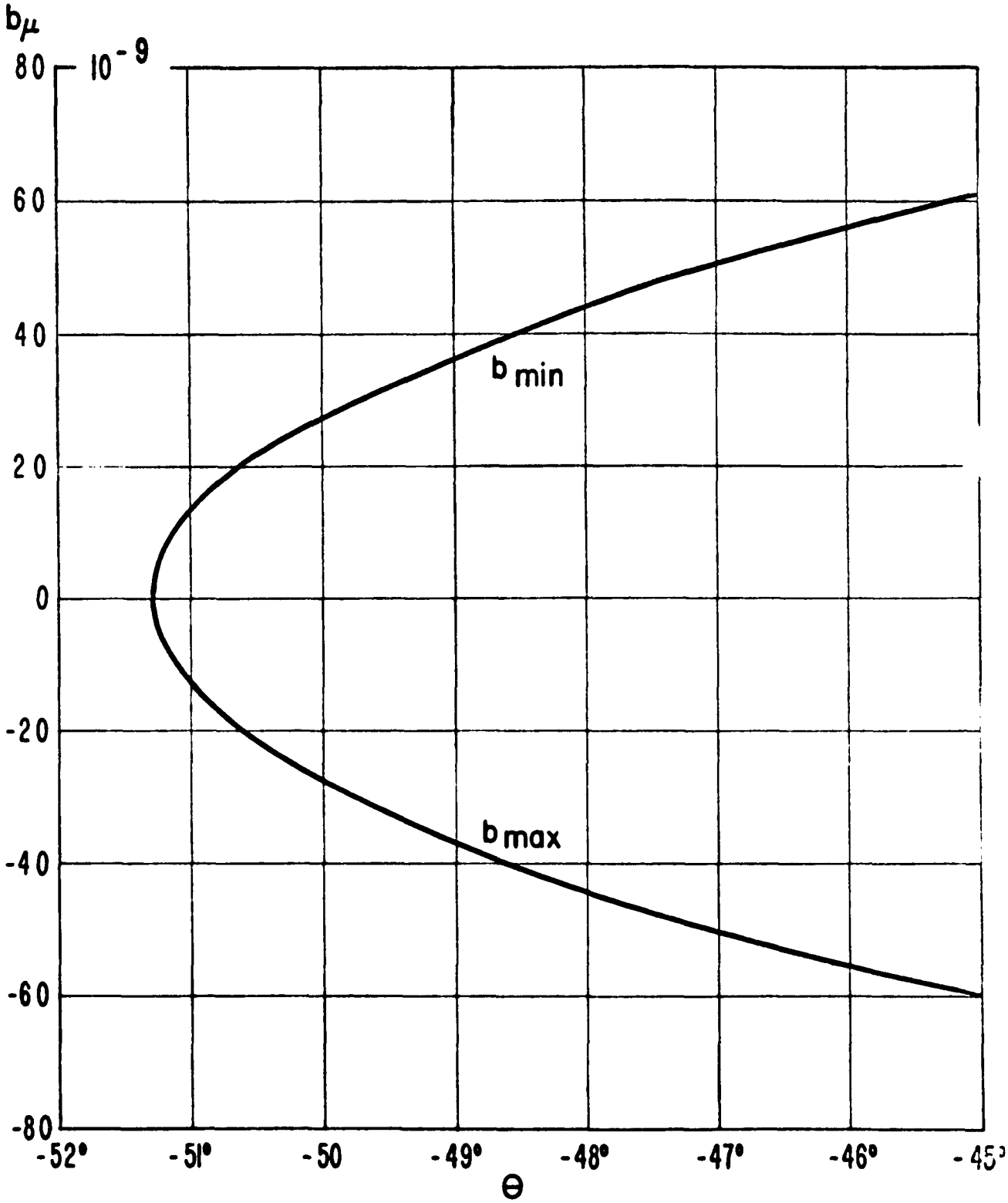

Fig. 39. Calculated values for the parabola constant b_μ in $10^{-9}/(°C)^2$ for the DT cut as a function of the orientation θ corresponding to the zero coefficient temperature curve of Fig. 35.

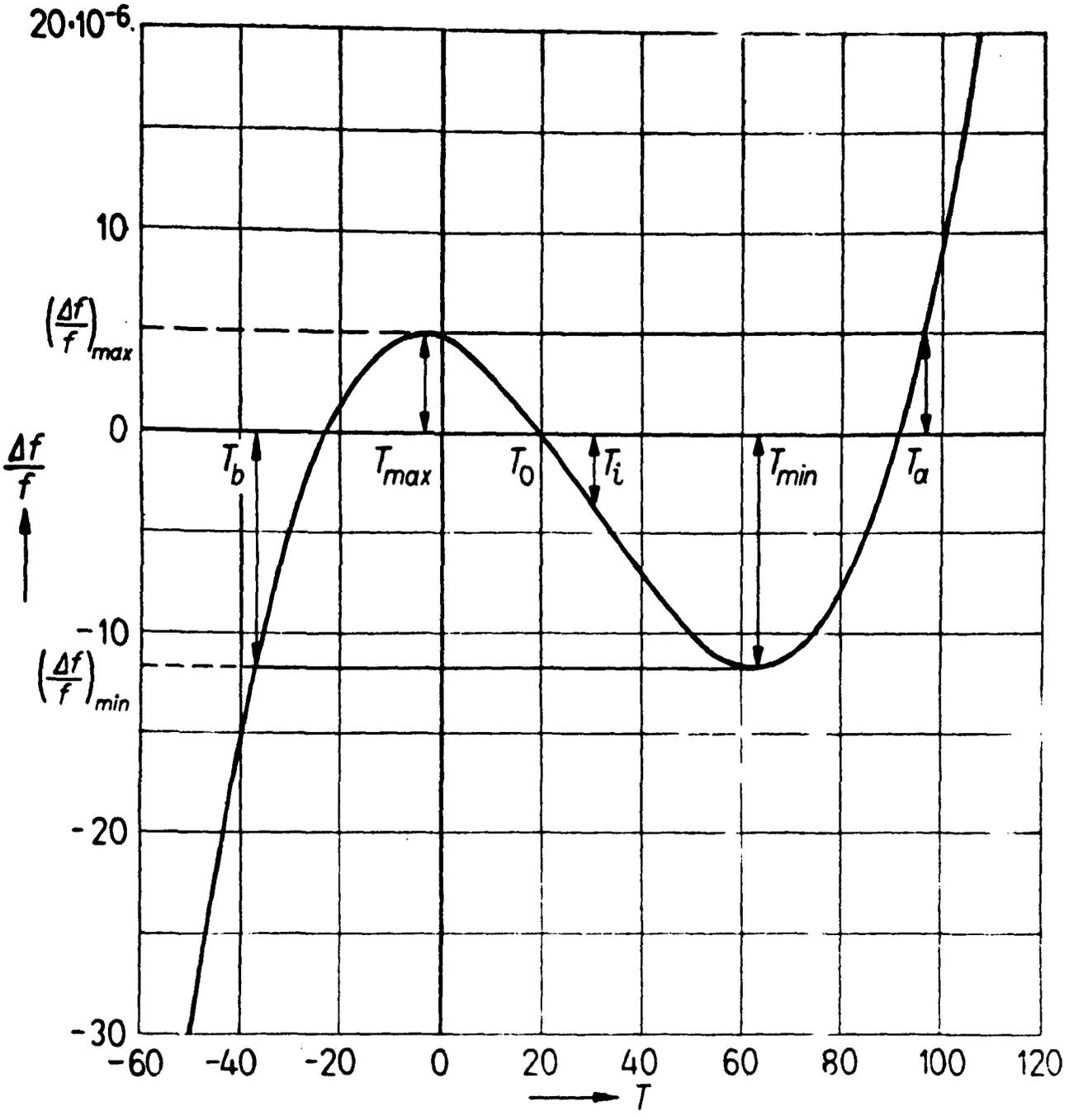

Fig. 40 Schematic frequency temperature behavior of an AT-cut in the vicinity of the first-order temperature coefficient θ

APPENDIX 1
VALUES FOR THE MATERIAL CONSTANTS USED IN THIS INVESTIGATION

In order to determine the values for $Tc_{\lambda\mu}^{(n)}$, $Ts_{\lambda\mu}^{(n)}$ (n = 1, 2, 3), the following values for the material constants of alpha-quartz have been used in the course of this investigation:

1) Elastic stiffnessess $c_{\lambda\mu}$ of alpha-quartz are given in Table 4; elastic compliances $s_{\lambda\mu}$ of alpha-quartz, in Table 10.

2)
$$e_{11} = 0.171$$
$$e_{14} = 0.0403$$

Piezoelectric stress constants in Cm^{-2} of alpha-quartz [9].

3)
$$\epsilon_{11}^{T} = \epsilon_{22}^{T} = 39.97 \qquad \epsilon_{11}^{S} - \epsilon_{11}^{T} = -0.76$$
$$\epsilon_{33}^{T} = 41.03 \qquad \epsilon_{33}^{S} - \epsilon_{33}^{T} = 0$$

Dielectric constants in 10^{-12} F m^{-1} of alpha-quartz.

4)
$$\alpha_{11}^{(1)} = \alpha_{22}^{(1)} = 13.71\ 10^{-6}/^{\circ}C$$
$$\alpha_{33}^{(1)} = 7.48$$
$$\alpha_{11}^{(2)} = \alpha_{22}^{(2)} = 6.5\ 10^{-9}/(^{\circ}C)^2$$
$$\alpha_{33}^{(2)} = 2.9$$
$$\alpha_{11}^{(3)} = \alpha_{22}^{(3)} = -\ 1.9\ 10^{-12}/(^{\circ}C)^3$$
$$\alpha_{33}^{(3)} = -\ 1.5$$

Coefficients of thermal expansion of alpha-quartz.

5)
$$\rho = 2.650\ 10^{3} Nm^{-4}s^{2}$$
$$T_{\rho}^{(1)} = -\ 34.92\ 10^{-6}/(^{\circ}C)$$
$$T_{\rho}^{(2)} = -\ 15.9\ 10^{-9}/(^{\circ}C)^2$$
$$T_{\rho}^{(3)} = 5.30\ 10^{-12}/(^{\circ}C)^3$$

Density and its temperature coefficients of alpha-quartz.

APPENDIX 2

ANALYTICAL EXPRESSIONS FOR THE FREQUENCY-TEMPERATURE CHARACTERISTICS

For practical application, as well as for theoretical consideration, it is necessary to define the frequency-temperature behavior quantitatively, introducing some constants—the temperature coefficients. The measured frequency f of a crystal unit as a function of the temperature T can be developed in a power series in the vicinity of the frequency f_o at the arbitrary temperature T_o:

$$\frac{f - f_o}{f_o} = \frac{\Delta f}{f_o} = a_o(\theta)[T - T_o] + b_o(\theta)[T - T_o]^2 + c_o(\theta)[T - T_o]^3 + \cdots, \tag{A2-1}$$

where $a_o(\theta)$, $b_o(\theta)$, and $c_o(\theta)$ are the first-, second- and third-order temperature coefficients of frequency as defined by

$$a_o(\theta) = \frac{1}{f_o}\left(\frac{\partial f}{\partial T}\right)_o, \quad b_o(\theta) = \frac{1}{2f_o}\left(\frac{\partial^2 f}{\partial T^2}\right)_o, \quad c_o(\theta) = \frac{1}{6f_o}\left(\frac{\partial^3 f}{\partial T^3}\right)_o. \tag{A2-2}$$

These constants are functions of the orientation and the other influences mentioned. The temperature coefficient of the frequency is given by

$$Tf = \frac{1}{f_o}\frac{\partial f}{\partial T} = a_o(\theta) + 2b_o(\theta)[T - T_o] + 3c_o(\theta)[T - T_o]^2. \tag{A2-3}$$

For the −60° to +100°C temperature range usually considered, temperature coefficients of order higher than three can be neglected. The three temperature coefficients can be related to the corresponding coefficients of the elastic constants involved and the coefficients of expansion.

Relating the power series to the temperature T_1 instead of the temperature T_o, we can write Eq. (A2-1) as

$$\frac{f - f_1}{f_1} = \frac{\Delta f}{f_1} = a_1(\theta)[T - T_1] + b_1(\theta)[T - T_1]^2 + c_1(\theta)[T - T_1]^3 + \cdots \tag{A2-4}$$

where the coefficients $a_1(\theta)$, $b_1(\theta)$, and $c_1(\theta)$ are referred to $a_o(\theta)$, $b_o(\theta)$, and $c_o(\theta)$ by the following equations

$$a_1 = \frac{1}{p}[a_o + 2b_o(T_1 - T_o) + 3c_o(T_1 - T_o)^2]$$

$$b_1 = \frac{1}{p}[b_o + 3c_o(T_1 - T_o)] \tag{A2-5}$$

$$c_1 = \frac{1}{p} c_o \qquad \text{(A2-5)}$$

$$p = 1 + a_o(T_1 - T_o) + b_o(T_1 - T_o)^2 + c_o(T_1 - T_o)^3.$$

A family of frequency-temperature curves is then given by the following expressions, assuming the change of the three temperature coefficients to be linear with angle of orientation:

$$\frac{\Delta f}{f} = a_o(\theta_o)[T - T_o] + b_o(\theta_o)[T - T_o]^2 + c_o(\theta_o)[T - T_o]^3 + \left\{ \frac{\partial a_o(\theta)}{\partial \theta}[T - T_o] + \frac{\partial b_o(\theta)}{\partial \theta}[T - T_o]^2 + \frac{\partial c_o(\theta)}{\partial \theta}[T - T_o]^3 \right\}(\theta - \theta_o), \qquad \text{(A2-6)}$$

where $\partial a_o(\theta)/\partial\theta$, $\partial b_o(\theta)/\partial\theta$, and $\partial c_o(\theta)/\partial\theta$ are the derivatives with respect to the angle of the three temperature coefficients, respectively. The linear terms are sufficient for a 1° range; higher terms for the derivatives of the temperature coefficients must be introduced when considering a wider range of orientation.

In the vicinity of a zero angle of orientation for the frequency, when a_o is zero or very small, two types of frequency-temperature behavior may be distinguished.

a. In case where b_o is rather small and c_o large, the frequency-temperature characteristic has a cubic form. An example is the AT-cut where generally b is smaller than $5 \cdot 10^{-9}/(°C)^2$ and c in the order $100 \cdot 10^{-12}/(°C)^3$. Another example is the GT-cut where both the second- and third-order temperature coefficients are very small.

b. In most of the other cuts, the second-order temperature coefficient is predominant, giving a parabolic frequency-temperature characteristic.

Considering first the frequency-temperature characteristics of an AT-type crystal, a typical frequency-temperature curve for an angle of orientation, giving a small negative value for the first-order temperature coefficient of frequency, is shown in Fig. 40. Some characteristic quantities for the frequency-temperature behavior are: maximum and minimum temperature (T_{max}, T_{min}), together with the corresponding maximum and minimum frequency change ($\Delta f/f_{max}$, $\Delta f/f_{min}$); the inflection temperature (T_i), i.e., the temperature for which the derivative of the temperature coefficient of frequency becomes zero; and the temperatures T_a and T_b, where in the case considered $T_a - T_b = 2(T_{min} - T_{max})$.

The analytical expressions for T_{min} and T_{max} follow from $Tf = 0$:

$$T_{\substack{min \\ max}} - T_o = \frac{-b_o \pm \sqrt{b_o^2 - 3a_o c_o}}{3c_o}. \qquad \text{(A2-7)}$$

The corresponding frequency deviation is given by

$$\frac{(\Delta f)}{f_{\substack{max \\ min}}} = \frac{\pm 2\sqrt{b_o^2 - 3a_oc_o}^{\,3} + 2b_o^3 - 9a_ob_oc_o}{27c_o^2}. \qquad \text{(A2-8)}$$

From this follows the expressions for the difference between the maximum and minimum temperatures

$$T_{min} - T_{max} = \frac{2\sqrt{b_o^2 - 3a_oc_o}}{3c_o}, \qquad \text{(A2-9)}$$

and the corresponding total frequency change

$$\left(\frac{\Delta f}{f}\right)_{max} - \left(\frac{\Delta f}{f}\right)_{min} = \frac{4}{27}\,\frac{\sqrt{b_o^2 - 3a_oc_o}^{\,3}}{c_o^2}. \qquad \text{(A2-10)}$$

The inflection temperature T_i is defined by $\frac{\partial Tf}{\partial T} = \frac{\partial^2 f}{\partial T^2} = 0$, hence

$$T_i - T_o = -\frac{b_o}{3c_o}. \qquad \text{(A2-11)}$$

The following equations are of practical interest:

$$\frac{\left(\frac{\Delta f}{f}\right)_{max} - \left(\frac{\Delta f}{f}\right)_{min}}{(T_{min} - T_{max})^3} = \frac{c_o}{2}, \qquad \text{(A2-12)}$$

and

$$\frac{\left(\frac{\Delta f}{f}\right)_{max} - \left(\frac{\Delta f}{f}\right)_{min}}{T_{min} - T_{max}} = \frac{2}{9} \cdot \frac{b_o^2 - 3a_oc_o}{c_o}. \qquad \text{(A2-13)}$$

Introducing the inflection temperature T_i as reference temperature instead of T_o, where $T_i - T_o = -b_o/3c_o$, then $b_i = 0$ and Eq. (A2-1) simplifies to

$$\frac{f - f_i}{f_i} = \frac{\Delta f}{f} = a_i(T - T_i) + c_i(T - T_i)^3, \qquad \text{(A2-14)}$$

where

$$a_i = \frac{1}{p}\,\frac{3a_oc_o - b_o^2}{3c_o}$$

$$c_i = \frac{1}{p}\,c_o \qquad \text{(A2-15)}$$

$$p = 1 + \frac{2b_o^3 - 9a_ob_oc_o}{27c_o^2} .$$

Equations (A2-7) and (A2-8) then simplify to

$$T_{\substack{\min\\ \max}} - T_i = \pm\sqrt{\frac{-a_i}{3c_i}} , \qquad \text{(A2-16)}$$

and

$$\left(\frac{\Delta f}{f}\right)_{\substack{\max\\ \min}} = \pm\, 2\sqrt{\frac{-a_i^3}{27c_i}} . \qquad \text{(A2-17)}$$

For Equations (A2-9) and (A2-10), we obtain

$$T_{min} - T_{max} = 3\sqrt{\frac{-a_i}{3c_i}} , \qquad \text{(A2-18)}$$

and

$$\left(\frac{\Delta f}{f}\right)_{max} - \left(\frac{\Delta f}{f}\right)_{min} = 4\sqrt{\frac{-a_i^3}{27c_i}} . \qquad \text{(A2-19)}$$

Equations (A2-12) and (A2-13) simplify to

$$\frac{\left(\frac{\Delta f}{f}\right)_{max} - \left(\frac{\Delta f}{f}\right)_{min}}{\left(T_{min} - T_{max}\right)^3} = \frac{c_i}{2} \; ; \; \frac{\left(\frac{\Delta f}{f}\right)_{max} - \left(\frac{\Delta f}{f}\right)_{min}}{T_{min} - T_{max}} = -\frac{2}{3}a_i . \qquad \text{(A2-20)}$$

The above formulae describe the frequency-temperature behavior of an AT cut with sufficient accuracy in the temperature range considered.

For the AT-type resonator, there is one special angle of orientation θ_J for which for the inflection temperature T_J, the first-order temperature coefficient a_J is zero, so that for this special orientation the frequency-temperature characteristic is represented by a single term

$$\frac{\Delta f}{f} = c_J(\theta_J)\,[T - T_J]^3 \; , \; a_J(\theta_J) = 0 \; , \; b_J(\theta_J) = 0 . \qquad \text{(A2-21)}$$

This equation may be called the main frequency-temperature characteristic.

In case of the BT-type quartz resonator and similar cuts with a parabolic frequency-temperature characteristic, the relations given above hold. In the temperature range considered, only one maximum of the frequency occurs. Instead of the inflection temperature T_i, the temperature T_{max} at which the frequency maximum occurs is a significant temperature.

The frequency-temperature characteristic related to its maximum is given by

$$\frac{\Delta f}{f} = b_m(\theta)\,[T - T_{max}]^2 + c_m(\theta)\,[T - T_{max}]^3 \,. \qquad \text{(A2-22)}$$

From Equation (A2-5), we obtain

$$\begin{aligned} a_m &= \frac{1}{p}\,[a_o + 2b_o\,(T_{max} - T_o) + 3c_o\,T_{max} - T_o)^2] = 0 \\ b_m &= \sqrt{b_o^2 - 3a_o c_o} \\ c_m &= c_o \,. \end{aligned} \qquad \text{(A2-23)}$$

Further, from Equation (A2-7),

$$\begin{aligned} T_{max} - T_o &= \frac{b_m - b_o}{3c_o} \\ &= -\frac{a_o}{b_o + b_m} \approx -\frac{a_o}{2b_o} \,. \end{aligned} \qquad \text{(A2-24)}$$

T_{max} as a function of the angle of orientation of the plate can be obtained from the derivatives of the temperature coefficients $a_o(\theta)$, $b_o(\theta)$, and $c_o(\theta)$ or from the derivatives of the temperature coefficients $b_m(\theta)$ and $c_m(\theta)$, with respect to the angle of orientation.

APPENDIX 3

COMPLETE EXPRESSIONS FOR $\frac{\partial T_m}{\partial \theta}$ WHERE T_m IS THE MAXIMUM OR MINIMUM TEMPERATURE OF THE FREQUENCY-TEMPERATURE CHARACTERISTICS

The expression for the frequency-temperature variation of a particular mode of motion, as given in Equation (8) and Appendix 2, is used to calculate the temperatures T_μ where the frequency deviation becomes a maximum or minimum:

$$T_\mu - T_o = \Delta T = \frac{-b_o}{3c_o} \pm \sqrt{\left(\frac{b_o}{3c_o}\right)^2 - \frac{a_o}{3c_o}}\,, \qquad \text{(A3-1)}$$

where a_o, b_o, and c_o are the temperature coefficients of frequency in Equation (8a) taken at the temperature T_o. These coefficients are functions of the orientation of the plate and determined from Equations (9), (10), and (11).

The variation of T_μ with respect to the angle θ follows from Equation (A3-1). The sign chosen is the same as that in Equation (A3-1).

$$\pm\sqrt{b_o^2 - 3a_oc_o}\;.\;\frac{\partial T_\mu}{\partial \theta} = -\frac{1}{2}\frac{\partial a_o}{\partial \theta} - \Delta T\;.\;\frac{\partial b_o}{\partial \theta} + \left(\frac{a_o}{2c_o} + \frac{b_o \Delta T}{c_o}\right)\frac{\partial c_o}{\partial \theta}. \qquad \text{(A3-2)}$$

$$p\;.\;b_\mu\;.\;\frac{\partial T_\mu}{\partial \theta} = -\frac{a}{2}(\theta_a - \theta_c) - b\;\Delta T\;(\theta_b - \theta_c)\,, \qquad \text{(A3-3)}$$

where b_μ is the parabola constant b at T_μ, and

$$p = 1 + a_o\Delta T + b_o\,\Delta T^2 + c_o\,\Delta T^3, \text{ where } \Delta T \approx 1, \qquad \text{(See A2-5)}$$

further, $\theta_x = \frac{1}{x}\frac{\partial x}{\partial \theta}$ is is the first-order coefficient of the quantity x with respect to the angle θ. Equations (A3-2) and (A3-3) yield $\frac{\partial T}{\partial \theta}$ when ϕ is substituted for θ.

APPENDIX 4

VALUES FOR THE TEMPERATURE COEFFICIENTS a, b, c WHEN THE REFERENCE TEMPERATURE T_o IS CHANGED TO T_1. (EXAMPLE: THICKNESS MODE C, (yxwl)10°,−33°.)

The first-, second-, and third-order temperature coefficients of frequency a_o, b_o, c_o in the power series (A2-4) are related to the reference temperature T_o when the reference temperature T_o is changed to the temperature T_1. Equation (A2-5) which transforms a_o, b_o, c_o to a_1, b_1, c_1 holds. The equation may be applied to the cut $\phi = 10°$, $\theta = -33°$ which has temperature coefficients related to the 25°C temperature, as shown in Table 5. The temperature coefficients a, b, c were transformed to the temperature 0°, −40°, −60°, and −80°C. The transformed values are as follow:

T_1	a $10^{-6}/°C$	b $10^{-9}/(°C)^2$	c $10^{-12}/(°C)^3$	Inflection Temperature
25°C	−0.87	−7.81	−21.5	−96°C
0°C	−0.532	−6.19	−21.5	−96°C
−40°C	−0.130	−3.62	−21.5	−96°C
−60°C	−0.011	−2.33	−21.5	−96°C
−80°C	0.06	−1.04	−21.5	−96°C

DISTRIBUTION LIST

	Copies
Commanding General U. S. Army Electronics Command ATTN: AMSEL-AD Fort Monmouth, New Jersey	3
Office of the Assistant Secretary of Defense (Research and Engineering) ATTN: Technical Library Room 3E1065, The Pentagon Washington 25, D. C.	1
Chief of Research and Development Department of the Army Washington 25, D. C.	2
Chief, United States Army Security Agency ATTN: ACofS, G4 (Technical Library) Arlington Hall Station Arlington 12, Virginia	1
Commanding Officer U. S. Army Electronics Research and Development Activity ATTN: Technical Library Fort Huachuca, Arizona	1
Commanding Officer U. S. Army Electronics Research and Development Activity ATTN: SELWS-AJ White Sands, New Mexico	1
Commanding Officer U. S. Army Electronics Research Unit P. O. Box 205 Mountain View, California	1
Commanding Officer U. S. Army Electronics Materiel Support Agency ATTN: SELMS-ADJ Fort Monmouth, New Jersey	1
Commanding General U. S. Army Satellite Communications Agency ATTN: Technical Documents Center Fort Monmouth, New Jersey	1
Commanding Officer Engineer Research and Development Laboratories ATTN: Technical Documents Center Fort Belvoir, Virginia	1
Commanding Officer U. S. Army Chemical Warfare Laboratories ATTN: Technical Library, Building 330 Army Chemical Center, Maryland	1
Commanding Officer Harry Diamond Laboratories ATTN: Library, Building 92, Room 211 Washington 25, D. C.	1
Headquarters, United States Air Force ATTN: AFCIN Washington 25, D. C.	2
Rome Air Development Center ATTN: RAALD Griffiss Air Force Base New York	1
Headquarters Ground Electronics Engineering Installation Agency ATTN: ROZMEL Griffiss Air Force Base New York	1
Commanding General U. S. Army Materiel Command ATTN: R&D Directorate Washington 25, D. C.	2

Distribution List (Cont)

	Copies
Aeronautical Systems Division ATTN: ASNXRR Wright-Patterson Air Force Base Ohio	1
U. S. Air Force Security Service ATTN: ESD San Antonio, Texas	1
Headquarters Strategic Air Command ATTN: DOCE Offutt Air Force Base, Nebraska	1
Headquarters Research & Technology Division ATTN: RTH Bolling Air Force Base Washington 25, D. C.	1
Air Proving Ground Center ATTN: PGAPI Eglin Air Force Base, Florida	1
Air Force Cambridge Research Laboratories ATTN: CRXL-R L. G. Hanscom Field Bedford, Massachusetts	2
Headquarters Electronic Systems Division ATTN: ESAT L. G. Hanscom Field Bedford, Massachusetts	2
AFSC Scientific/Technical Liaison Office U. S. Naval Air Development Center Johnsville, Pa.	1
Chief of Naval Research ATTN: Code 427 Department of the Navy Washington 25, D. C.	1
Bureau of Ships Technical Library ATTN: Code 312 Main Navy Building, Room 1528 Washington 25, D. C.	1
Chief, Bureau of Ships ATTN: Code 454 Department of the Navy Washington 25, D. C.	1
Chief, Bureau of Ships ATTN: Code 686B Department of the Navy Washington 25, D. C.	1
Director U. S. Naval Research Laboratory ATTN: Code 2027 Washington, D. C. 20390	1
Commanding Officer & Director U. S. Navy Electronics Laboratory ATTN: Library San Diego 52, California	1
Commander U. S. Naval Ordnance Laboratory White Oak Silver Spring 19, Maryland	1
Commander Defense Documentation Center ATTN: TISIA Cameron Station, Bldg. 5 Alexandria, Virginia 22314	20
USAELRDL Liaison Officer U. S. Army Tank-Automotive Center Warren, Michigan 48090	1
USAELRDL Liaison Officer Naval Research Laboratory ATTN: Code 1071 Washington, D. C. 20390	1
USAELRDL Liaison Officer Massachusetts Institute of Technology Building 26, Room 131 77 Massachusetts Avenue Cambridge 39, Massachusetts	1

Distribution List (Cont)

	Copies
USAELRDL Liaison Office Aeronautical Systems Division ATTN: ASDL-9 Wright-Patterson Air Force Base Ohio	1
U. S. Army Research Liaison Office Lincoln Laboratory P. O. Box 73 Lexington, Massachusetts	1
USAELRDL Liaison Officer Rome Air Development Center ATTN: RAOL Griffiss Air Force Base New York	1
USAELRDL Liaison Officer U. S. Army Combat Developments Command, CDCLN-EL Fort Belvoir, Virginia	1
USAEMSA Liaison Office, Far East Signal Office, USARPAC APO 958, U. S. Forces San Francisco, California	1
Technical Dir., SELRA/CS Headquarters, USAELRDL	1
USAELRDA-White Sands Liaison Office SELRA/LNW, USAELRDL	1
AFSC Scientific/Technical Liaison Office SELRA/LNA, USAELRDL	1
Director, USAEGIMRADA Attn: ENGGM-SS Fort Belvoir, Virginia	1
Marine Corps Liaison Office SELRA/LNR, USAELRDL	1
USACDC Liaison Office SELRA/LNF, USAELRDL	2
Chief, Technical Information Division Headquarters, USAELRDL	6
USAELRDL Technical Documents Center SEIRA/ADT, Hexagon	1
Chief Scientist U. S. Army Electronics Command Attn: AMSEL-SC Fort Monmouth, N. J.	1
File Unit Nr. 1 Rm. 3D-116, Hexagon	1
Commanding Officer U. S. Army Security Agency Processing Center Fort Monmouth, N. J.	1
National Bureau of Standards Boulder Laboratories Attn: Library Boulder, Colorado	1
Director National Bureau of Standards Attn: Library Washington 25, D. C.	1
Professor R. D. Mindlin Columbia University 632 West 125th St. New York 27, N. Y.	2
Union Thermoelectric Corp. 7212 Circle Ave. Forest Park, Illinois	1
Director, Solid State and Frequency Control Division	18
Director, Electronic Components Department	1
Piezoelectric Crystal and Circuitry Branch	65

ARMY, FT. MONMOUTH, NJ-MON 3996-63

AD ______________ Div. ______________

Army Electronics Research and Development Laboratory, Fort Monmouth, N. J.
HIGHER ORDER TEMPERATURE COEFFICIENTS OF THE ELASTIC STIFFNESSES AND COMPLIANCES OF ALPHA-QUARTZ, by R. Bechmann, A. D. Ballato, T. J. Lukaszek. September 1963, 79 p. incl. illus. tables, 29 refs. (AELRDL Technical Report 2261) (DA Task 3A99-15-001-02) Unclassified report

The first-, second-, and third-order temperature coefficients of the elastic stiffnesses and compliances of alpha-quartz have been determined using thickness modes of double-rotated quartz plates based on the Christoffel theory of thickness vibrations. The temperature dependence of all possible thickness modes can be calculated from the values of the elastic stiffnesses and their

UNCLASSIFIED

1. Alpha-Quartz--Elastic Properties, Temperature Coefficients (Higher Order)
2. Elasticity of Quartz
3. Vibrators--Quartz
4. Temperature Coefficients--Elastic Constants

I. Bechmann, R. Ballato, A. D. Lukaszek, T. J.
II. Army Electronics Research and Development Laboratory, Fort Monmouth, N. J.
III. DA Task 3A99-15-001-02

AD ______________ Div. ______________

Army Electronics Research and Development Laboratory, Fort Monmouth, N. J.
HIGHER ORDER TEMPERATURE COEFFICIENTS OF THE ELASTIC STIFFNESSES AND COMPLIANCES OF ALPHA-QUARTZ, by R. Bechmann, A. D. Ballato, T. J. Lukaszek. September 1963, 79 p. incl. illus. tables, 29 refs. (AELRDL Technical Report 2261) (DA Task 3A99-15-001-02) Unclassified report

The first-, second-, and third-order temperature coefficients of the elastic stiffnesses and compliances of alpha-quartz have been determined using thickness modes of double-rotated quartz plates based on the Christoffel theory of thickness vibrations. The temperature dependence of all possible thickness modes can be calculated from the values of the elastic stiffnesses and their

UNCLASSIFIED

1. Alpha-Quartz--Elastic Properties, Temperature Coefficients (Higher Order)
2. Elasticity of Quartz
3. Vibrators--Quartz
4. Temperature Coefficients--Elastic Constants

I. Bechmann, R. Ballato, A. D. Lukaszek, T. J.
II. Army Electronics Research and Development Laboratory, Fort Monmouth, N. J.
III. DA Task 3A99-15-001-02

AD ______________ Div. ______________

Army Electronics Research and Development Laboratory, Fort Monmouth, N. J.
HIGHER ORDER TEMPERATURE COEFFICIENTS OF THE ELASTIC STIFFNESSES AND COMPLIANCES OF ALPHA-QUARTZ, by R. Bechmann, A. D. Ballato, T. J. Lukaszek. September 1963, 79 p. incl. illus. tables, 29 refs. (AELRDL Technical Report 2261) (DA Task 3A99-15-001-02) Unclassified report

The first-, second-, and third-order temperature coefficients of the elastic stiffnesses and compliances of alpha-quartz have been determined using thickness modes of double-rotated quartz plates based on the Christoffel theory of thickness vibrations. The temperature dependence of all possible thickness modes can be calculated from the values of the elastic stiffnesses and their

UNCLASSIFIED

1. Alpha-Quartz--Elastic Properties, Temperature Coefficients (Higher Order)
2. Elasticity of Quartz
3. Vibrators--Quartz
4. Temperature Coefficients--Elastic Constants

I. Bechmann, R. Ballato, A. D. Lukaszek, T. J.
II. Army Electronics Research and Development Laboratory, Fort Monmouth, N. J.
III. DA Task 3A99-15-001-02

AD ______________ Div. ______________

Army Electronics Research and Development Laboratory, Fort Monmouth, N. J.
HIGHER ORDER TEMPERATURE COEFFICIENTS OF THE ELASTIC STIFFNESSES AND COMPLIANCES OF ALPHA-QUARTZ, by R. Bechmann, A. D. Ballato, T. J. Lukaszek. September 1963, 79 p. incl. illus. tables, 29 refs. (AELRDL Technical Report 2261) (DA Task 3A99-15-001-02) Unclassified report

The first-, second-, and third-order temperature coefficients of the elastic stiffnesses and compliances of alpha-quartz have been determined using thickness modes of double-rotated quartz plates based on the Christoffel theory of thickness vibrations. The temperature dependence of all possible thickness modes can be calculated from the values of the elastic stiffnesses and their

UNCLASSIFIED

1. Alpha-Quartz--Elastic Properties, Temperature Coefficients (Higher Order)
2. Elasticity of Quartz
3. Vibrators--Quartz
4. Temperature Coefficients--Elastic Constants

I. Bechmann, R. Ballato, A. D. Lukaszek, T. J.
II. Army Electronics Research and Development Laboratory, Fort Monmouth, N. J.
III. DA Task 3A99-15-001-02

AD ________________ Div. ________________

Army Electronics Research and Development Laboratory, Fort Monmouth, N. J.
HIGHER ORDER TEMPERATURE COEFFICIENTS OF THE ELASTIC STIFFNESSES AND COMPLIANCES OF ALPHA-QUARTZ, by R. Bechmann, A. D. Ballato, T. J. Lukaszek. September 1963, 79 p. incl. illus. tables, 29 refs. (AEIRDL Technical Report 2261) (DA Task 3A99-15-001-02) Unclassified report

The first-, second-, and third-order temperature coefficients of the elastic stiffnesses and compliances of alpha-quartz have been determined using thickness modes of double-rotated quartz plates based on the Christoffel theory of thickness vibrations. The temperature dependence of all possible thickness modes can be calculated from the values of the elastic stiffnesses and their

UNCLASSIFIED

1. Alpha-Quartz--Elastic Properties, Temperature Coefficients (Higher Order)
2. Elasticity of Quartz
3. Vibrators--Quartz
4. Temperature Coefficients--Elastic Constants

I. Bechmann, R.
Ballato, A. D.
Lukaszek, T. J.

II. Army Electronics Research and Development Laboratory, Fort Monmouth, N. J.

III. DA Task 3A99-15-001-02

AD ________________ Div. ________________

Army Electronics Research and Development Laboratory, Fort Monmouth, N. J.
HIGHER ORDER TEMPERATURE COEFFICIENTS OF THE ELASTIC STIFFNESSES AND COMPLIANCES OF ALPHA-QUARTZ, by R. Bechmann, A. D. Ballato, T. J. Lukaszek. September 1963, 79 p. incl. illus. tables, 29 refs. (AEIRDL Technical Report 2261) (DA Task 3A99-15-001-02) Unclassified report

The first-, second-, and third-order temperature coefficients of the elastic stiffnesses and compliances of alpha-quartz have been determined using thickness modes of double-rotated quartz plates based on the Christoffel theory of thickness vibrations. The temperature dependence of all possible thickness modes can be calculated from the values of the elastic stiffnesses and their

UNCLASSIFIED

1. Alpha-Quartz--Elastic Properties, Temperature Coefficients (Higher Order)
2. Elasticity of Quartz
3. Vibrators--Quartz
4. Temperature Coefficients--Elastic Constants

I. Bechmann, R.
Ballato, A. D.
Lukaszek, T. J.

II. Army Electronics Research and Development Laboratory, Fort Monmouth, N. J.

III. DA Task 3A99-15-001-02

AD ________________ Div. ________________

Army Electronics Research and Development Laboratory, Fort Monmouth, N. J.
HIGHER ORDER TEMPERATURE COEFFICIENTS OF THE ELASTIC STIFFNESSES AND COMPLIANCES OF ALPHA-QUARTZ, by R. Bechmann, A. D. Ballato, T. J. Lukaszek. September 1963, 79 p. incl. illus. tables, 29 refs. (AEIRDL Technical Report 2261) (DA Task 3A99-15-001-02) Unclassified report

The first-, second-, and third-order temperature coefficients of the elastic stiffnesses and compliances of alpha-quartz have been determined using thickness modes of double-rotated quartz plates based on the Christoffel theory of thickness vibrations. The temperature dependence of all possible thickness modes can be calculated from the values of the elastic stiffnesses and their

UNCLASSIFIED

1. Alpha-Quartz--Elastic Properties, Temperature Coefficients (Higher Order)
2. Elasticity of Quartz
3. Vibrators--Quartz
4. Temperature Coefficients--Elastic Constants

I. Bechmann, R.
Ballato, A. D.
Lukaszek, T. J.

II. Army Electronics Research and Development Laboratory, Fort Monmouth, N. J.

III. DA Task 3A99-15-001-02

AD ________________ Div. ________________

Army Electronics Research and Development Laboratory, Fort Monmouth, N. J.
HIGHER ORDER TEMPERATURE COEFFICIENTS OF THE ELASTIC STIFFNESSES AND COMPLIANCES OF ALPHA-QUARTZ, by R. Bechmann, A. D. Ballato, T. J. Lukaszek. September 1963, 79 p. incl. illus. tables, 29 refs. (AEIRDL Technical Report 2261) (DA Task 3A99-15-001-02) Unclassified report

The first-, second-, and third-order temperature coefficients of the elastic stiffnesses and compliances of alpha-quartz have been determined using thickness modes of double-rotated quartz plates based on the Christoffel theory of thickness vibrations. The temperature dependence of all possible thickness modes can be calculated from the values of the elastic stiffnesses and their

UNCLASSIFIED

1. Alpha-Quartz--Elastic Properties, Temperature Coefficients (Higher Order)
2. Elasticity of Quartz
3. Vibrators--Quartz
4. Temperature Coefficients--Elastic Constants

I. Bechmann, R.
Ballato, A. D.
Lukaszek, T. J.

II. Army Electronics Research and Development Laboratory, Fort Monmouth, N. J.

III. DA Task 3A99-15-001-02